

# Stationary storage for improving the energy recovery in DC trolley grids.

by

E.E. Bronkhorst

to obtain the degree of Master of Science  
at the Delft University of Technology,  
to be defended publicly on Friday May 28, 2021 at 10:30 AM.

|                   |                               |          |
|-------------------|-------------------------------|----------|
| Student number:   | 4318927                       |          |
| Project duration: | June 1, 2020 – May 28, 2021   |          |
| Thesis committee: | Prof. dr. ir P. Bauer,        | TU Delft |
|                   | dr.ir. Gautham Chandra Mouli, | TU Delft |
|                   | dr. Pedro P. Vergara,         | TU Delft |

*This thesis is confidential and cannot be made public until May 28, 2023.*

An electronic version of this thesis is available at <http://repository.tudelft.nl/>.



# Preface

Technology, the miraculous mixture of science and math that changes our lives everyday has always been the most fascinating topic for me. It started at the school for vocational education, where I was subject to the practical side of the beautiful phenomena called electricity. From that moment on, I wanted to learn more. For that, I needed to crawl my way up to get what I wanted, being a student at the Technical University of Delft.

The thesis you're about to read may be a normal stack of paper to you, but for me it's the closure of a part of my life. Starting in 2013, ending in 2021. This period means a lot to me, not only on the educational side of studying, but also on the side of personal development. Moving to Delft, being a member of the study association ETV and standing on my own feet for the first time was sometimes a challenge for me. But luckily I quickly found out that you don't have to be alone. I'm grateful for all the friends I made in Delft. Especially my fellow board members, the people who got to know me pretty good in our one-year adventure. And of course, Kevin, the guy who got me in Delft, the study association, and a perfect friendship. Thank you all for the wonderful time.

About a year ago Ibrahim introduced me to the trolleybus project, and the decision to accept the challenge was made fast. A trolleybus, something you can touch, something you can explain to your friends and a technology that can significantly help to make our world a better place. With the support of dr.ir. Gautham Chandra Mouli, and under the supervision of Prof. dr. ir P. Bauer, Ibrahim and I found our way in the process of writing this thesis. I am grateful for all the support I received from these people, thank you.

This thesis is written in a time that the whole world came to a standstill due to the coronavirus. People were forced to work from home, cutting out the important moments of social interaction. I'm thankful for the ones that support me in this time, listening to my boring monologues on trolleybuses and making these dark days brighter. Great thanks to my family, friends and especially Jan and Sietze for adopting me back in my hometown after leaving Delft.

Technology may change our lives everyday, but we should never forget the importance of friends and family.

With warm regards,

*Erné*  
*Gorinchem, May 2021*



# Summary

Trolleybus systems are a known sustainable replacement for regular diesel powered busses. However, the sustainability of these systems can be improved by implementing wayside stationary storage. In this work, implementing stationary storage will be considered for the reduction of transmission losses and increased braking energy recovery. Based on measurements of the Arnhem grid, a case-study on the implementation of such systems is simulated. Results show that for this grid, implementing storage only for the reduction of transmission losses is not beneficial. However, when the recuperation of braking energy is considered, a significant energy reduction can be achieved (up to 17% for some specific sections in the grid). A recommendation on location, sizing and charge scheme is given based on the simulation results. Furthermore, a study has been performed on using stationery storage for reducing feeding substation peak demands, creating headroom for other services (e.g. EV charging) to be implemented on the trolley-grid.



# Contents

|  |           |
|--|-----------|
| <b>List of Figures</b>                                 | <b>ix</b> |
| <b>List of Tables</b>                                  | <b>xi</b> |
| <b>1 Introduction</b>                                  | <b>1</b>  |
| 1.1 Problem statement . . . . .                        | 1         |
| 1.1.1 Grid setup . . . . .                             | 2         |
| 1.1.2 Busses . . . . .                                 | 2         |
| 1.1.3 Bus behaviour . . . . .                          | 4         |
| 1.1.4 Power flow . . . . .                             | 4         |
| 1.1.5 Challenges . . . . .                             | 5         |
| 1.2 Energy Storage Systems. . . . .                    | 5         |
| 1.2.1 Battery based ESS . . . . .                      | 6         |
| 1.2.2 Capacitor based ESS . . . . .                    | 6         |
| 1.2.3 Hybrid ESS . . . . .                             | 7         |
| 1.2.4 Other ESS technologies . . . . .                 | 7         |
| 1.3 ESS in trolleybus grids . . . . .                  | 7         |
| 1.4 Thesis objective . . . . .                         | 9         |
| 1.5 Contribution . . . . .                             | 9         |
| 1.6 Summary of Results . . . . .                       | 10        |
| 1.7 Project workflow and Report Organization . . . . . | 10        |
| 1.8 Conclusion . . . . .                               | 10        |
| <b>2 Literature Review</b>                             | <b>11</b> |
| 2.1 Bus simulation . . . . .                           | 11        |
| 2.2 Storage type . . . . .                             | 12        |
| 2.3 Charge scheme. . . . .                             | 12        |
| 2.4 Storage in trolleybus grids . . . . .              | 13        |
| 2.5 Trolleybus grid capacity increase . . . . .        | 14        |
| 2.6 Research Gap . . . . .                             | 14        |
| 2.7 Conclusions. . . . .                               | 15        |
| <b>3 Dataset exploration</b>                           | <b>17</b> |
| 3.1 Grid layout . . . . .                              | 17        |
| 3.1.1 Sections. . . . .                                | 17        |
| 3.1.2 Forked section simplification. . . . .           | 18        |
| 3.1.3 Substations . . . . .                            | 19        |
| 3.2 Measurements . . . . .                             | 20        |
| 3.3 Velocity profiles . . . . .                        | 20        |
| 3.4 Power Profiles . . . . .                           | 21        |
| 3.5 Bus lines & scheduling . . . . .                   | 21        |
| 3.5.1 Scenario distribution . . . . .                  | 22        |
| 3.6 Energy measurements . . . . .                      | 22        |
| 3.7 Validation . . . . .                               | 22        |
| 3.7.1 Position profile validation. . . . .             | 22        |
| 3.7.2 Bus energy validation . . . . .                  | 23        |
| 3.8 Regenerative braking energy analysis . . . . .     | 24        |
| 3.8.1 Recuperation power ratio . . . . .               | 24        |
| 3.8.2 Potential regenerative energy . . . . .          | 25        |
| 3.9 Conclusions. . . . .                               | 26        |

|          |   |           |
|----------|---|-----------|
| <b>4</b> | <b>Simulation methodology</b>   | <b>27</b> |
| 4.1      | Position simulation . . . . .   | 27        |
| 4.2      | Simulation scenarios . . . . .  | 28        |
| 4.3      | Power simulation . . . . .  | 29        |
| 4.3.1    | Grid model . . . . .  | 29        |
| 4.3.2    | Simulation of the braking resistor . . . . .  | 31        |
| 4.3.3    | Generation of summer power profiles . . . . .   | 31        |
| 4.4      | Base simulation cycle . . . . .   | 32        |
| 4.5      | Sample frequency . . . . .  | 33        |
| 4.6      | ESS Objectives . . . . .  | 33        |
| 4.7      | ESS Implementation . . . . .  | 34        |
| 4.7.1    | Charge/Discharge efficiency . . . . .   | 34        |
| 4.7.2    | SOC Limits . . . . .  | 34        |
| 4.7.3    | Sizing . . . . .  | 34        |
| 4.8      | Charge scheme . . . . .   | 35        |
| 4.8.1    | CS1: Simple recuperation . . . . .  | 35        |
| 4.8.2    | CS2: Advanced recuperation . . . . .  | 36        |
| 4.9      | ESS simulation cycle . . . . .  | 37        |
| 4.10     | List of assumptions . . . . .   | 38        |
| 4.11     | Conclusions . . . . .   | 39        |
| <b>5</b> | <b>Baseline results</b>   | <b>41</b> |
| 5.1      | Substation utilisation . . . . .  | 41        |
| 5.2      | Substation power . . . . .  | 42        |
| 5.3      | Substation energy . . . . .   | 43        |
| 5.3.1    | Substation energy validation . . . . .  | 43        |
| 5.4      | Available regenerative energy . . . . .   | 44        |
| 5.5      | Braking resistor energy . . . . .   | 45        |
| 5.6      | Energy distribution . . . . .   | 46        |
| 5.6.1    | Grid level . . . . .  | 46        |
| 5.6.2    | Bus level . . . . .   | 47        |
| 5.7      | Transmission losses . . . . .   | 48        |
| 5.8      | Peak substation power . . . . .   | 48        |
| 5.9      | Conclusions . . . . .   | 49        |
| <b>6</b> | <b>Simulation results &amp; Discussion</b>  | <b>51</b> |
| 6.1      | Stationary storage for reduction of transmission losses . . . . .                     | 51        |
| 6.1.1    | Simulation setup . . . . .  | 51        |
| 6.1.2    | Isolated section results . . . . .  | 51        |
| 6.1.3    | Connected section results . . . . .   | 53        |
| 6.1.4    | Full grid results . . . . .   | 55        |
| 6.1.5    | CS2 for reduction of transmission losses and implementation of bus location . . . . . | 55        |
| 6.2      | Stationary storage storage for recuperation of braking energy . . . . .               | 56        |
| 6.2.1    | Simulation setup . . . . .  | 56        |
| 6.2.2    | Operation of stationary storage used for recuperation of braking energy . . . . .     | 56        |
| 6.2.3    | Full grid simulation . . . . .  | 57        |
| 6.3      | Stationary storage for increased substation capacity . . . . .                        | 59        |
| 6.4      | Recommendation on sizing . . . . .  | 60        |
| 6.5      | Conclusions . . . . .   | 61        |
| <b>7</b> | <b>Conclusions</b>  | <b>63</b> |
| 7.1      | Grid analysis . . . . .   | 63        |
| 7.2      | Reduction of transmission losses . . . . .  | 64        |
| 7.3      | Maximal recuperation of braking energy . . . . .                                      | 64        |
| 7.4      | Increase of grid power capacity . . . . .   | 64        |
|          | <b>Bibliography</b>   | <b>65</b> |

# List of Figures

|      |  |    |
|------|--|----|
| 1.1  | Trolleybus grid layout . . . . .   | 2  |
| 1.2  | Trolleybus in Arnhem [46] . . . . .  | 3  |
| 1.3  | Schematic overview of trolleybus-catenary interface . . . . .  | 4  |
| 1.4  | Trolleybus grid power flow a) during bus acceleration b) during bus-to-bus interaction c) to EV or storage system d) to o-board storage e) to braking resistor . . . . . | 5  |
| 1.5  | Design of electrical layout of a trolleybus: a) without on-board storage b) with on-board storage . . . . .  | 8  |
| 1.6  | Stationary energy storage system . . . . .   | 8  |
| 1.7  | Stationary storage in Gdynia [7] . . . . .   | 9  |
| 2.1  | A typical ride cycle of: (a) rail traction vehicle; (b) trolleybus (* ride with quasi constant speed), $t$ – time, $v$ – velocity [3] . . . . .                          | 11 |
| 2.2  | Visual representation of storage type parameters [29] . . . . .  | 12 |
| 2.3  | Charge scheme details [8] . . . . .  | 13 |
| 3.1  | Map of the Arnhem trolley-grid showing sections and substations. . . . .   | 18 |
| 3.2  | Example of implemented section simplification . . . . .  | 19 |
| 3.3  | Section-substation relationship of substation 1, connecting sections 23 and 24 . . . . .   | 19 |
| 3.4  | Example bus velocity profile line 1: Velp to Oosterbeek from HAN measurement . . . . .   | 20 |
| 3.5  | Example bus power profile line 1: Velp to Oosterbeek from HAN measurement . . . . .  | 21 |
| 3.6  | Measured substation location energy profiles . . . . .   | 22 |
| 4.1  | Overview of simulation framework . . . . .   | 27 |
| 4.2  | Example of bus velocity and position profile . . . . .   | 28 |
| 4.3  | Example of bus position on section and section profile . . . . .   | 28 |
| 4.4  | Example of HVAC plateau . . . . .  | 29 |
| 4.5  | Equivalent circuit for trolley grid: a) real-world situation b) equivalent simplified circuit . . . . .  | 30 |
| 4.6  | Comparing overhead lines: a) without parallel connection b) with parallel connection . . . . .   | 30 |
| 4.7  | Overview of the grid model used in the simulation framework . . . . .  | 31 |
| 4.8  | Flowchart of pre-simulation power distribution (PSPD) . . . . .  | 31 |
| 4.9  | Summer profile generation . . . . .  | 32 |
| 4.10 | Simulation flowchart without ESS . . . . .   | 33 |
| 4.11 | Comparing sampled measurement data with re-sampled data for simulation . . . . .   | 33 |
| 4.12 | ESS model used in the simulation framework . . . . .   | 34 |
| 4.13 | Braking resistor power peak indication used for sizing . . . . .   | 35 |
| 4.14 | Flowchart describing operation of charge scheme 1 (CS1) . . . . .  | 36 |
| 4.15 | Operation of CS1 . . . . .   | 36 |
| 4.16 | Flowchart describing operation of charge scheme 2 (CS2) . . . . .  | 37 |
| 4.17 | Operation of CS2 . . . . .   | 37 |
| 4.18 | Simulation flowchart for section with ESS connected (direct or indirect) . . . . .   | 38 |
| 5.1  | Substation time-based utilization . . . . .  | 41 |
| 5.2  | Distribution of number of busses fed by the same substation during full-grid operation . . . . .   | 42 |
| 5.3  | Example substation power profile . . . . .   | 43 |
| 5.4  | Substation energy for all scenarios . . . . .  | 43 |
| 5.5  | Simulated vs. measured substation location energy consumption based on measurement data and simulation outcomes . . . . .  | 44 |
| 5.6  | Braking resistor power profile, outcome of pre-simulation power distribution (PSPD) calculation for a bus on line 6 departing at 05:00 . . . . .                         | 45 |

---

|      |  |    |
|------|--|----|
| 5.7  | Braking energy per substation . . . . .  | 46 |
| 5.8  | Energy distribution of trolley-grid. . . . .   | 46 |
| 5.9  | Excess energy share in different scenarios . . . . .   | 48 |
| 5.10 | Transmission losses for all substations . . . . .  | 48 |
| 5.11 | Daily substation current profile . . . . .   | 49 |
|      |  |    |
| 6.1  | Map and simplified representation of the isolated model of section 24 . . . . .                  | 52 |
| 6.2  | Reduction in transmission losses for section 24 in isolated state . . . . .                      | 52 |
| 6.3  | Map and simplified representation of the connected model of section 24 . . . . .                 | 53 |
| 6.4  | Reduction in transmission losses for section 24 in connected state . . . . .                     | 54 |
| 6.5  | ESS Simulation results; CS2, 1-day full grid simulation, regular workday, max profiles . . . . . | 57 |
| 6.6  | Analysis on ESS efficiency in different sections based on known section parameters. . . . .      | 58 |
| 6.7  | Substation headroom without tuned threshold . . . . .  | 60 |
| 6.8  | Substation headroom with tuned threshold . . . . .   | 60 |
| 6.9  | ESS Operation with over-sized storage . . . . .  | 61 |
| 6.10 | ESS Operation with properly sized storage . . . . .  | 61 |

# List of Tables

|     |  |    |
|-----|--|----|
| 1.1 | Summary of some important trolleybus properties . . . . .  | 3  |
| 1.2 | Comparison of different ESS technologies [45] . . . . .  | 6  |
| 3.1 | Substation locations . . . . .   | 20 |
| 3.2 | Overview of Arnhem trolley-lines . . . . .   | 21 |
| 3.3 | Arnhem annual schedule distribution . . . . .  | 22 |
| 3.4 | Analysis of integrated velocity profiles vs measured section lengths . . . . .   | 23 |
| 3.5 | Analysis of energy consumption per kilometer based on measured power profiles . . . . .  | 23 |
| 3.6 | Analysis of energy consumption per kilometer using only bus traction power . . . . .   | 24 |
| 3.7 | Analysis of available regenerative energy per line measurement . . . . .   | 25 |
| 3.8 | Analysis of available regenerated energy per kilometer . . . . .   | 25 |
| 4.1 | Time analysis for number of busses N fed by substation . . . . .   | 29 |
| 5.1 | Time analysis for number of busses N fed by substation . . . . .   | 42 |
| 5.2 | Available regenerative energy in the Arnhem grid . . . . .   | 45 |
| 5.3 | Increase in braking resistor power over different scenarios, absolute and relative to the total energy consumption . . . . .   | 46 |
| 5.4 | Increase in braking resistor power over different scenarios, absolute and relative to the total energy consumption . . . . .   | 47 |
| 5.5 | Excess energy destination analysis . . . . .   | 47 |
| 6.1 | Change in transmission losses for section 24 (Connected), a) absolute, b) relative to baseline, c) impact of location . . . . .  | 53 |
| 6.2 | Section 24 results for both connected and isolated operation . . . . .   | 54 |
| 6.3 | Full grid simulations on reduction of transmission losses. a) Positive effect is green. b) row based colouring on optimal location per charge scheme (green is best, red is worst, orange is in between) . . . . . | 55 |
| 6.4 | Relative reduction in substation energy [%] for CS1 and CS2 implemented stationary storage. a) CS1 b) CS2 (Efficiency colouring from green to red, green is best, red is worse) . . . . .                          | 58 |
| 6.5 | Comparing difference in substation energy reduction between implementation of CS1 and CS2, row coloured on efficiency, green is better . . . . .   | 59 |



# Introduction

*In this chapter, an introduction to trolleybuses and the trolley-grid components is presented. The operation and its challenges are discussed and a framework is given for this thesis based on a set of research questions.*

Urban transportation is indispensable in the current society. On an average workday in the Netherlands, around 4 million people make use of public transport [1]. Companies in the transport sector consume about 30% of energy usage worldwide [4]. Due to growth in environmental awareness by society, and the increasing prices of fossil fuels such as oil and gas, the urban transport sector is searching for opportunities in energy saving and the integration of renewable energy sources.

With the introduction of trolleybuses around 1899 (back then called the "Electromote"), the first electrically powered road vehicle was introduced. Since then the amount of trolleybuses increased rapidly. Nowadays a total of around 40.000 electrical trolleybuses are being deployed in approximately 310 cities worldwide [33]. Since the busses are driven by electricity instead of fossil fuel (they are regularly equipped with electrical machines instead of combustion engines), the implementation of renewable energy is attractive. Also, any electrical machine is able to work in two directions of energy flow. In the case of traction motors, this means the possibility of generator operation during braking of the vehicle, involving the conversion of vehicle kinetic energy into electrical energy [4]. This gives the opportunity to store the braking energy of the bus, instead of dumping this energy into a so called braking resistor, transferring it to heat.

The trolleybus is powered through a medium voltage DC grid. The actual feeding line, also known as the catenary, delivers power from the DC grid to the bus. The usage of the catenary limits the physical mobility of the bus. Recent research is focused on the option of catenary-free operation, by storing energy in the bus through so called in-motion charging (IMC). The application of in-motion charging is increasing the load on the existing DC grid, since it not only has to provide the traction power, but also power to the charger that is charging the required on-board battery.

Due to the introduction of bidirectional energy flows in the grid and by recovering braking energy, in-motion charging among others, the grid is used more extensively than what it was initially built for. This opens opportunities to use the grid for other applications, for example the charging of electrical vehicles and other auxiliary services that can be connected. Using renewable energy sources to feed the DC grid can make the grid, and all connected services, more energy neutral.

## 1.1. Problem statement

In order to investigate the trolleybus grid, one has to consider many characteristics. In this section the grid system (feeder), busses (consumer) and power flow will be discussed.

### 1.1.1. Grid setup

Typical trolleybus grids consist out of a bipolar DC link with a typical potential difference of 600-750 volt. This DC link is fed by unidirectional 6/12 pulse rectifiers placed in substations. The DC grid is comprised out of sections with a length of 1 to 1.5 kilometers. Figure 1.3 shows the layout of a substation. A substation may be feeding multiple sections. These different sections are connected to the same busbar in the substation, and are thereby fed by the same rectifier. Sections of overhead lines, hereafter called catenary, are connected with the substation using (underground) feeder lines. The losses in these feeder lines are strongly depending on the distance from the substation to the point of connection with the catenary, which are considered as constant. The actual power that is lost in these feeding lines is depending on the current flowing through them. Sections fed from different substations are isolated or connected via so called bilateral connections. In the case of isolated sections, the bus is able to pass the isolator using its momentum. A bilateral connection between two sections can be closed in order to exchange power between different sections. This gives the opportunity to, for example, use regenerated power from a bus in one section on an accelerating bus in the other section.

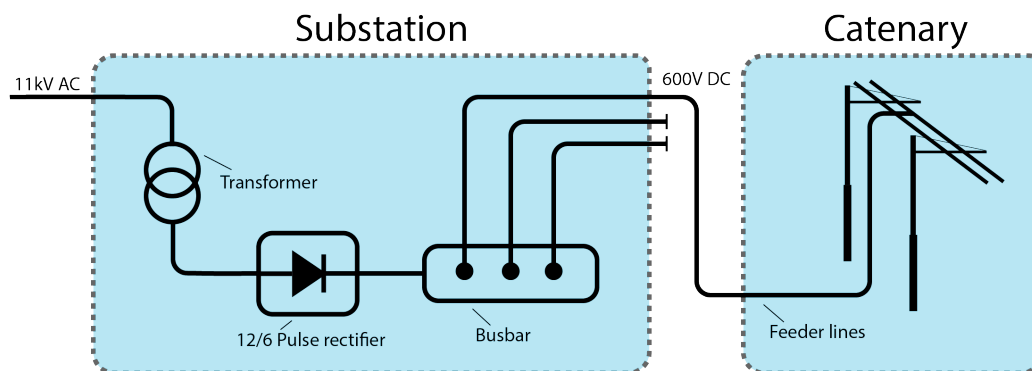


Figure 1.1: Trolleybus grid layout

### 1.1.2. Busses

Figure 1.3 shows a schematic layout of a trolleybus. The power delivered by the catenary is picked up by the busses through the current collector first. Two sliding brushes (contact shoes) make contact to the positive and negative catenary wires. The current flows through the roof-mounted trolley poles to the on board power electronics. The trolley poles can be disconnected from the catenary by winding up the pole ropes. Trolleybus current collectors are characterized by the maximum allowed load current of 600 A [28]. The power from the current collector is directed to the motor, HVAC (Heating, Ventilation and Air Conditioning) and other auxiliary services in the bus through an on-board power electronic converter as can be seen in figure 1.5a. Also, the bus is equipped with a braking resistor. This resistor acts as a fail safe in case the DC voltage is increased over a set value. Figure 1.4.e shows a schematic of this braking resistor. The energy consumption of a trolleybus varies between 1.8-2.8 kWh/km [5], they are available with a maximum speed of 80 km/h and the maximum acceleration and deceleration can go up to  $2 \text{ m/s}^2$  and  $-2 \text{ m/s}^2$ . These properties are summarized in table 1.1. Figure 1.2 shows an actual trolleybus.

Table 1.1: Summary of some important trolleybus properties

| <b>Trolleybus property</b>        |                          |
|-----------------------------------|--------------------------|
| Feeder voltage                    | 600-750 [V]              |
| Maximum load current              | 600 [A]                  |
| Typical energy consumption        | 1.8-2.8 [kWh/km]         |
| Maximum velocity                  | 80 [km/h]                |
| Maximum acceleration/deceleration | $-2 < a < 2$ [ $m/s^2$ ] |



Figure 1.2: Trolleybus in Arnhem [46]

In order to improve the mobility of the trolleybus, research is performed on catenary-free operation of the trolleybus. This new technique enables the bus to disconnect from the catenary to for example extend a line to places without catenary. The implementation of this catenary-free operation requires the bus to have on-board energy storage. This energy storage can be charged during normal operation, where the bus is connected to the catenary, even while driving. This concept is called in-motion-charging (IMC) and increases the power demand from the existing trolley grid.

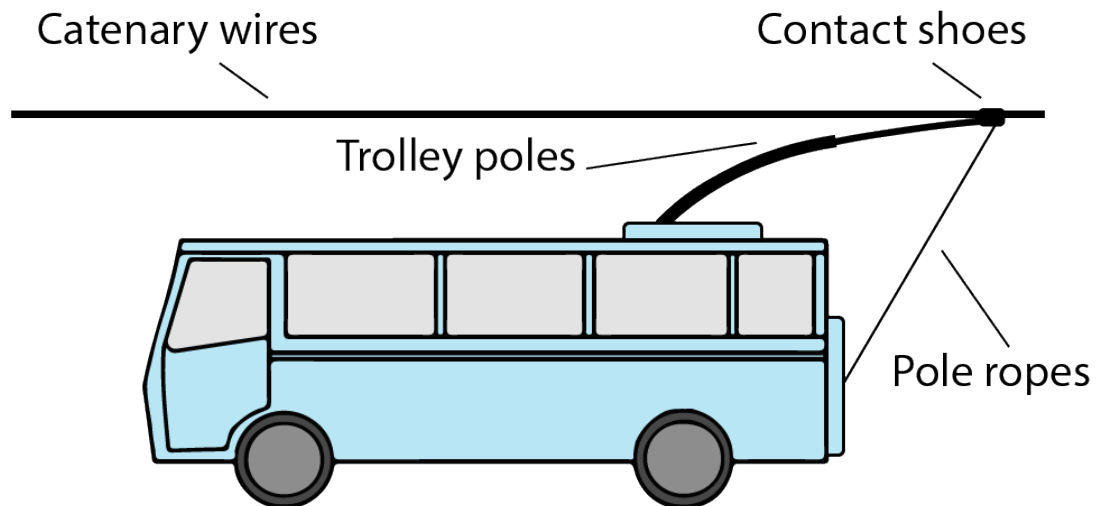


Figure 1.3: Schematic overview of trolleybus-catenary interface

### 1.1.3. Bus behaviour

The trolleybus grid has some similarities with metro, tram and train-systems, but the main difference is in the behaviour of the trolleybus. First, the bus is not depending on railway lines or tracks, and moves on its own trajectory, this is primarily interesting when investigating the IMC busses, where the mobility of the bus is not limited by tracks or the catenary. Therefore, when for example a way is blocked, the bus is able to deviate from the normal route to pass the blocking. The second and probably biggest difference between trolleybuses and other light-rail transportation is the traffic dependence of the bus. The trolleybus can be considered as normal traffic member, riding along with other traffic without any priority over others. This difference makes it even harder to model the velocity profiles of the bus, since traffic in general is heavily unpredictable.

### 1.1.4. Power flow

Due to the unidirectional nature of the feeding rectifier, and the possibility of regenerative braking, the power flow in trolleybus-grids is complex to control. Since no droop control is implemented in the substation, the voltage across the line is heavily depending on the resistive losses and power drawn over the line. Power control is performed by scheduling and slowing vehicles down. In practice, when the voltage drops below a certain value (typically 10%), the busses slow down or comes to a complete stop. Figure 1.4.a shows the normal operation of the bus, fed from the substation. When a bus is braking, around 30% of the energy can be regenerated and fed back to the DC grid. When another bus is accelerating at the same time the power that is injected from the braking bus is transferred to the accelerating bus. Figure 1.4.b shows this phenomena which is called natural sharing. The regenerative braking causes the line voltage to increase when no natural sharing occurs. An increasing line voltage can be used for various purposes. First, the excess energy can be used to support the grid when another bus is accelerating at the same moment, on the same section or through a bilateral connection to another section. Second, the power can be used to charge any IMC bus or EV charger, or storage system connected to the grid. When no other energy destination is available and the voltage keeps on rising, the on-board braking resistor starts burning away the energy and it is converted to heat.

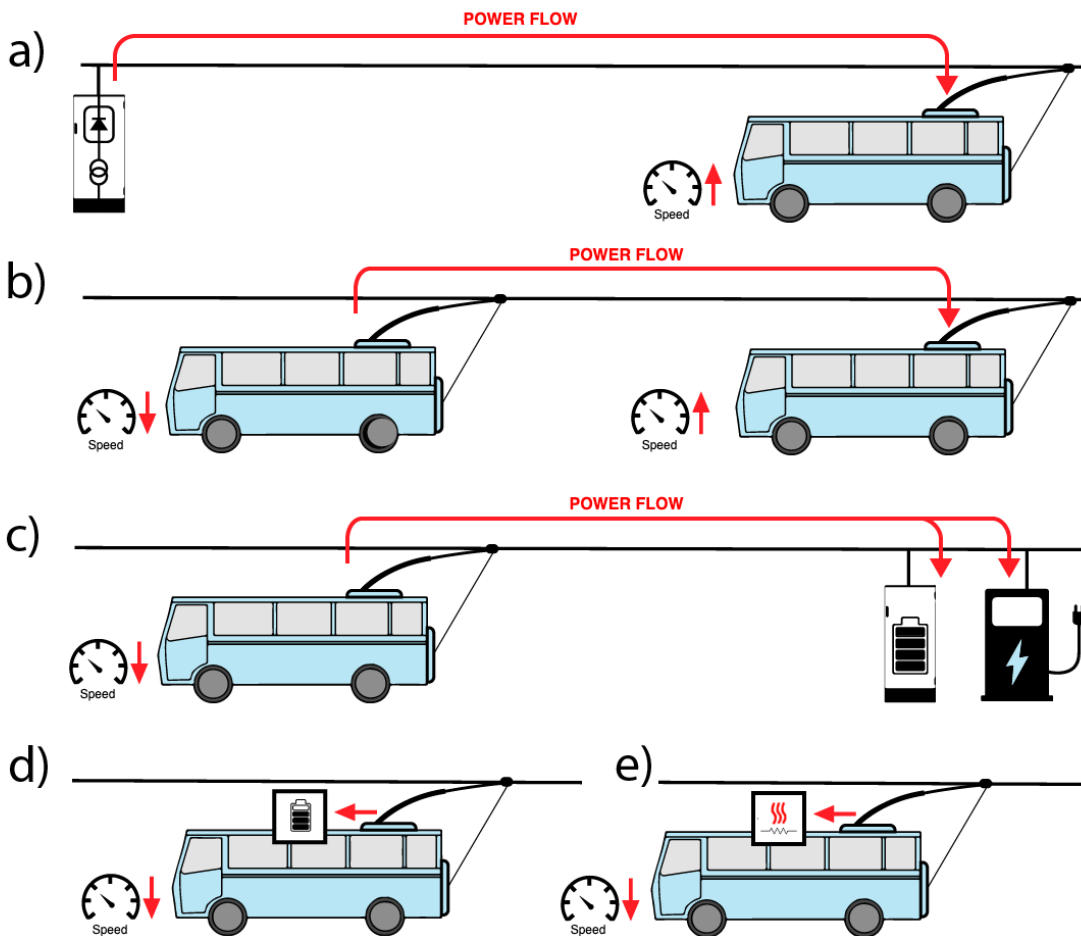


Figure 1.4: Trolleybus grid power flow a) during bus acceleration b) during bus-to-bus interaction c) to EV or storage system d) to o-board storage e) to braking resistor

### 1.1.5. Challenges

As described, the trolleybus has two main sources of power losses, the **power lost in the braking resistor** due to line over-voltages and the **power lost in the catenary wires** due to the high current passing through the long cables. These losses increase the amount of energy consumed by the total grid, and thereby increasing the cost of operation of the grid. Also, the implementation of in-motion charging busses introduce **increased capacity demand** from the substation. This increase may even cause the substation to overload sometimes, tripping the breakers and disconnection the whole DC grid. In this thesis, work will be performed on reduced power losses, and increased substation capacity.

## 1.2. Energy Storage Systems

Energy storage systems (ESS), convert electrical energy to some form of energy that can be stored and released when needed [45]. Various types of energy storage systems exist, each having specific benefits and disadvantages over each other. Important properties to consider are;

- **Energy efficiency**

The energy efficiency describes the ratio between the energy stored and recovered and the energy lost in the process of storing and recovering energy. This ratio can be used to account for losses, and indicate the effective efficiency of the ESS.

- **Power density**

The power density is a value which indicates how much power can be stored/recovered from a

kilogram of the specified storage. The power density plays an important role while designing an ESS. Using the power demand profile, one is able to determine the size of the ESS.

- **Energy density**

The power density is a value which indicates how much energy can be stored/recovered from a kilogram of the specified storage. The energy density plays an important role while designing an ESS. Using the energy demand profile, one is able to determine the size of the ESS.

- **Cycle life**

All ESS technologies encounter some form of degradation while using it. For most ESS technologies the amount of cycles plays an important role in the degradation. Using the application specific cycle profile, one can determine the lifetime of the ESS based on the cycle life.

- **Self discharge**

Some ESS technologies undergo so called self-discharge. This is the process of loss of potential energy when the ESS is not used. Self discharge plays an important role while dimensioning a ESS. One has to determine if the ESS is able to store the energy long enough to be recovered when needed. If any energy is lost during storage, this energy has to be considered as loss source.

These properties can be used to dimension an ESS for a specific application, but they are also important when selecting a specific ESS technology. Typical parameters for ESS technologies are displayed in figure 1.2. In order to get more insight in the available ESS technologies, some of them will be discussed.

Table 1.2: Comparison of different ESS technologies [45]

| Type                 | Energy Efficiency (%) | Energy Density ( $Wh/kg$ ) | Power Density ( $W/kg$ ) | Cycle Life (cycles) | Self Discharge |
|----------------------|-----------------------|----------------------------|--------------------------|---------------------|----------------|
| Pb-Acid              | 70–80                 | 20–35                      | 25                       | 200–2000            | Low            |
| Ni-Cd                | 60–90                 | 40–60                      | 140–180                  | 500–2000            | Low            |
| Ni-MH                | 50–80                 | 60–80                      | 220                      | < 3000              | High           |
| Li-Ion               | 70–85                 | 100–200                    | 360                      | 500–2000            | Med            |
| Li-polymer           | 70                    | 200                        | 250–1000                 | > 1200              | Med            |
| NaS                  | 70                    | 120                        | 120                      | 2000                | –              |
| VRB                  | 80                    | 25                         | 80–150                   | > 16000             | Negligible     |
| EDLC                 | 95                    | < 50                       | 4000                     | > 50000             | Very high      |
| Pumped hydro         | 65–80                 | 0.3                        | –                        | > 20 years          | Negligible     |
| CAES                 | 40–50                 | 10–30                      | –                        | > 20 years          | –              |
| Flywheel (steel)     | 95                    | 5–30                       | 1000                     | > 20000             | Very high      |
| Flywheel (composite) | 95                    | > 50                       | 5000                     | > 20000             | Very high      |

### 1.2.1. Battery based ESS

One of the most known and currently broadly applied ESS technology is the battery technology. For example, batteries are used in cars as starter battery, in uninterruptible power supplies for data centres, in nearly all mobile devices (phones, laptops) and also in electric vehicles (EV's) this technology is used. The technology is characterized by a relatively high energy and power density, making them ideal for portable applications. Since the introduction of the Lithium-Ion batteries, this type of storage is applied even more. Lithium-Ion batteries have even higher power and energy densities than the broadly applied lead-acid batteries.

### 1.2.2. Capacitor based ESS

Super-capacitors, also known as EDLC (Electrostatic double-layer capacitors), are capacitors with a higher capacitance rating than regular capacitors. This ESS technology is ideal for applications where a high power density is needed. For example, super-capacitors can be used in automotive application,

when storing regenerative braking energy, or in grid stabilisation systems. The main drawback of super-capacitors is their high self discharge rate. This property makes the storage technology not usable when storing energy for a long time.

### 1.2.3. Hybrid ESS

In some applications, the demand profile not only requires a high energy density, but also needs to be able to handle instantaneous power peaks, requiring a high power density. For example in electric vehicles, the energy rating of the storage determines the range of the vehicle. Battery technology would be suitable for this application, but during acceleration or deceleration, the amount of power transferred from and to the batteries is too high, and the internal resistance causes the battery to overheat. To overcome this problem the hybrid ESS is introduced. A combination of batteries and capacitors provides a large energy content, while being able to deliver power peaks at the same time.

### 1.2.4. Other ESS technologies

The discussed ESS technologies focus on portable storage application, but non-portable systems also exist. Flywheels can be used in stationary storage systems. Flywheels use their momentum to store energy in rotating kinetic energy. They are characterized by a high power density, and a rather low energy density. Flywheels can be used in portable applications as well, for example almost every combustion engine has a flywheel, but as storage system they are mostly used in stationary application. Another not portable storage system is the pumped hydro, mainly used in grid applications. Flow batteries (vanadium redox battery (VRB)) store their energy in a liquid form. Flow batteries are bulky in general, and therefore only used in grid-based applications.

The results of this thesis can be used to determine a suitable technology for stationary storage, however the actual recommendation on the storage type is not in the scope of this thesis. The information presented in the previous sections serves as a background to be used in further research on the recommended storage type.

## 1.3. ESS in trolleybus grids

As described in section 1.1.5, the main challenges in trolleybus grids consist out of reducing energy losses and increasing substation capacity. For both cases, an energy storage system could help achieving these goals. When using an ESS for reducing energy losses, one can use the regenerated energy while braking to charge a storage, and use this energy again when the bus accelerates. During braking, the ESS reduces the voltage increase, and thereby reduce the utilization of the braking resistor. When the bus accelerates again the power can be fed from an ESS that is closer to the bus, or in the bus, thereby reducing the current through the catenary and reducing the resistive losses in the catenary wires. Also, when the ESS is charged during low power demand moments on the substation, its energy can be released on high power demand, thereby reducing the substation load, and increasing the substation capacity.

#### On-board battery

ESS in trolleybus grids can be placed at multiple locations. One of these locations is on-board of the bus. Figure 1.4.d shows the flow of regenerative braking energy when on-board storage is implemented. The main advantage of on-board storage is the ability to utilize catenary-free operation on the bus, when the required energy demand is delivered from the on-board battery. Also, regenerative braking energy can be stored directly in the on-board ESS, thereby not using the catenary wires and reducing wire losses. When the energy is stored on board, it moves along with the bus movement, making the usage of the ESS independent of the bus's location on the line. Figure 1.5a shows a typical electrical layout of a normal bus, without on-board storage implemented. Figure 1.5b shows a bus with a super-capacitor module. This module includes the super-capacitors itself, as well as the possible required power electronics to control the charge and discharge power in the storage.

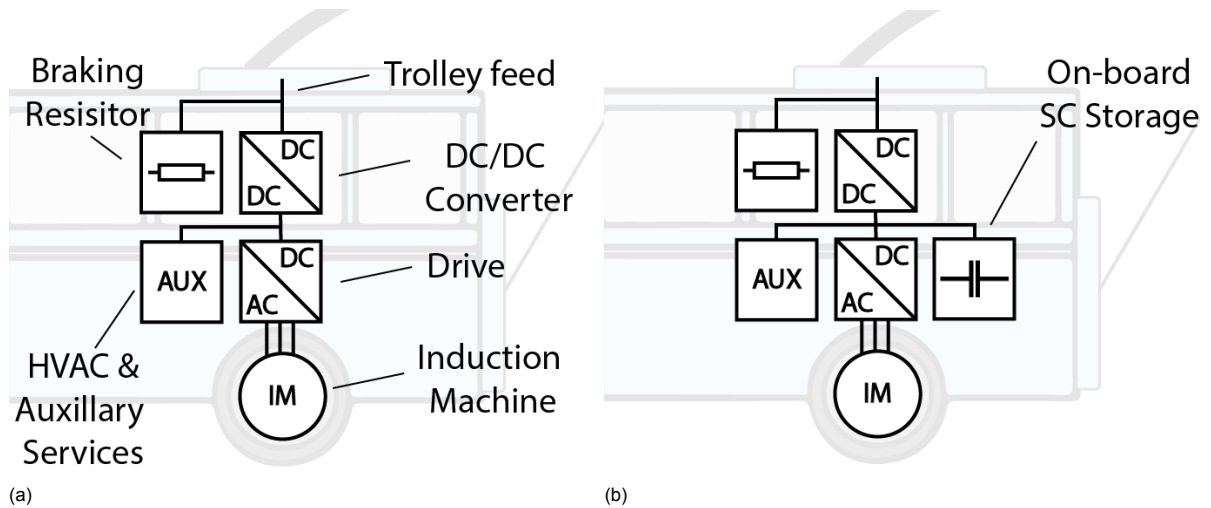


Figure 1.5: Design of electrical layout of a trolleybus: a) without on-board storage b) with on-board storage

### Stationary storage

In comparison to on-board storage, one could also position the ESS off-board. This is known as stationary storage. Figure 1.6 shows the layout of such a system. The main advantage of stationary ESS is that the ESS is helping a specific section/substation instead of a load. For example, a stationary storage can help reducing catenary wire losses by adding a feeding point on a different location on the line. Also, stationary storage can be used to support a specific high-loaded substation. Next to these advantages, stationary storage is available in the section at all times, and not depending on the location of the bus. This is specifically interesting when renewable energy sources are used to feed the grid. For example, if a PV installation is connected to the grid, feeding it with DC power on solar illumination, the energy can only be stored when a ESS is present in the section. In the case of IMC-busses, this would mean that if no bus is present in the line, the PV is not able to transfer any power. Figure 1.4.c shows the flow of regenerative braking energy when stationary storage is implemented. Figure 1.7 shows an actual implemented ESS in Gdynia, Poland.

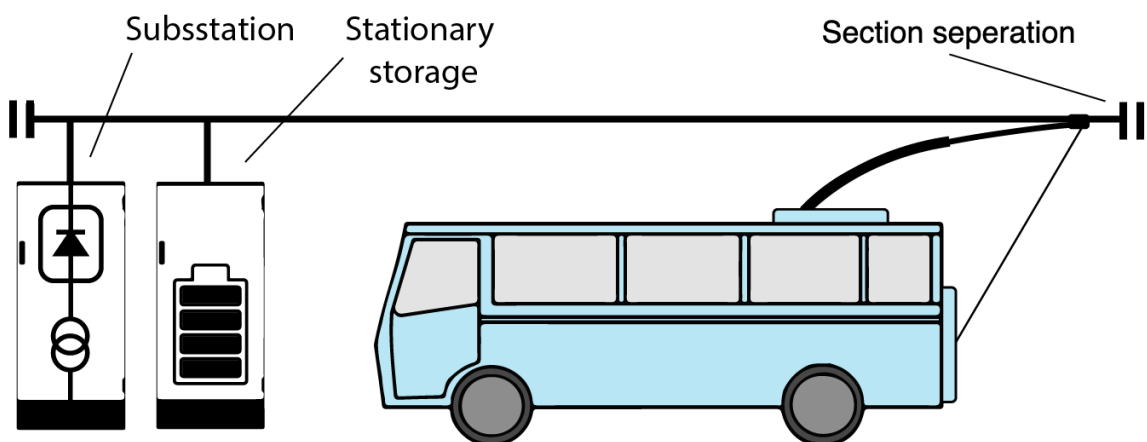


Figure 1.6: Stationary energy storage system



Figure 1.7: Stationary storage in Gdynia [7]

## 1.4. Thesis objective

In section 1.1.5, the main challenges of the trolleybus grid were introduced. For each of these challenges, a stationary storage device could contribute to a solution. One can ask the following questions:

- How far can stationary energy storage systems in trolleybus grids provide a place for excess energy to go to while braking, instead of the braking resistor, and thereby **reducing the power wasted**?
- All energy lost in the catenary wires depends on the magnitude of the current and the distance to the storage device. By how much can low-current charging of an energy storage system along the line **reduce the power lost in catenary wires** and thereby make the complete grid more energy efficient?
- When used for peak shaving, can stationary storage systems provide the power due to the **increased substation capacity demand by implementing services as in-motion charging or EV chargers**?

In order to research the feasibility of stationary storage as a solution to these challenges, respecting the minimum bus voltage  $V_{\min}$ , the maximum section current  $I_{\max}$  and substation capacity  $P_{\max}$ , the research is split up into several research questions. For the research, the Arnhem trolley-grid will be used as a case study. This study can be covered in the first research question:

**RQ1:** *What is the magnitude of transmission losses and braking resistor energy distribution in the Arnhem grid?*

Next, when stationary storage is implemented in order to reduce transmission losses, the location and sizing of these systems are important design parameters, therefore:

**RQ2:** *What location, size and charge scheme of stationary storage allows the least transmission losses?*

Since available regenerative braking energy is converted into heat, a lot of energy is lost. An ESS could be implemented in order to decrease the braking resistor utilisation, therefore;

**RQ3:** *What location, size and charge scheme of stationary storage allows the largest recuperation of regenerative braking energy?*

## 1.5. Contribution

Combining measured velocity and power profiles in ESS simulations can give more realistic insights in the energy flows in a trolley-grid. From these insights, recommendations can be made on the implementation of stationary storage in the Arnhem grid.

## 1.6. Summary of Results

The combination of scheduling and seasonal power profile changes determines the share in excess energy. These factors are found to be not independent. Simulation shows that the transmission losses are nearly constant while using different schedules and (seasonal changing) power profiles. Extending the grid with, for example EV chargers, is limited by some (rare) peaks in substation current demand that go beyond the substation capacity. Using stationary storage only for reduction of transmission losses with the proposed charge schemes is not beneficial due to the small impact on the total energy consumption. When stationary storage is implemented, the best (or least negative) impact on the reduction of the transmission losses is when it is positioned halfway down the line. The section-substation relationship has a negative effect on the reduction of transmission losses using stationary ESS since the proposed charge schemes are not a function of the actual bus location. Placing stationary ESS for the increase of recuperation of braking energy is beneficial. Up to 17% of reduction in substation energy can be achieved in some sections with high braking resistor utilisation. The reduction of total substation energy is related to the amount of excess energy in the section (or connected sections). Implemented storage with a special charge scheme set to maximum recuperation of braking energy gives worse results than with an aggressive charge scheme. Tuning a charge scheme allows for specific applications apart from the maximum recuperation of braking energy. For example increase of the substation power headroom for the application of constant power loads on the trolley-grid like EV chargers or the implementation of in-motion charging busses. A method is presented to determine proper sizing based on the simulation results, not violating any of the SOC limitations of the storage medium.

## 1.7. Project workflow and Report Organization

This thesis is divided in several chapters;

- In chapter 1 the thesis objective is formulated and background is given on trolleybus grids and energy storage systems. The research questions are defined and a methodology is presented.
- In chapter 2, the state of the art is presented based on current literature. In this chapter, information can be found on previous work in charge schemes, storage types for energy storage systems, present work on energy storage systems in trolleybus grids and work performed on future grid demand.
- In chapter 3, the available data set from the Arnhem grid is explored and various assumptions will be made in order to prepare the simulation.
- In chapter 4, the simulation methodology is explained explained by setting up the framework for simulation.
- In chapter 5, the current state of the Arnhem grid will be investigated. A study on braking energy distribution and the magnitude transmission losses in the Arnhem grid will give insights in the present state.
- In chapter 6, the actual implementation of stationary storage solutions is investigated. A recommendation on sizing, location and charge scheme is made based on the simulation results for both reduction in transmission losses and decreased utilisation of the braking resistor. This chapter also involves a study on using stationary storage for substation peak demand reduction.
- Chapter 7 concludes the work performed in chapter 4-6 and gives clear recommendations on the implementation of stationary storage in the Arnhem grid.

## 1.8. Conclusion

In this chapter, an introduction to trolleybuses and the trolley-grid is presented. The research questions are defined in order to determine if stationary storage can decrease the transmission losses, reduce the utilization of the braking resistor and increase substation capacity for auxiliary services that can be fed from the trolley-grid. In the next chapter, a literature study will present the state of the art on storage in urban transportation, multiple storage technologies and their properties and define the research gap.

# 2

## Literature Review

*In this chapter the state of the art on the implementation of storage in urban transportation systems and the research gap will be discussed.*

Stationary storage systems are not unknown in the transport industry. Many work is already performed on the design, integration and evaluation of regenerative braking recovery systems for metros, trains and EVs [2]. For this thesis, topics to investigate are; bus modelling, storage types, ESS charge schemes and the specific implementation in a trolleybus grid. Some performed work will be discussed.

### 2.1. Bus simulation

Various methods for simulating the bus behaviour have been discussed in literature, mainly focusing on the simulation of velocity profiles and corresponding power profiles. [10] [30] [20] [26] These methods include a simplification of the trolleybus behaviour, splitting up the modes of operation in four classes:

- I Acceleration
- II Constant speed
- III Coasting
- IV Braking

Figure 2.1.a shows a simplified velocity profile for both a rail traction vehicle and a trolleybus. Comparing these profiles shows that the velocity profile of a trolleybus is more dynamic than that of a rail traction vehicle. This dynamic behaviour originates from the traffic dependence of a trolleybus, whereas it has to interact with other traffic, traffic lights and crossings.

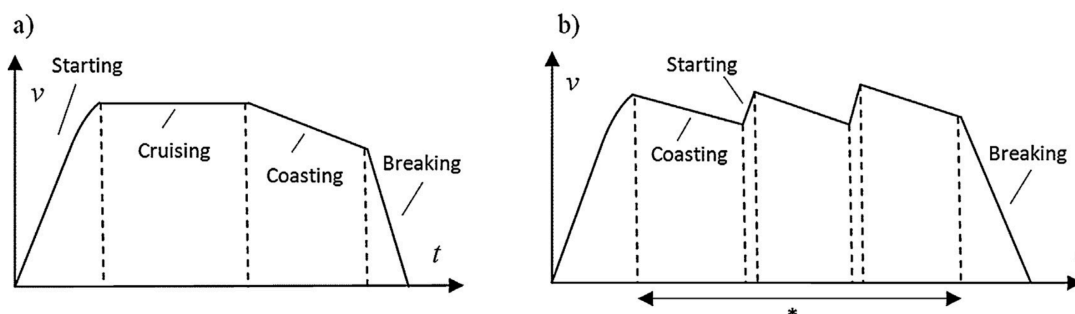


Figure 2.1: A typical ride cycle of: (a) rail traction vehicle; (b) trolleybus (\* ride with quasi constant speed),  $t$  – time,  $v$  – velocity [3]

Due to the unpredictable nature of the trolleybus behaviour, Hamacek *et al.* [3] presented work on behavioural analysis using Monte Carlo simulation. The goal of their work is to increase the extend of regenerative braking by using super-capacitor storage or a change in the topology of the power supply system. The Monte Carlo simulation is used to randomly initialise the system during simulation. For that, some driving behaviour models are used. Figure 2.1.b shows the model used for a typical ride cycle of a trolleybus.

## 2.2. Storage type

Sauer *et al.* [29] present a detailed comparison on wayside energy recovery storage types in urban railway systems. Super-capacitors [18] [21] [27], flywheels, battery storage systems [31] [47] and inverters are compared. This work shows operating ranges of these storage types, as well as their power and energy density. While the papers is based on railway systems, the various storage type parameters can be used in selecting and dimensioning of the storage system in this thesis. Figure 2.2 shows a visual representation of some storage types and their available parameters (Power density / Energy density).

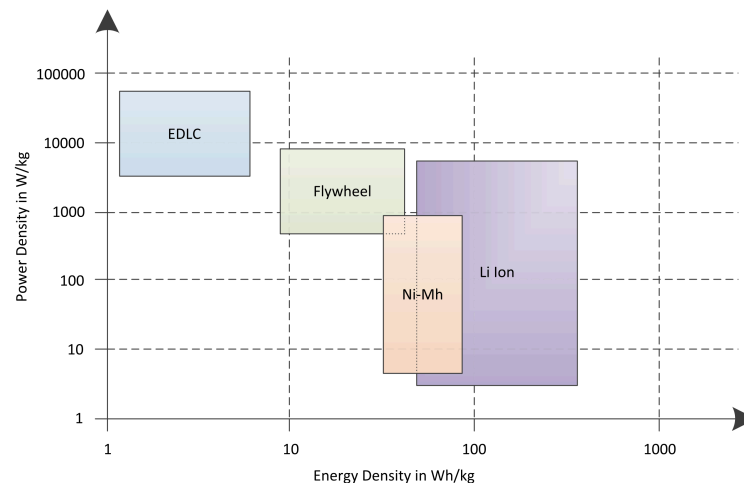


Figure 2.2: Visual representation of storage type parameters [29]

The application of battery technology in electric vehicles has been researched in extend. [22] [47]. The Li-ion technology is also deployed broadly in EVs and various research has been performed on the aging and cycle life of this technology. [32] [12] [11]. These state-of-the-art batteries are known for their high energy density and power density. In some real high-power applications, the ELDC is a better solution, since it has even higher power ratings than batteries.

Hybrid storage combines battery and super-capacitor technology into one solution. These systems are capable of delivering both high energy density with the use of batteries, and high power density with the implemented super-capacitors. Many work has been performed on the implementation of on-board hybrid storage systems, but not for stationary storage. [44] [23] [42] [14] [39]

Sizing of on-board hybrid solutions has been researched in extend in [37], [35] and [36], but not a lot of research has been performed on the sizing of stationary storage. In [3], a suggestion on sizing is made upon the simulation of an existing trolley grid, but no measurement data is used in this case study.

## 2.3. Charge scheme

Rufer *et al.* presented work in the implementation of a super-capacitor based storage system at the end of a trolleybus-line in the city of Lausanne, Switzerland. [27] In this work, the storage is placed

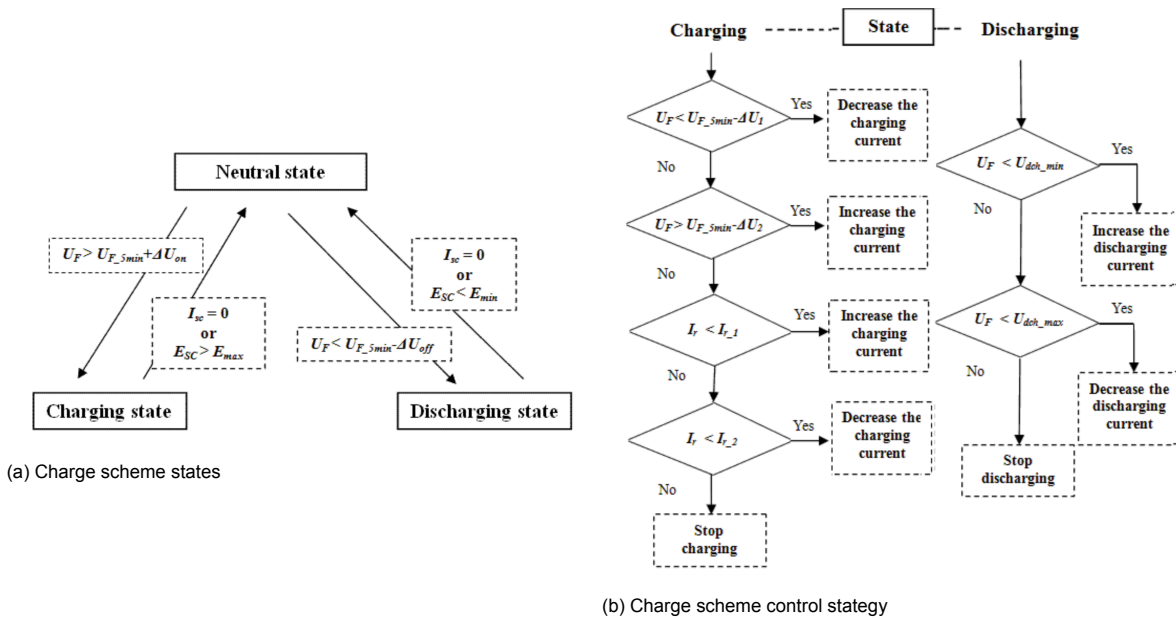


Figure 2.3: Charge scheme details [8]

stationary at the end of line, in order to reduce transmission losses and increase the utilisation of regenerative braking energy. A comparison is made between building a new substation, or the usage of the SC-storage. A detailed control scheme to charge and discharge the ESS is presented in their work. The super-capacitor ESS is build up out of 2 DC/DC converters, with an intermediate DC bus between them. The proposed control scheme is therefore build based on this topology, and may be to specific to use in the work in this thesis. The paper concludes with a recommendation for SC-ESS.

Shiokawa *et al.* [40] propose a charge scheme model for stationary energy storage systems in train grids. In their work, an optimisation is performed on this model, using a grid simulator in order to measure the efficiency of the scheme. This model and method of optimising can be used on trolleybus grids, and is based on voltage control.

In M. Barłomiejczyk's work [7] [8], a review is performed of the analysis of a super-capacitor energy storage system in the city of Gdynia. A charge scheme is introduced based on the voltage level of the bus and the rectifier load current. A distinction is made between small and big rectifier currents when controlling the ESS charging. During small currents through the rectifier ( $\leq 69$  A), the charging is stopped so that the super-capacitor bank is only charged when regenerated energy is delivered from the bus. In order to prevent oscillations to occur, states were introduced. Figures 2.3a and 2.3b show the introduced states and corresponding decision diagrams.

## 2.4. Storage in trolleybus grids

Regenerative braking is one of the main reasons behind the high levels of energy efficiency achieved in railway electric traction systems. [17] This work can be extended to trolleybus grids. Although they are often the subject of studies [25] [15] [16] [43] [3], these studies are usually limited to the accumulation of electricity in the storage devices alone. There is no literature on the methods of increasing the scale of recuperation energy re-use from the global perspective, i.e. with regard to re-using such energy by auxiliaries and other electrical vehicles. [19]

Papanikolaou *et al.* [2] created a model for a trolleybus, and proposed the implementation of an energy storage system. This work includes a extensive model of the supply grid, inverter and synchronous motor. Also, the in-traffic behaviour of the bus is modeled, including traffic density and the amount of passengers using the bus. Combining these models results in a consumption estimation.

These consumption results are used in the analysis of the efficiency increase by implementing a storage system for energy recovery. The analysis results in a potential energy saving of 24%. Important to note is that the simulation is performed in Athens, Greece, and the geographical data is included as well. The potential energy in a bus is also depending on the bus altitude, and therefore the energy savings can be lower when the system is applied in a area without hills. Also, line losses are not modeled in the regenerative braking system, and may be different when stationary storage is applied.

Polom *et al.* [9] analyse the transmission losses in overhead lines, and the potential of recuperated energy recovery in trolleybus grids. The measurements and simulation of the grid shows a strong relationship in the spatial structure of the supply grid and traffic intensity and the effective use of regenerated energy. The paper suggests the use of bilateral connections and a decentralised overhead line power supply system. The papers concludes that power flowing from vehicle to vehicle is the cheapest and most effective way to use the regenerated energy in these grids. In the context of this work one can use the results of the bilateral connections simulation, and consider what could be the impact of these connections when stationary storage is implemented.

Ratniyomchai *et al.* [34] propose a optimisation problem for optimal sizing and positioning of super-capacitor storage in light rail vehicle system. The work consists out of a grid model and simulation of one train. The paper concludes that with introduction of super-capacitors the energy consumption can be decreased by 65%, and energy losses can be reduced by 70%. Important to mention is that this work is performed on light-rail vehicle systems, and these numbers may not apply to trolleybus systems. Also, the work is performed on a one train simulator and the storage analyses is limited to the use of super-capacitors.

In the work of Stana *et al.* [41], an analysis is performed on all the possible scenarios for power interaction between two busses. The goal of this work is to investigate if on-board or off-board storage have any potential, when considering the transmission losses in the catenary. Also, the losses that are introduced by the bus-bar when a power flow passes through a substation have been modelled. This work shows the potential of implementing storage over the line, but is mainly focused on the power flow between two busses and provides detailed loss models.

## 2.5. Trolleybus grid capacity increase

Bartlomiejczyk [6] discusses the implementation of in-motion-charging (IMC) in trolleybus grids. The impact on the collector is investigated and limits are described on the operation (charging powers during acceleration, cruising and stopping) and an analyses is performed on the possibility of catenary-free operation. The paper concludes that is is only necessary to electrify 33%-50% of the grid. This can be used to extend lines of existing grids, and opens the opportunity to create routes trough historical city centres without the need of installing unwanted catenary. More research on autonomous driving has been performed in [5], showing an analysis of the electrification of one specific line. In this work, the sizing and type of storage are interesting.

Iannuzzi *et al.* [24] performed work on simulating a energy storage system together with a dc-dc converter to boost the line voltage in old tramways. Sizing of this storage is performed by optimisation. The solution reduces the substation current peaks while minimising the investment costs. Numerical simulations have been performed on an tramway in the city of Naples. Also, for this paper, it is performed on tramways, which does not take the trolleybus behaviour into account.

In [26] Iannuzzi *et al.* show that, using a simple velocity profile and a non probabilistic traffic approach, a suggestion can be made on the most efficient location to place stationary storage. This study shows that the result of the optimisation is heavily dependent on the assigned weights of the objective function, and thus on may not be applicable for the trolley-grid.

## 2.6. Research Gab

Based on literature, research has been performed on the implementation of stationary storage, using trapezoidal velocity profiles. This simplification is expected to have a significant effect on the stationary

storage location and sizing recommendations. Combining measured velocity and power profiles in ESS simulations can give more realistic insights in the energy flows in a trolley-grid. From these insights, better recommendations could be made on the implementation of stationary storage. Performed work show that the combination of charge-scheme optimisation and location dependence is not investigated yet, and can be researched in this thesis. Also, from the results of this thesis, the energy and power demand profiles of stationary storage can be determined. These profiles can be used to find a suitable storage technology for the application in the stationary storage. Also, combining seasonal changes in power-profiles and scheduling, placing storage at different positions on a section and simulating the full grid for a complete day gives results to be used for sizing storage.

## **2.7. Conclusions**

In this chapter, the state of the art is discussed. Research has been performed on stationary storage using trapezoidal velocity profiles as input. Using actual measurement data, seasonal changes in power profiles and scheduling and full grid analysis in simulations is found to be not researched yet, and will therefore be the research gap for this thesis. In the next chapter, the measurement data to be used in the simulations from the Arnhem grid will be introduced.



# 3

## Dataset exploration

*In this chapter, the available data-set of the Arnhem grid will be explored. The data contains bus velocity and power profiles, as well as layout of the grid components. Also in this chapter some of these measurements will be validated based on expected results from literature.*

The simulations in this work are done based on the Arnhem trolley-grid. From this grid, multiple data is available to be used as an input for the simulation framework to be implemented. There is also data available which can be used to validate the outcome of the simulations. The layout is available for the different sections and substations, position and power profiles are available for the busses, scheduling data is available for the bus schedules and energy measurements from the grid's substations are provided.

### 3.1. Grid layout

The Arnhem grid is build up out of multiple sections of overhead lines. These sections are connected to substations from where the energy is being fed. A section can be connected to another section (end-to-end) via a bilateral connection. These bilateral connections can either be open or closed. In closed position, energy can flow from one section to another. This enables energy sharing between busses from different sections. The goal of these bilateral connections is to provide a more robust grid, sections which are used intensively can be helped by other sections, and thus reduce large voltage deviations and transmission losses. In this work, the implementation of bilateral connections is omitted.

#### 3.1.1. Sections

Figure 3.1 shows the section overview of the Arnhem grid. The different colors on this map shows which sections are fed by the same rectifier. The boxes containing letters indicate section to section crossings. Orange boxes indicate bilateral connections, meaning these sections can be connected to each other. The other boxes indicate isolated section to section connections. The dots on the map indicate section feeding points. This is the location where the feeder cable between the rectifier in the substation and the section are connected. The feeder cables have a resistive character, and their lengths are known, but the losses in these cables are omitted in this work.



Figure 3.1: Map of the Arnhem trolley-grid showing sections and substations.

### 3.1.2. Forked section simplification

The grid model that is going to be used in the simulations only accepts one-dimensional section layouts. In the real world, not all sections have this one-dimensional layout. Figure 3.2 shows an example of such a section. In this case, section 12 of the Arnhem grid has a split in the middle of the section, resulting in a multi-dimensional layout. Since the grid model to be used does not accept this layout as an input, these sections will be simplified into one-dimensional layouts. This simplification will mainly have an effect on the transmission losses, whereas the actual transmission losses would be lower when the multi-dimensional problem could be solved.

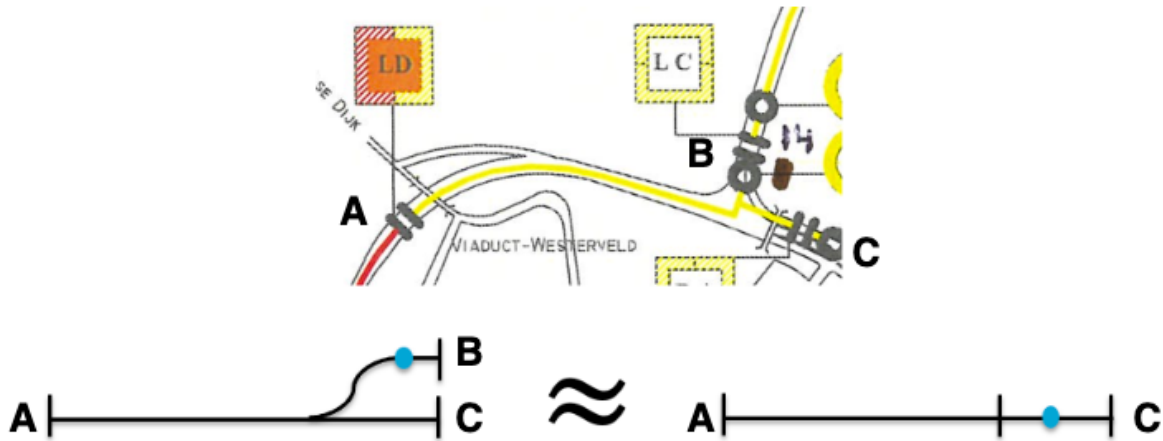


Figure 3.2: Example of implemented section simplification

### 3.1.3. Substations

Every section is fed from a diode rectifier, which is located in a substation. Sections fed from the same rectifier are connected to each other through the busbar that is in the substation. This connection enables the so called section-substation relationship, where sections are able to share energy with other sections connected to the same busbar. For example, when a bus is braking in section 24, and a bus is accelerating in section 23, the regenerative energy from the bus in section 24 is able to flow to the bus in section 23 as can be seen in figure 3.3. Multiple sections connected to a rectifier is considered to be a substation, but multiple rectifiers can be in at the same substation location. Therefore a distinction is made between substation and substation location. Table 3.1 shows an overview of substation locations and connected substations.

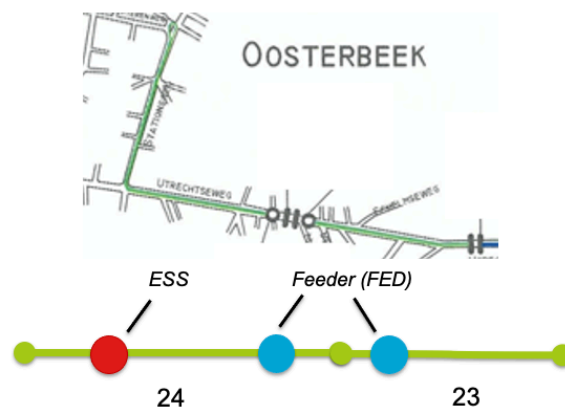


Figure 3.3: Section-substation relationship of substation 1, connecting sections 23 and 24

Table 3.1: Substation locations

| Location | Connected substation |
|----------|----------------------|
| 1        | 7                    |
| 2        | 5                    |
| 3        | 14                   |
| 4        | 4, 32, 9             |
| 5        | 15                   |
| 6        | 17                   |
| 7        | 13                   |
| 8        | 7                    |
| 9        | 2                    |
| 10       | 3, 6                 |
| 11       | 12                   |
| 12       | 10                   |
| 13       | 11                   |
| 14       | 1                    |
| 15       | 16                   |
| 16       | 19                   |
| 17       | 18                   |
| 18       | 20                   |

## 3.2. Measurements

For all six trolley lines in the Arnhem grid, two measurements of one run in every direction are available. The two measurements are the minimal, and maximal measurements on the day of measuring. From these two measurements, a velocity profile and power profile have been recorded. In this work, the max profiles will be used as the input for simulation, to be sure that sizing the results are over-estimated instead of under-estimated, resulting in energy dumped in to the braking resistor.

## 3.3. Velocity profiles

Figure 3.4 shows an example bus velocity profile for one line. The data is recorded from the moment of departure from the start of the line, to the moment that the bus is at the end of the line. For some lines, a bus is at a standstill for a long time at one specific station. In figure 3.4 such a stop can be observed around 05:18. Every bus velocity sample recording has a corresponding timestamp which can be used when the data has to be re-sampled for simulation.

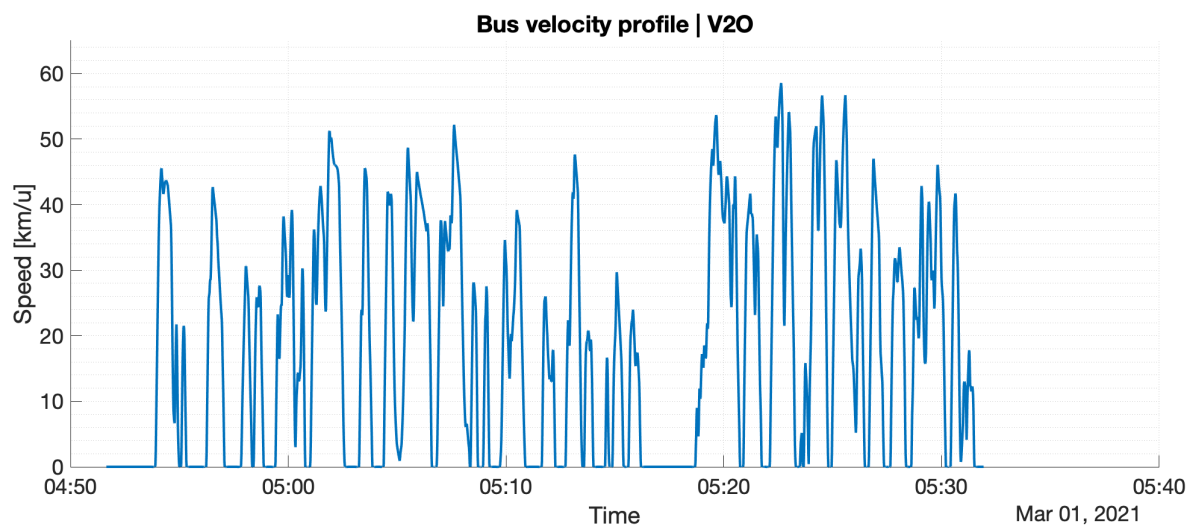


Figure 3.4: Example bus velocity profile line 1: Velp to Oosterbeek from HAN measurement

### 3.4. Power Profiles

Figure 3.5 shows an example bus power profile for one run. The data is recorded from the moment of departure from the start of the line, to the moment that the bus is at the end of the line. Every bus power sample recording has a corresponding timestamp which can be used when the data has to be re-sampled for simulation.

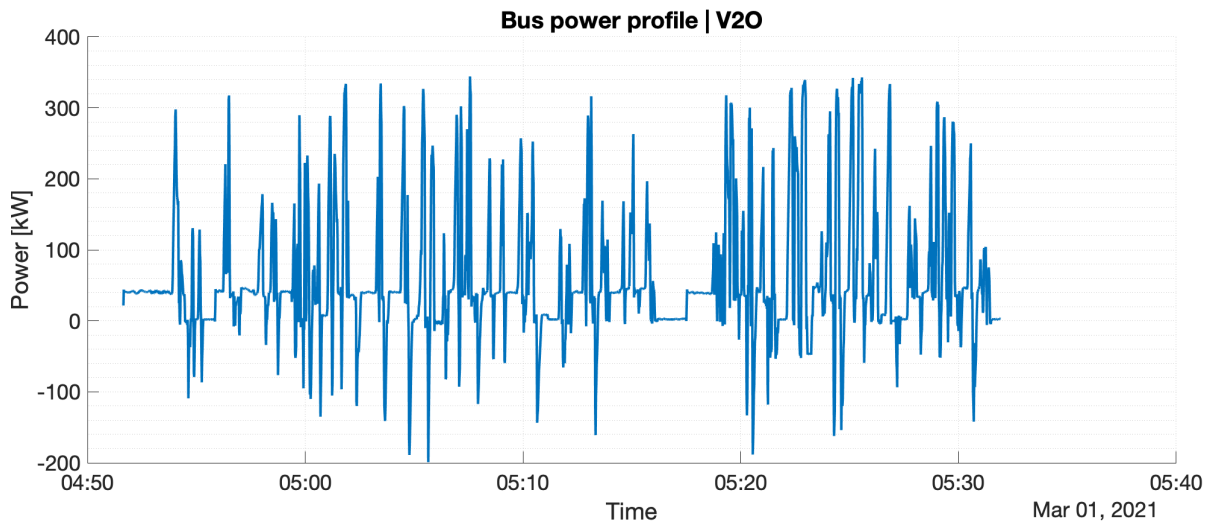


Figure 3.5: Example bus power profile line 1: Velp to Oosterbeek from HAN measurement

### 3.5. Bus lines & scheduling

The Arnhem trolley-grid consists out of six different sequences of stops called lines. Every line can be followed in both directions. Table 3.2 shows the six lines in both direction, their start location, end location and unique identifier used in the simulating framework. Not in all cases the busses move from the line startpoint to the line endpoint, in some cases (mainly during the beginning and ending of the day schedule) busses can depart from locations halfway down the line. For example, busses entering line 1 for the first time on a day, start from Central Station (CS) and not from Oosterbeek or Velp. Since this only holds for a small fraction of busses in a day, this phenomena will be ignored in the simulations. Busses only start and end on the stated start and end locations.

Table 3.2: Overview of Arnhem trolley-lines

| Identifier | Line | Start           | End             |
|------------|------|-----------------|-----------------|
| 1_O2V      | 1    | Oosterbeek      | Velp            |
| 1_V2O      | 1    | Velp            | Oosterbeek      |
| 2_AC2ZL    | 2    | Arnhem Centraal | Zuid-Laren      |
| 2_ZL2AC    | 2    | Zuid-Laren      | Arnhem Centraal |
| 3_BZ2D     | 3    | Burgers' Zoo    | Duifje          |
| 3_D2BZ     | 3    | Duifje          | Burgers' Zoo    |
| 5_PR2SC    | 5    | Presikchaaf     | Schuyfgraaf     |
| 5_SC2PR    | 5    | Schuyfgraaf     | Presikchaaf     |
| 6_DL2EZ    | 6    | De Laar West    | Elsweide        |
| 6_EZ2DL    | 6    | Elsweide        | De Laar West    |
| 7_GK2RW    | 7    | Rijkerswoerd    | Geitenkamp      |
| 7_GK2RW    | 7    | Geitenkamp      | Rijkerswoerd    |

The busses move along these defined lines at scheduled times. The schedule [13] varies over the day in the week and the time of the year to compensate for the change in bus transport demand. In one week, a distinction can be made in the regular workday schedule (Mon-Fri), the Saturday schedule

and the Sunday schedule. Also, throughout the year the actual departure times of busses changes, in summertime, when less bus transport demand is needed, less busses are scheduled.

### 3.5.1. Scenario distribution

As described in section 3.5, different schedules are active throughout the year. For some special holidays in the year, the Sunday schedule is applied (for example on Christmas). In this work, some annual calculations will be performed. For these calculations, the yearly occurrence of the different schedules is used. Table 3.3 shows for every schedule the amount of days it will be active in a year to be used in the annual calculations.

Table 3.3: Arnhem annual schedule distribution

| Schedule        | Season | Occurrence |
|-----------------|--------|------------|
| Regular workday | Winter | 196        |
| Saturday        | Winter | 45         |
| Sun/Holiday     | Winter | 50         |
| Regular workday | Summer | 60         |
| Saturday        | Summer | 7          |
| Sunday          | Summer | 7          |

## 3.6. Energy measurements

For every substation location, measurements of the annual energy consumption are available. These measurements can be used to validate the simulation framework from a substation energy perspective. Figure 3.6 shows the annual energy consumption distribution between the different substation locations. Note that these are the locations as defined in section 3.1.3, and not the actual substations. From this figure one can see that some locations consume a lot more energy than others. This difference may originate from the feeding sections and substations, whereas some locations feed sections that have a higher traffic density than others.

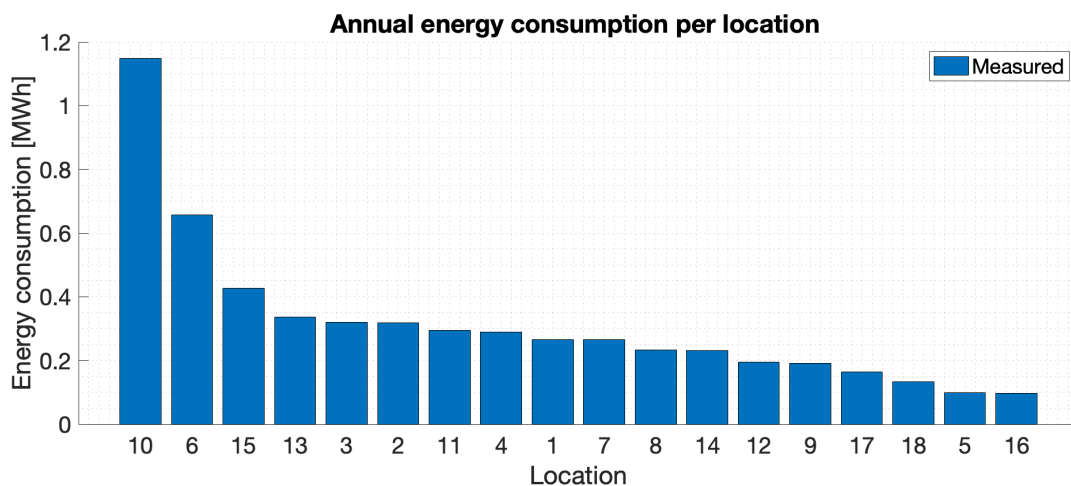


Figure 3.6: Measured substation location energy profiles

## 3.7. Validation

### 3.7.1. Position profile validation

The position profile used during simulation is deducted from the measured bus velocity profile. The total line length is defined as the total distance from the line start point to the line end point. In order to validate the position profiles, one can compare the integrated velocity profiles with measured section lengths combined with the sections included in a line. Table 3.5 shows the difference between the integrated velocity profiles and the sum of section lengths.

Table 3.4: Analysis of integrated velocity profiles vs measured section lengths

| Line    | $x_{data}$ [km] | $\Sigma x_{section}$ [km] | $\Delta x$ [km] | $\Delta$ [%] |
|---------|-----------------|---------------------------|-----------------|--------------|
| 1_O2V   | 11.60           | 11.66                     | 0.06            | 0.55         |
| 1_V2O   | 11.54           | 11.65                     | 0.11            | 0.97         |
| 2_AC2ZL | 8.49            | 8.44                      | -0.05           | -0.64        |
| 2_ZL2AC | 8.30            | 8.51                      | 0.21            | 2.52         |
| 3_BZ2D  | 10.47           | 10.59                     | 0.13            | 1.23         |
| 3_D2BZ  | 9.98            | 10.74                     | 0.76            | 7.63         |
| 5_PR2SC | 15.14           | 14.06                     | -1.08           | -7.16        |
| 5_SC2PR | 14.32           | 15.37                     | 1.05            | 7.31         |
| 6_DL2EZ | 11.92           | 12.27                     | 0.36            | 3.00         |
| 6_EZ2DL | 11.89           | 12.10                     | 0.21            | 1.77         |
| 7_GK2RW | 12.42           | 12.65                     | 0.23            | 1.86         |
| 7_RW2GK | 12.71           | 12.72                     | 0.00            | 0.02         |

From table 3.5 one can deduct that the maximum difference between the measured and integrated distance is around 8%, but most of the line lengths differences are around 1%. The line with the biggest deviation, line 5, is different from the other lines, due to the actual route. The busses on this line can follow multiple routes on this line, but not all of these routes are available at the moment of writing. One important thing to mention is that these differences are mainly in the tails of the route, where less interaction with other busses is expected. Therefore, the influence of the difference in line lengths will not influence the results on the more busy and interactive sections, and can be neglected.

### 3.7.2. Bus energy validation

The power profiles from the measurements can be validated by checking if the total energy consumed per kilometer in a measurement is in line with the expected energy consumption of a trolleybus. The energy consumption of a trolleybus varies between 1.8-2.8 kWh/km as described in literature [5]. The average energy consumption of the measured profiles can be determined by integrating over the power profiles and dividing this energy over the total line length. The average consumption is based only on positive power values (consumption), thereby neglecting the negative power available (regeneration). Equation 3.1 shows how the average energy consumption is calculated from the power profiles.

$$E_{avg} = \frac{\int_{t=0}^{t=t_{max}} P(P > 0, t) dt}{\int_{t=0}^{t=t_{max}} v(t) dt} \left[ \frac{\text{kWh}}{\text{km}} \right] \quad (3.1)$$

Table 3.5: Analysis of energy consumption per kilometer based on measured power profiles

| Line           | $\int P(P > 0)$ [kWh] | $x_{line}$ [km] | $E_{avg}$ [kWh/km] |
|----------------|-----------------------|-----------------|--------------------|
| 1_O2V          | 40.00                 | 11.60           | 3.45               |
| 1_V2O          | 40.96                 | 11.54           | 3.55               |
| 2_AC2ZL        | 25.37                 | 8.49            | 2.99               |
| 2_ZL2AC        | 25.41                 | 8.30            | 3.06               |
| 3_BZ2D         | 25.61                 | 10.47           | 2.45               |
| 3_D2BZ         | 34.93                 | 9.98            | 3.50               |
| 5_PR2SC        | 45.76                 | 15.14           | 3.02               |
| 5_SC2PR        | 39.29                 | 14.32           | 2.74               |
| 6_DL2EZ        | 36.74                 | 11.92           | 3.08               |
| 6_EZ2DL        | 33.33                 | 11.89           | 2.80               |
| 7_GK2RW        | 35.91                 | 12.42           | 2.89               |
| 7_RW2GK        | 43.14                 | 12.71           | 3.39               |
| <b>Average</b> |                       |                 | 3.39               |

From Table 3.5 one can find an average energy consumption of 3.39 kWh/km, this value is above the expected 1.8-2.8 kWh/km. This difference is related to the implemented HVAC system in the bus, which can cause a higher energy consumption. The measurements were sampled in January, where the HVAC system is responsible for heating the bus. In order to validate the energy consumption, one should consider the actual traction power instead of the total power consumed by the bus. The measurement data includes a profile for the HVAC power, which can be used to determine the actual traction power. Table 3.6 shows the results of the same analysis, but now only considering the traction power.

Table 3.6: Analysis of energy consumption per kilometer using only bus traction power

| Line           | $\int P_{tr}(P_{tr} > 0)$ [kWh] | $x_{line}$ [km] | $E_{avg}$ [kWh/km] |
|----------------|---------------------------------|-----------------|--------------------|
| 1_O2V          | 24.19                           | 11.60           | 2.09               |
| 1_V2O          | 25.60                           | 11.54           | 2.22               |
| 2_AC2ZL        | 16.26                           | 8.49            | 1.91               |
| 2_ZL2AC        | 13.70                           | 8.30            | 1.65               |
| 3_BZ2D         | 14.75                           | 10.47           | 1.41               |
| 3_D2BZ         | 20.47                           | 9.98            | 2.05               |
| 5_PR2SC        | 26.31                           | 15.14           | 1.74               |
| 5_SC2PR        | 22.67                           | 14.32           | 1.58               |
| 6_DL2EZ        | 25.90                           | 11.92           | 2.17               |
| 6_EZ2DL        | 17.90                           | 11.89           | 1.51               |
| 7_GK2RW        | 18.88                           | 12.42           | 1.52               |
| 7_RW2GK        | 27.75                           | 12.71           | 2.18               |
| <b>Average</b> |                                 |                 | 2.18               |

Table 3.6 shows that, when considering only traction power, the average energy consumption per kilometer is in line with the expected 1.8-2.8 kWh/km and thereby validating the power profiles.

## 3.8. Regenerative braking energy analysis

### 3.8.1. Recuperation power ratio

An indication of the available recuperation power can be given as the ratio between the bus energy demand  $E_{dem}$  and the available recuperation power  $E_{rec}$ . Equation 3.2 shows how the energy demand can be determined by integrating over the positive values of the bus power profile. Equation 3.3 shows how the available recuperated energy can be determined by integrating over the negative values of the total bus power profile. Table 3.7 shows the calculation of these energies and the ratio between them. The average available regenerative power is 10.11%. In this analysis, the total bus demand is considered, including HVAC.

$$E_{dem} = \int_{t=0}^{t=t_{max}} P(P > 0, t) dt \text{ [kWh]} \quad (3.2)$$

$$E_{rec} = \int_{t=0}^{t=t_{max}} P(P < 0, t) dt \text{ [kWh]} \quad (3.3)$$

Table 3.7: Analysis of available regenerative energy per line measurement

| Line           | $E_{dem}$ [kWh] | $E_{rec}$ [kWh] | Ratio [%] |
|----------------|-----------------|-----------------|-----------|
| 1_O2V_min      | 28.95           | 4.62            | 15.97     |
| 1_O2V_max      | 39.99           | 5.62            | 14.04     |
| 1_V2O_min      | 29.21           | 2.32            | 7.95      |
| 1_V2O_max      | 40.95           | 4.08            | 9.96      |
| 2_AC2ZL_min    | 18.01           | 1.67            | 9.30      |
| 2_AC2ZL_max    | 25.36           | 3.86            | 15.22     |
| 2_ZL2AC_min    | 18.05           | 1.16            | 6.45      |
| 2_ZL2AC_max    | 25.41           | 1.54            | 6.06      |
| 3_BZ2D_min     | 20.98           | 2.30            | 10.96     |
| 3_BZ2D_max     | 25.60           | 0.10            | 0.37      |
| 3_D2BZ_min     | 26.87           | 2.87            | 10.68     |
| 3_D2BZ_max     | 34.93           | 3.55            | 10.15     |
| 5_PR2SC_min    | 27.01           | 1.32            | 4.90      |
| 5_PR2SC_max    | 45.75           | 4.91            | 10.72     |
| 5_SC2PR_min    | 27.30           | 3.12            | 11.43     |
| 5_SC2PR_max    | 39.29           | 3.79            | 9.64      |
| 6_DL2EZ_min    | 30.37           | 4.23            | 13.92     |
| 6_DL2EZ_max    | 36.73           | 6.50            | 17.69     |
| 6_EZ2DL_min    | 28.20           | 1.89            | 6.69      |
| 6_EZ2DL_max    | 33.32           | 3.48            | 10.46     |
| 7_GK2RW_min    | 27.66           | 2.53            | 9.15      |
| 7_GK2RW_max    | 35.91           | 4.16            | 11.58     |
| 7_RW2GK_min    | 36.30           | 3.10            | 8.53      |
| 7_RW2GK_max    | 43.14           | 4.71            | 10.92     |
| <b>Average</b> |                 |                 | 10.11     |

### 3.8.2. Potential regenerative energy

The same process as in 3.7.1 can be applied to the negative power values, in order to indicate the potential regenerative energy available. Equation 3.4 is used to determine this potential regenerative energy. Table 3.8 shows the results of this analysis. The average available regenerative braking energy is 0.66 kWh/km.

$$E_{avg} = \frac{\int_{t=0}^{t=t_{max}} P(P < 0, t) dt}{\int_{t=0}^{t=t_{max}} v(t) dt} \left[ \frac{kWh}{km} \right] \quad (3.4)$$

Table 3.8: Analysis of available regenerated energy per kilometer

| Line           | $\int P_{tr}(P_{tr} > 0)$ [kWh] | $x_{line}$ [km] | $E_{avg}$ [kWh/km] |
|----------------|---------------------------------|-----------------|--------------------|
| 1_O2V          | 9.73                            | 11.60           | 0.84               |
| 1_V2O          | 7.57                            | 11.54           | 0.66               |
| 2_AC2ZL        | 6.27                            | 8.49            | 0.74               |
| 2_ZL2AC        | 4.17                            | 8.30            | 0.50               |
| 3_BZ2D         | 2.91                            | 10.47           | 0.28               |
| 3_D2BZ         | 6.67                            | 9.98            | 0.67               |
| 5_PR2SC        | 8.61                            | 15.14           | 0.57               |
| 5_SC2PR        | 7.96                            | 14.32           | 0.56               |
| 6_DL2EZ        | 9.99                            | 11.92           | 0.84               |
| 6_EZ2DL        | 6.01                            | 11.89           | 0.51               |
| 7_GK2RW        | 7.98                            | 12.42           | 0.64               |
| 7_RW2GK        | 8.39                            | 12.71           | 0.66               |
| <b>Average</b> |                                 |                 | 0.66               |

### **3.9. Conclusions**

In this chapter, the data-set to be used in the simulation framework is explored and validated. The outcomes of the validation shows that the measurement data is usable as an input for the simulations. In the next chapter, the simulation framework will be discussed, of which the measurements discussed in this chapter will be used as inputs.

# 4

## Simulation methodology

Using the data-set as discussed in chapter 3 and the knowledge on the operation of a trolley-grid from chapter 1, the actual simulation framework can be built. This chapter will discuss the design, different components and operation of the simulation framework.

In order to investigate the potential of the implementation of storage systems, simulations will be performed on a model of the Arnhem grid. This chapter describes the method of simulation, formatting of the input variables, running the simulation and defining the simulation outputs. Figure 4.1 shows an overview of the complete simulation framework.

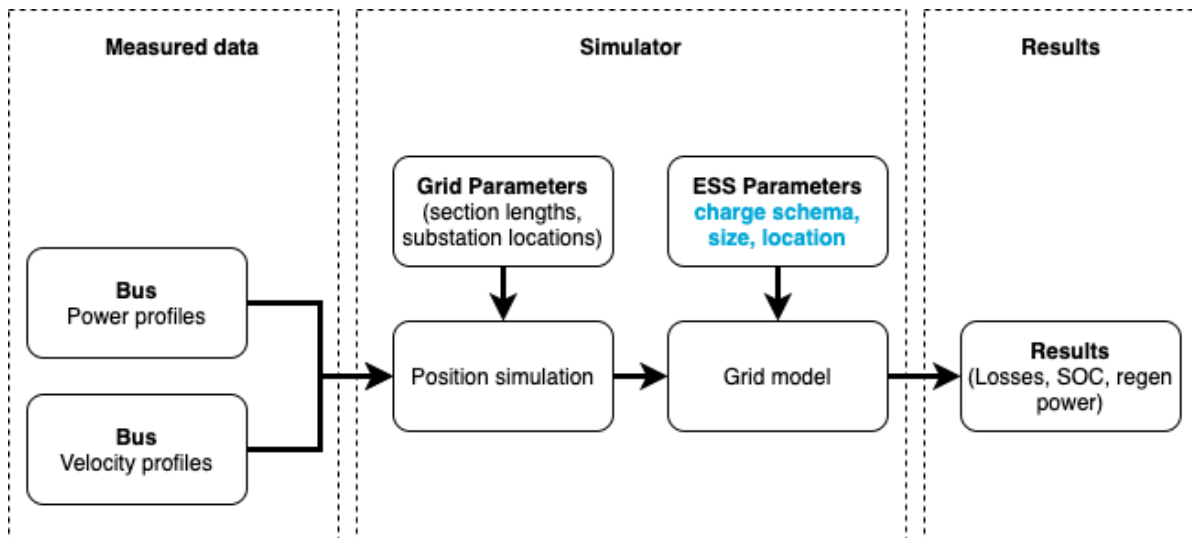


Figure 4.1: Overview of simulation framework

### 4.1. Position simulation

The bus velocity profiles for each line are available in the measured data. Using equation 4.1 the position of a bus on a line  $x(t)$  can be determined. Figure 4.2 shows an example of the measured velocity profile, and the integrated position profile.

$$x_{\text{bus}(t)} = \int_{t=0}^{t=t_{\text{max}}} v_{\text{bus}(t)} dt \quad (4.1)$$

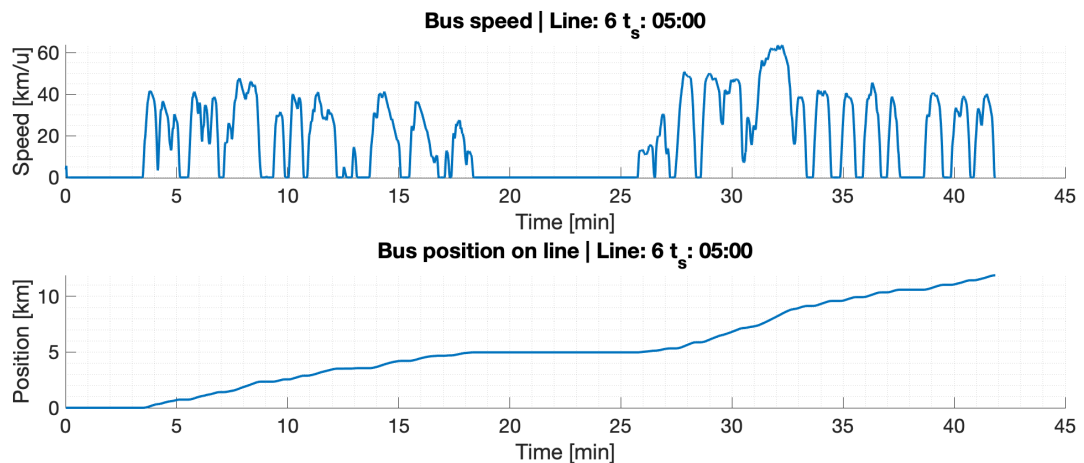


Figure 4.2: Example of bus velocity and position profile

A bus run on a line consists out of a sequence of (directional) sections. Combining the bus position profiles with the available data on section lengths and directions, the exact location of a bus on a section at time  $t$  can be determined. Figure 4.3 shows an example output of the bus position on a section, and the current section over time. Note that, based on the direction of the bus, the position on a section can start at a high high value and decrease while running.

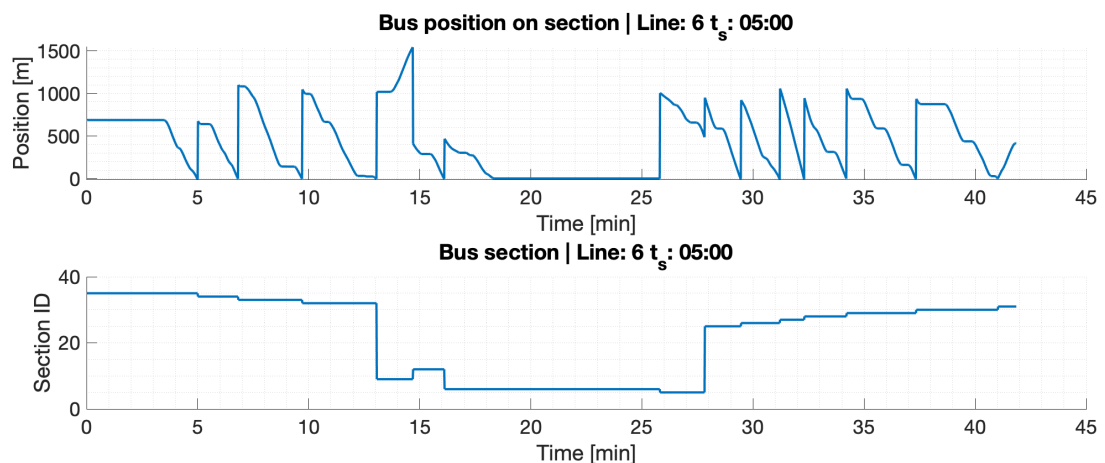


Figure 4.3: Example of bus position on section and section profile

From these profiles, the simulator is able to determine the bus location, section and exact position on the section for every time instance  $t$ .

## 4.2. Simulation scenarios

In order to simulate the seasonal impact on the operation of the trolley-grid, multiple scenarios are formulated. There are two important factors determining the seasonal change:

- **Scheduling:** As described in section 3, the Arnhem grid operates in different schedules. There is a regular schedule and a summer schedule, each having different timetables for regular work-days, Saturdays and Sun-/Holidays. This change in timetable has an impact on the number of busses driving simultaneously, and therefore might have a significant impact on the shared energy between busses.
- **Power profiles:** The bus power profiles are heavily depending on the HVAC operation. While heating, the HVAC can consume nearly 40 kW. Since the measured data is measured on a day in

winter, these profiles clearly show an power plateau during heating. Figure 4.4 shows an example of this plateau. A method will be discussed on how to remove the HVAC impact on the profiles, and generate a summer profile from a filtered version of the measurements. These generated profiles can be used during simulation in summertime.

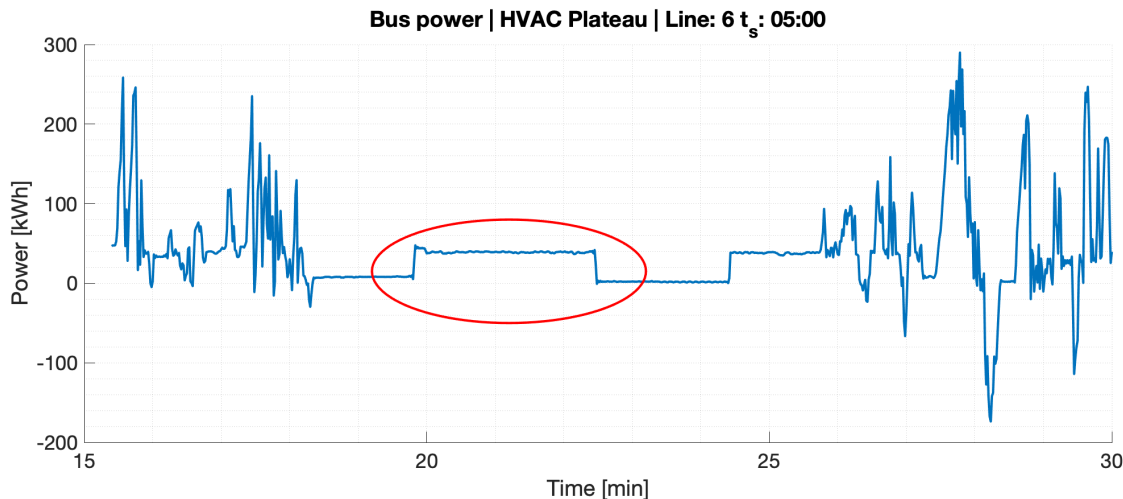


Figure 4.4: Example of HVAC plateau

In order to get insight into the seasonal change (i.e. HVAC demand), two extreme seasonal situations will be considered, one week in summertime, and one week in wintertime, for each day in the week. Table 4.1 shows an overview of the six scenarios that will be used during simulation. The temperature during the measurements is unknown.

Table 4.1: Time analysis for number of busses N fed by substation

|               | Workday schedule  |                   | Saturday schedule  |                    | Sun-/Holiday schedule  |                        |
|---------------|-------------------|-------------------|--------------------|--------------------|------------------------|------------------------|
|               | Winter            | Summer            | Winter             | Summer             | Winter                 | Summer                 |
| Reference     | S1                | S4                | S2                 | S5                 | S3                     | S6                     |
| Power profile | Measured          | Generated         | Measured           | Generated          | Measured               | Generated              |
| Schedule      | Winter<br>Workday | Summer<br>Workday | Winter<br>Saturday | Summer<br>Saturday | Winter<br>Sun-/Holiday | Summer<br>Sun-/Holiday |
| Temperature   | -                 | 30°C              | -                  | 30°C               | -                      | 30°C                   |

## 4.3. Power simulation

Modelling the energy flow in the trolley-grid required definition of nodes, whereas every node has a power and a position. The power flow in the trolley-grid is directly related to the nodes powers and their locations. Busses are considered as constant power nodes, storage systems are considered as power nodes as well, meaning that an ESS is set to a specific power value for every sample. In order to model the transmission losses, node voltage and currents and total energy demand, a grid model will be used.

### 4.3.1. Grid model

Figure 4.5 shows the equivalent circuit of the trolley-grid containing one bus at a set location. In this circuit, the bus is a power source with a voltage  $V_{bus}$  at the terminals. Equation 4.2 shows the relation between the line resistance ( $R_{line}$ ) and the bus location ( $x_{bus}$ ). Using superposition, the series connected line resistances on the feed and return lines can be combined into one line resistance  $2R_{line}$ .

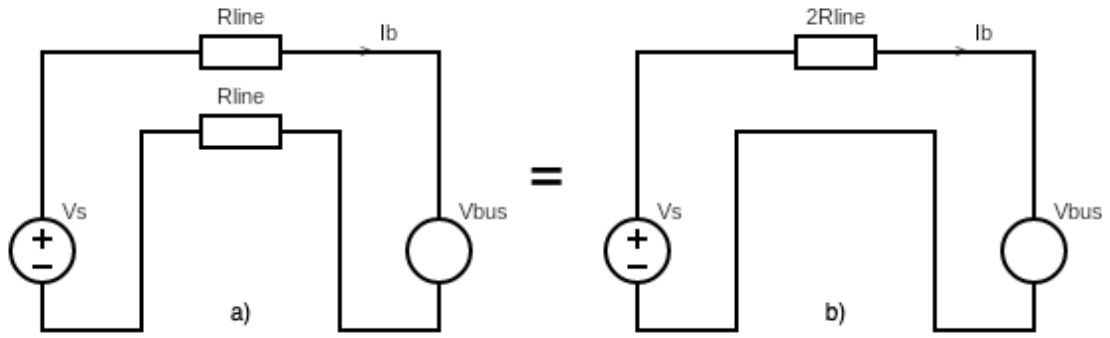


Figure 4.5: Equivalent circuit for trolley grid: a) real-world situation b) equivalent simplified circuit

$$R_{\text{line}} = \frac{\rho_{\text{Cu}} L}{A} \approx 0.000172 x_{\text{bus}} \Omega \quad (4.2)$$

In order to determine the losses in the transmission lines, node voltage and currents and source powers, the circuit can be solved. Equation 4.3 shows the relation between  $V_s$  and  $V_{\text{bus}}$ . When this (quadratic) equation is solved, all the voltages, powers and current in the circuit can be calculated.

$$V_{\text{bus}}^2 - V_s V_{\text{bus}} + P_{\text{bus}} 2R_{\text{line}} = 0 \quad (4.3)$$

In the Arnhem grid, most line sections consist out of a set of wires (positive and negative potential) for each direction, resulting in the situation as shown in figure 4.6. When a connection is made between the two sets of wires, a so-called parallel connection, the line resistance can be reduced since the total resistance of the combination will be lower. Combining the line resistance and the implemented parallel lines results in equation 4.4 for the actual value of  $R_{\text{line}}$  to be used during simulation.

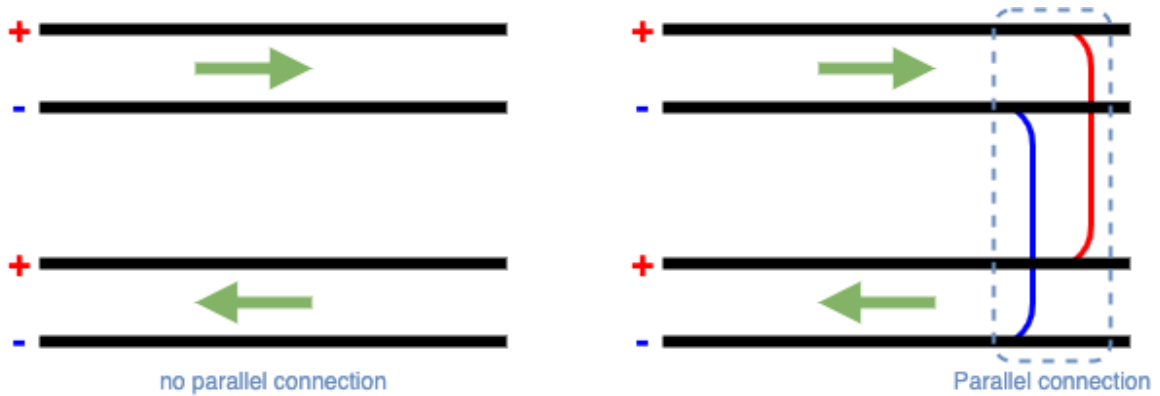


Figure 4.6: Comparing overhead lines: a) without parallel connection b) with parallel connection

$$R_{\text{line}} = \frac{2}{2} R_{\text{line}} = 0.000172 x_{\text{bus}} \Omega \quad (4.4)$$

When the number of nodes on the grid is increased, the circuit needs to be solved numerically. In order to do so, a grid model is used. Figure 4.7 shows an overview of the in- and outputs of this model.  $P(t)$  and  $x(t)$  are vectors containing the position and power information of the nodes which can be a bus or an ESS.  $V_s$  and  $x_s$  are respectively the substation voltage and location on the line. The outputs of the grid model are vectors  $I(t)$  and  $V(t)$ , containing the node voltages and currents. Also, the total amount of power is that is lost in the lines is calculated and available as  $P_{\text{loss}}$ .

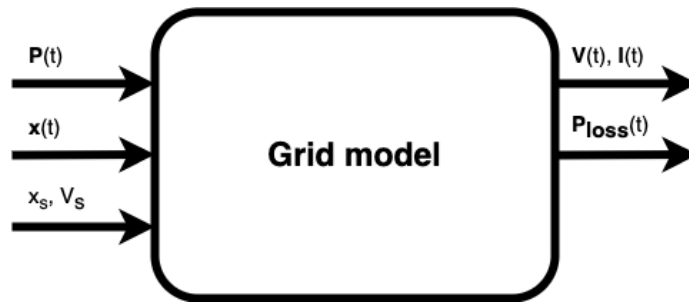


Figure 4.7: Overview of the grid model used in the simulation framework

### 4.3.2. Simulation of the braking resistor

Since the used grid model does not consider the utilisation of the braking resistor on board of the bus, the calculation of the braking power will be done before running the grid model during the pre-simulation power distribution (PSPD). Figure 4.8 shows a flowchart on the operation of the PSPD phase of the simulation. In this figure,  $\mathbf{P}$  is the vector containing all the power nodes that are connected to a section on time  $t$  and  $N$  is the size of this vector. Following this flowchart, one can see that if excess power is available in the section, it will be distributed across the different consuming nodes. If any power is still left over after this distribution, it will be burned in a braking resistor. Note that, when no excess power is available, none of the braking resistors will be operational.

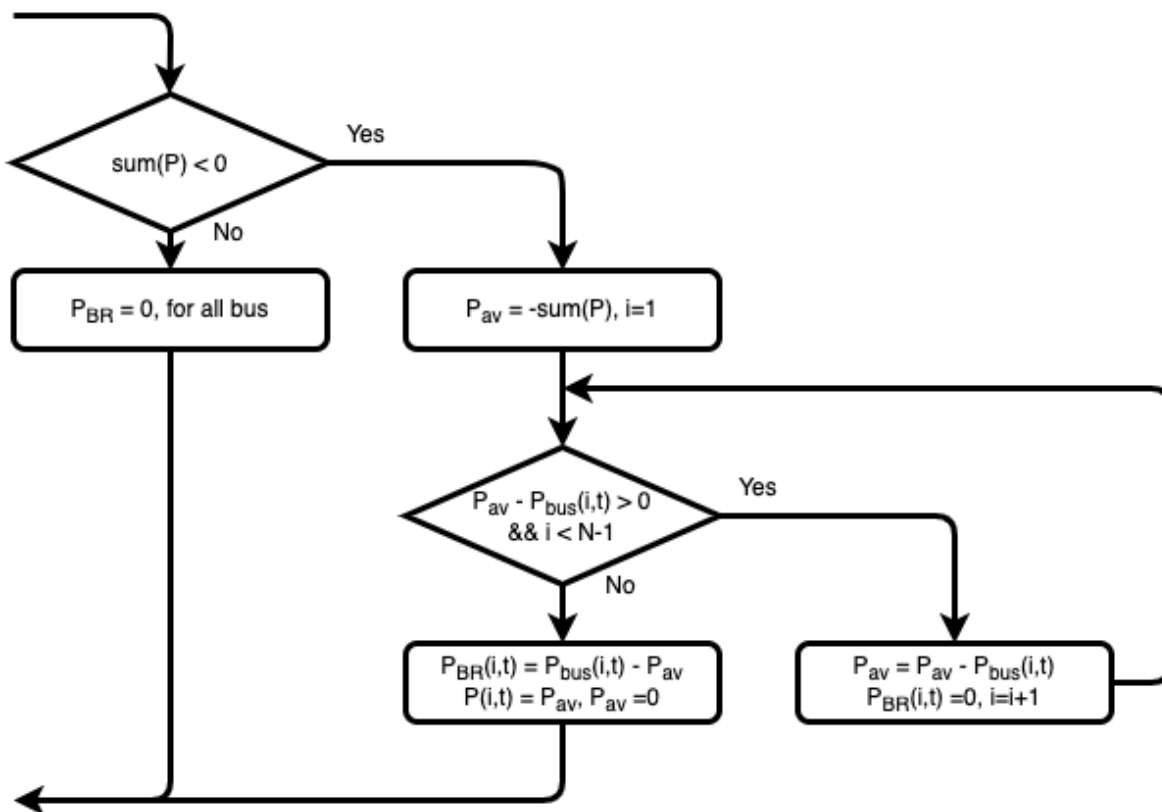


Figure 4.8: Flowchart of pre-simulation power distribution (PSPD)

### 4.3.3. Generation of summer power profiles

As described in section 4.2, measured power profiles for summer time are not available, and therefore will be generated based on the winter measurements. The HVAC plateau has the biggest impact on the power profile when comparing seasonal power profiles, and needs to be removed from the winter measurements. After removing the HVAC from the winter measurements, a simulated summer HVAC

profile is added again. The HVAC is modeled as a PWM-modulated power load, with changing duty cycle over different temperatures. Figure 4.9 shows the different stages in the process of generating the summer profile. First, the HVAC is removed from the measurements, resulting in nearly zero power consumption during standstill, and a more negative power value during regenerative braking. This implies that, when the bus is braking, the available power will be used by the HVAC first, and then send in to the grid (self-consumption). This is actually what is happening in the busses. After removal the simulated HVAC is added, finally resulting in the power profile to be used in summer simulations.

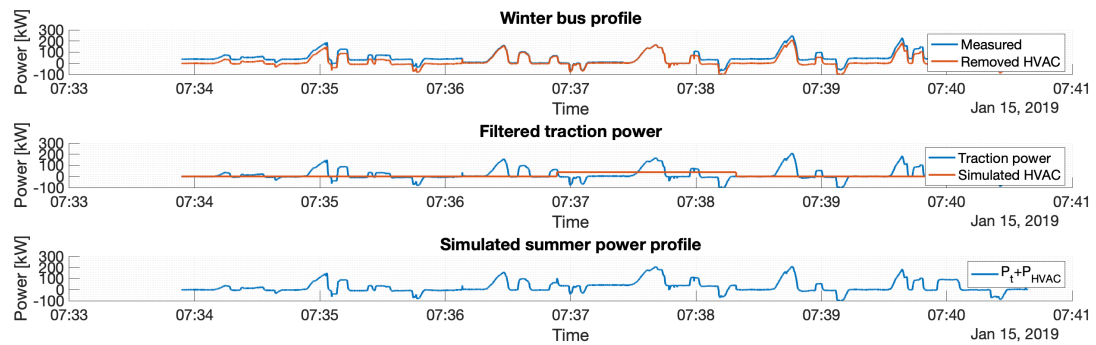


Figure 4.9: Summer profile generation

#### 4.4. Base simulation cycle

The full grid simulation is performed using the flowchart shown in figure 4.10. For every time sample in the simulation, the total power distribution in each substation is simulated by running the grid-model on every section connected to that substation. Note that the power vectors used in the grid model are the output of the PSPD phase as described in section 4.3.2 on substation level, so that the operation of the braking resistor is considered. The simulation framework stores the following output vectors for every time sample:

- $V_{bus}(t)$  Bus feeder voltage for every bus
- $I_{bus}(t)$  Bus feeder current for every bus
- $P_{br}(t)$  Bus braking power for every bus
- $I_{sec}(t)$  Section feeder current for every section
- $P_{loss}(t)$  Transmission loss power for every section

These outputs can be used to generate various results when they are combined to known parameters. For example, substation energy can be determined by multiplying the section feeder current vector with the known section feeder voltage, and integrate over time.

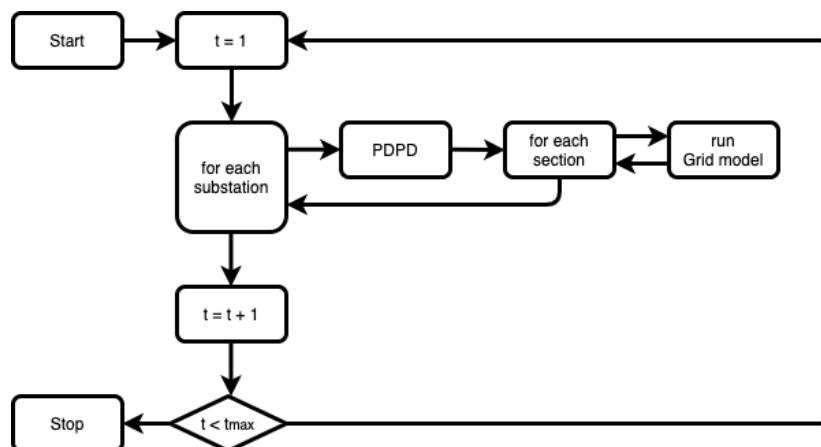


Figure 4.10: Simulation flowchart without ESS

## 4.5. Sample frequency

The simulation framework is based upon sample based discrete data. The measured input data is sampled with a frequency of approximately 13 samples per second. However, if this (rather high) sample frequency would be used throughout the complete simulation, the total simulation time would be long and therefore impractical. Therefore, the input data is re-sampled to a lower frequency of one sample per second. The re-sampled data still shows the fundamental profiles of bus power and velocity and filters out any measurement errors. Figure 4.11 shows an example of the original measured data and the re-sampled data profile used in the simulations.

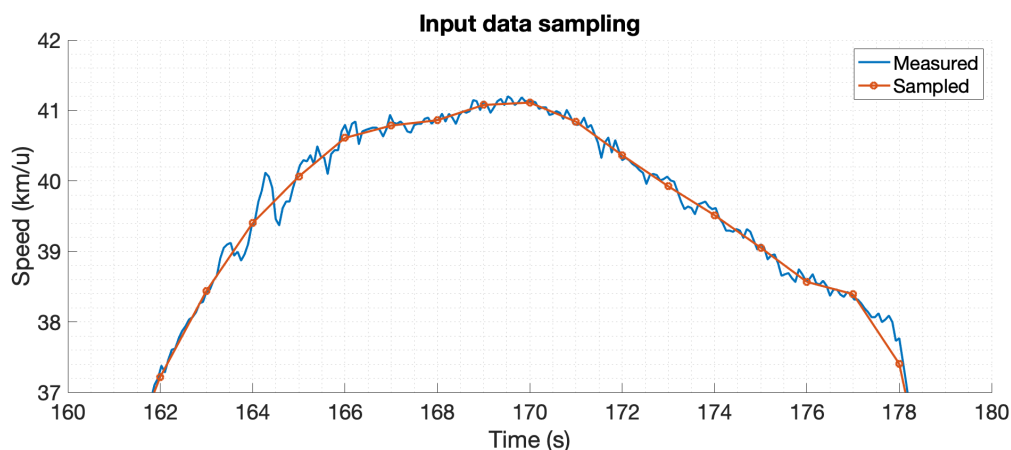


Figure 4.11: Comparing sampled measurement data with re-sampled data for simulation

## 4.6. ESS Objectives

Energy storage systems can be deployed for multiple purposes. In this work, there will be three major ESS objectives:

- **Recuperation of braking energy** is possible when energy that would normally be wasted in the braking resistor, is temporarily stored in a storage solution. Later, when there is an energy demand in the connection section, the stored energy can be used to feed the section, thereby reusing the braking energy and reducing the substation energy demand.
- **Reduction of transmission losses** can be achieved when energy that is stored in a storage system is discharged closer to the consuming bus than the distance that it would travel when fed from the substation. The transmission losses are dependent on the line resistance, which decreases when the distance between feeding node and consuming node is smaller.

- **Increase of substation headroom** can be achieved when energy that is stored in a storage system is discharged when peak demands are requested from the substation. These peaks can be covered by the ESS and thereby create headroom in the substation energy demand profile. This (constant) headroom can be used when for example EV charger or in-motion charging busses are deployed in the trolley-grid. Note that for this application, some energy has to be available at all times and thereby have an impact on the sizing of the storage.

## 4.7. ESS Implementation

Energy storage systems can be modelled as a power node on the grid with a specific location and power set-point over time. Since in this thesis the focus is on stationary storage, the location of the storage is fixed for every simulation. The set-point however can change based on the implemented charge schema and the input parameters of the storage. Figure 4.12 shows the ESS model used in the simulations. The charge schema has two inputs, SOC is the current state of charge of the storage and  $P_{\text{sum}}$  is the sum of the available power in the connected section and the sections connected through the section-substation relationship. The output  $P_{\text{set}}$  of the charge schema is the set-point of the power from and to the storage. Note that  $P_{\text{set}}$  can either be positive while discharging, and negative while charging.

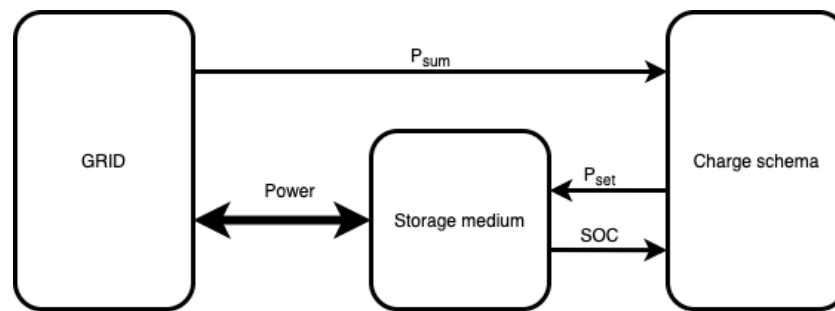


Figure 4.12: ESS model used in the simulation framework

### 4.7.1. Charge/Discharge efficiency

Since every storage medium is affected by losses during charging and discharging, the efficiency of the storage is not always 100%. In order to model the losses in the storage, a charge/discharge efficiency of 95% is considered. This efficiency ( $\eta$ ) is implemented in the calculation of  $\Delta E$ , the amount of energy added in, or subtracted from the storage during operation. Equation 4.5 shows the calculation of  $\Delta E$ .

$$\Delta E(t) = \eta \int_{t-1}^t P_{\text{set}}(t) dt \quad (4.5)$$

### 4.7.2. SOC Limits

The operating range of the storage medium is not always the full capacity of the storage. A lower limit on the SOC prevents the storage medium of deep-discharging. An upper limit leaves a safety margin for high power peaks feeding to the storage. The operating range of the storage is limited by 20%-80% SOC.

### 4.7.3. Sizing

Sizing the storage is dependent on the available regenerative energy, the operating charge schema and the charge/discharge efficiency. When considering only regenerative braking energy recuperation, the storage has to be sized big enough to store the maximum energy mismatch. When other applications of storage are implemented (e.g. peak shaving), the size can increase or decrease based on this specific application. When considering the reduction of transmission losses, and the storage of recuperating braking energy, the storage size will be sized infinite, meaning that in any case, all the regenerative braking energy can be stored. In order to determine the size of this infinite storage during simulation, equation 4.6 is used to determine the biggest regenerative braking energy peaks. In this equation,  $P_{\text{br}}$  is the sum of the braking resistor power profiles in a section at time  $t$ , and  $t_0$  and  $t_1$  the start and endpoint for every peak in this braking resistor power profile. Figure 4.14 shows this area.

$$E_{\max} = \max \left( \int_{t_0}^{t_1} P_{\text{br}}(t) dt \right) \quad (4.6)$$

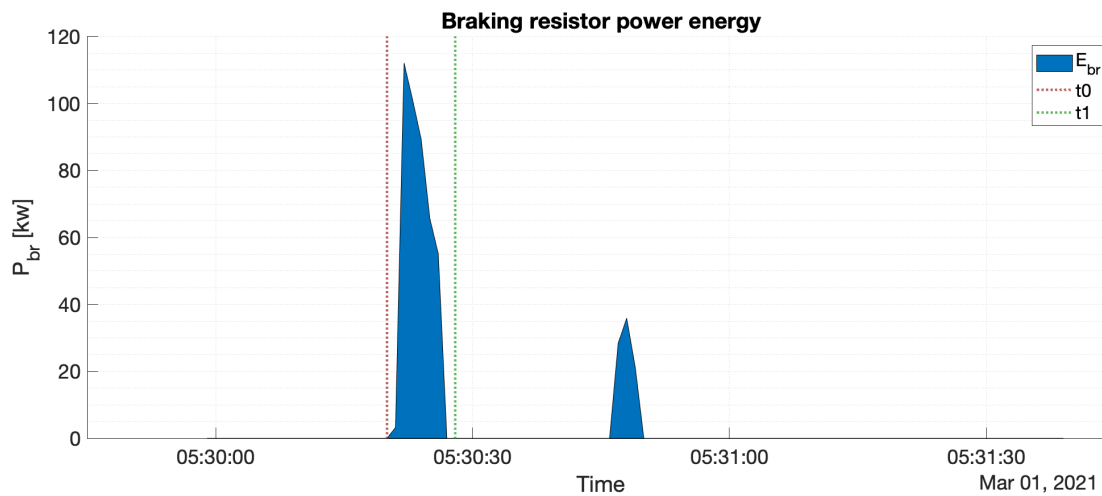


Figure 4.13: Braking resistor power peak indication used for sizing

Running this equation over all the available power profiles gives a maximum value of  $E_{\max}$  of 0.57 kWh, therefore, in the simulations where storage size is considered to be infinite, a value of 1 kWh is considered.

## 4.8. Charge scheme

The operation of the storage is defined by the implemented charge scheme. Two charge schemes will be considered defined as CS1 and CS2. This section will introduce the two charge schemes and show their operation.

### 4.8.1. CS1: Simple recuperation

The most simple implementation of an ESS charge scheme is represented by CS1. The main goal of this charge scheme is store all the available braking resistor energy in a section at every time, and discharge this stored energy when there is a demand. Figure 4.14 shows a flowchart of the operation of this charge scheme.

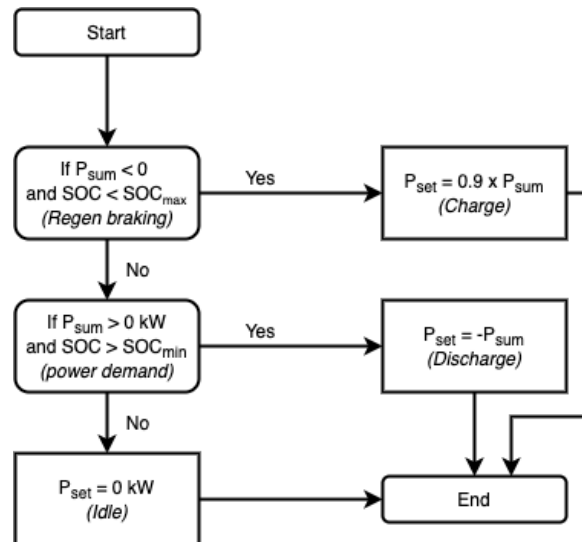


Figure 4.14: Flowchart describing operation of charge scheme 1 (CS1)

When the sum of the power in the connected section ( $P_{\text{sum}}$ ) (or connected section through the section-substation relationship) is negative, and the SOC of the storage is below the upper limit, the charge scheme will enter the charge state. The charge set-point of the storage is defined by the amount of available power in the section multiplied by a factor 0.9. This factor accounts for the introduced transmission losses when the energy is transferred from the bus to the storage. If this factor would be left out (and thus equal to 1), any additional transmission losses during the storage of the recuperated braking energy, will be fed from the substation and thus increase the total energy demand. When  $P_{\text{sum}}$  is positive, there is a demand for power in the section. In this scenario, if the storage SOC is higher than the lower SOC limit, the storage enters the discharge state. The discharge set-point is set to  $P_{\text{sum}}$ . In any other case, the storage is in the idle state. Figure 4.15 shows an example of operation of the charge scheme.

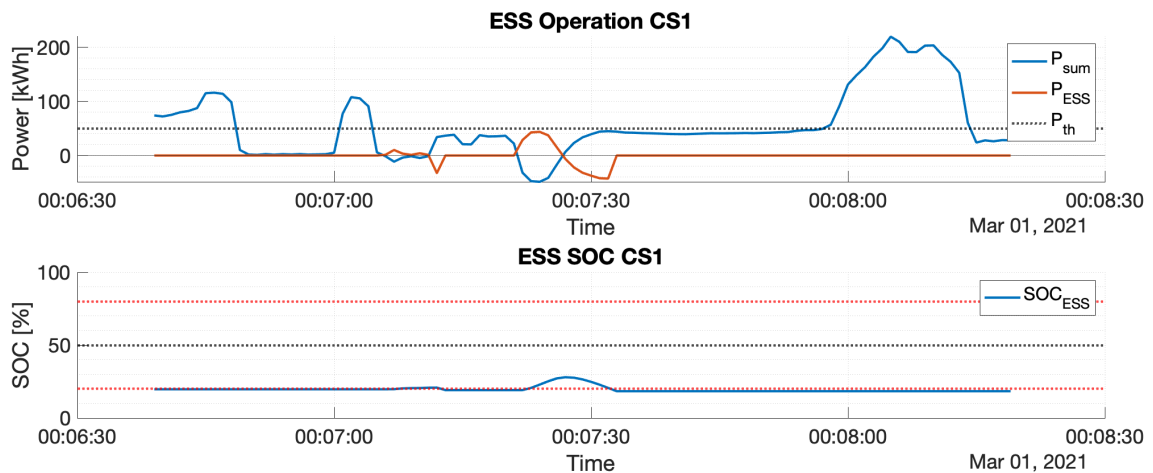


Figure 4.15: Operation of CS1

#### 4.8.2. CS2: Advanced recuperation

In order to get more control on the energy flows from and to the storage, a more advanced charge scheme can be used. CS2 is proposed as the charge scheme for advanced recuperation. This charge scheme is capable of only supporting the grid when the power demand is higher than a set threshold. Figure 4.16 shows a flowchart of the operation of this charge scheme.

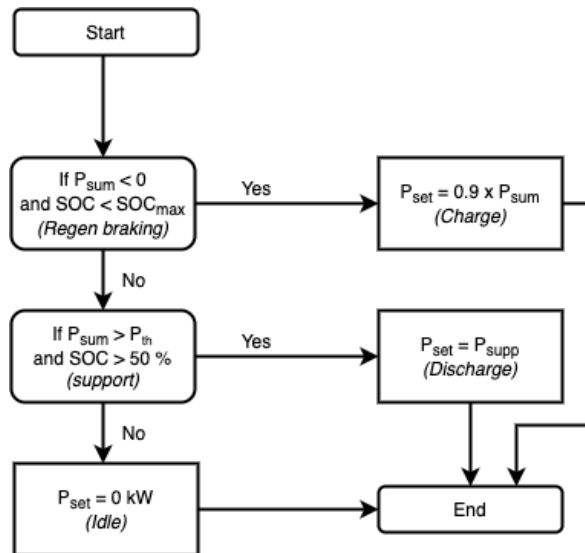


Figure 4.16: Flowchart describing operation of charge scheme 2 (CS2)

When the sum of the power in the connected section ( $P_{sum}$ ) (or connected section through the section-substation relationship) is negative, and the SOC of the storage is below the upper limit, the charge scheme will enter the charge state. The charge set-point of the storage is defined by the amount of available power in the section multiplied by a factor 0.9, as in CS1. When  $P_{sum}$  is higher than a the variable  $P_{th}$ , and the storage SOC is higher than the lower SOC limit, the storage enters the discharge state. The discharge set-point is set to a fixed value of  $P_{supp}$ . In any other case, the storage is in the idle state. Figure 4.17 shows an example of operation of the charge scheme.

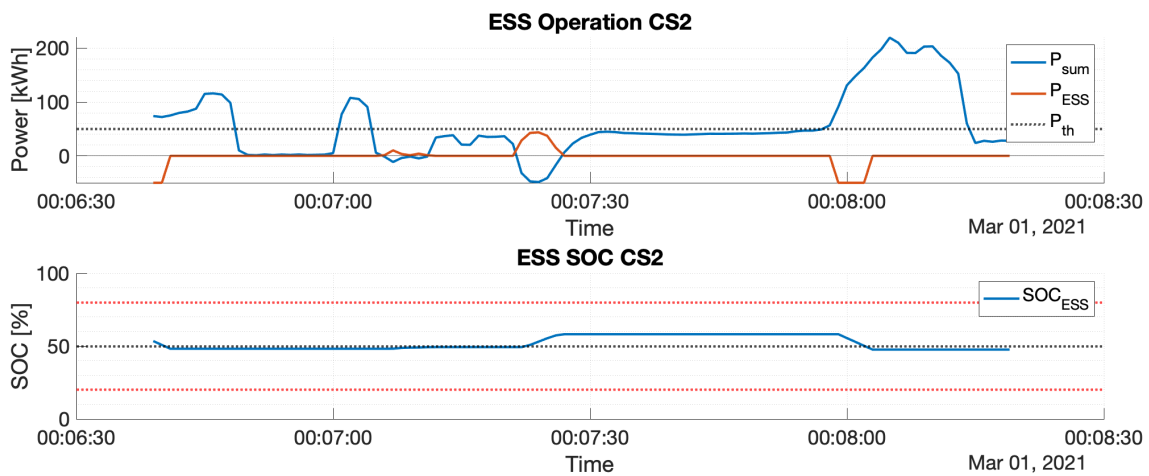


Figure 4.17: Operation of CS2

As can be seen in the operation of CS2, this charge scheme is able to only discharge at peak demand. Since transmission losses are higher at these peak demands, this charge scheme could, if positioned correct (closer to the bus than feeding from the substation), help reducing the transmission losses. Also, when tuning parameter  $P_{th}$  and the size of the storage, substation power peaks can be reduced.

### 4.9. ESS simulation cycle

In order to determine the set-point of the storage, the power flows in a section has to be determined when no ESS would be present. The total energy ( $P_{sum}$ ) is positive when there is a pure demand in the

section, and negative when excess energy is available. Figure 4.18 shows a flowchart of the simulation cycle that will be executed when storage is implemented in a section (or a section connected to a section with storage through the section-substation relationship). The flowchart consist out of a base simulation where normal (no ESS) operation of the grid is simulated. After this simulation, the whole process is repeated with the added ESS power node on the set-point based on the charge scheme of the storage.

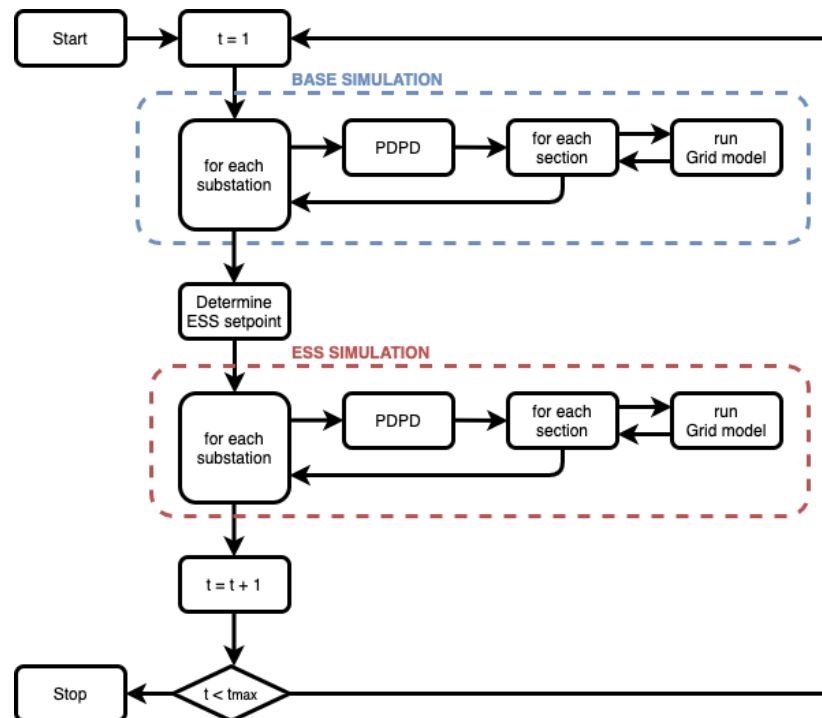


Figure 4.18: Simulation flowchart for section with ESS connected (direct or indirect)

The simulation framework stores the following output vectors for every time sample to be used for further analysis:

- $V_{\text{bus}}(t)$  Bus feeder voltage for every bus
- $I_{\text{bus}}(t)$  Bus feeder current for every bus
- $P_{\text{br}}(t)$  Bus braking power for every bus
- $V_{\text{ESS}}(t)$  ESS voltage for every ESS
- $I_{\text{ESS}}(t)$  ESS current for every ESS
- $\text{SOC}_{\text{ESS}}(t)$  ESS SOC for every ESS
- $I_{\text{sec}}(t)$  Section feeder current for every section
- $P_{\text{loss}}(t)$  Transmission loss power for every section

#### 4.10. List of assumptions

This section provides a list of assumptions made in the simulations;

- The feeder cables from the substation to the point of connection on the catenary have a resistive character, and their lengths are known, but the losses in these cables are omitted in this work.
- Forks in sections have been simplified as described in section 3.1.2.
- Storage lifetime and cycle degradation is not simulated in the framework.
- Negative values in the power profiles is available regenerative power, either used for natural sharing, storage or to be burned in the braking resistor.

## 4.11. Conclusions

This chapter gives a detailed explanation of the design considerations and operation of the simulation framework. Two ESS charge schemes are proposed for both the reduction of transmission losses and maximum recuperation. In the next chapter, baseline simulations will be performed on the Arnhem grid. These simulations will give insights in the energy distribution when no storage is implemented. After these baseline simulations, the same simulation framework will be used to determine the operation and efficiency increase for the Arnhem grid with the implementation of storage.



# 5

## Baseline results

With the simulation methodology as described in chapter 4 one is able to simulate the full grid operation with or without implementing an energy storage system. In this chapter, the Arnhem grid is considered without implementation of storage systems. These simulations can be used as a baseline for comparison with the situation where storage is implemented.

### 5.1. Substation utilisation

Since the different lines of the Arnhem grid have different routes, each line has a different sequence of sections to pass. Some sections are passed by multiple lines, and some sections are only utilised by one single line. This distribution in section utilization (and thereby also substation utilization) may be of interest when looking at the implementation of storage. Using equation 5.1, the relative utilization of a substation can be determined.  $N_{sec}(t)$  keeps track of the number of busses fed by a substation at time  $t$ . Figure 5.3 shows the distribution of the relative utilization. This figure also shows the difference in utilization distribution between the winter and summer schedule. As can be seen, no big differences in utilization can be observed between the two schedules. Substation 4 has the highest utilisation and substation 19 the lowest. This makes sense, since substation 4 is feeding sections that are passed by many lines, and substation 19 is only utilized by one line.

$$\rho = \frac{\int_{t=0}^{t=t_{max}} N_{sec}(t) dt}{\int_{t=0}^{t=t_{max}} N_{total}(t) dt} \cdot 100\% [\%] \quad (5.1)$$

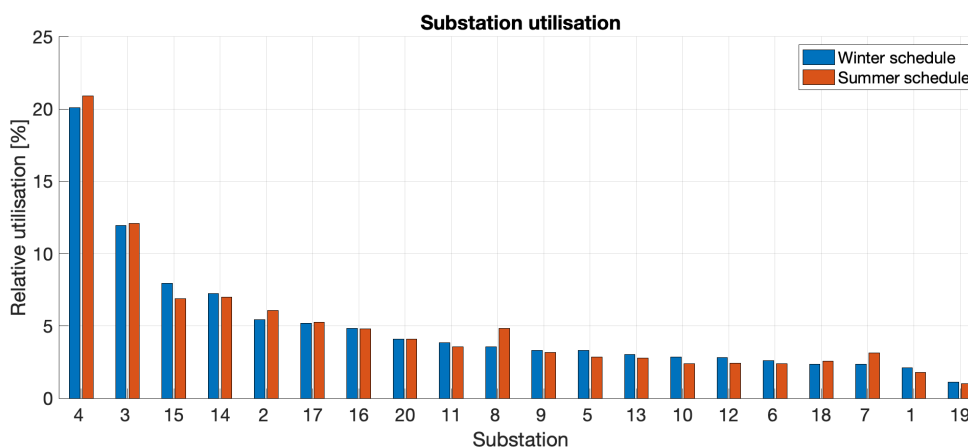


Figure 5.1: Substation time-based utilization

During the summer schedule, the number of busses and runs is decreased to the demand of transportation. This decrease in the number of active busses on the grid may have an impact on the distri-

bution of the number of busses fed by a substation at a given time  $t$ . Due to this change in substation utilisation, the amount of energy being shared from bus to bus, while fed from the same substation is expected to be reduced. Figure 5.2 shows the distribution of the number of busses fed from the same substation for the full grid operation. On the y-axis, the total time is presented. This distribution is created for the regular workday, Saturdays and Sun-/Holidays. From this figure we can see that the total utilisation is decreased in the summer, but also that the number busses available to share energy with is decreased in summer.

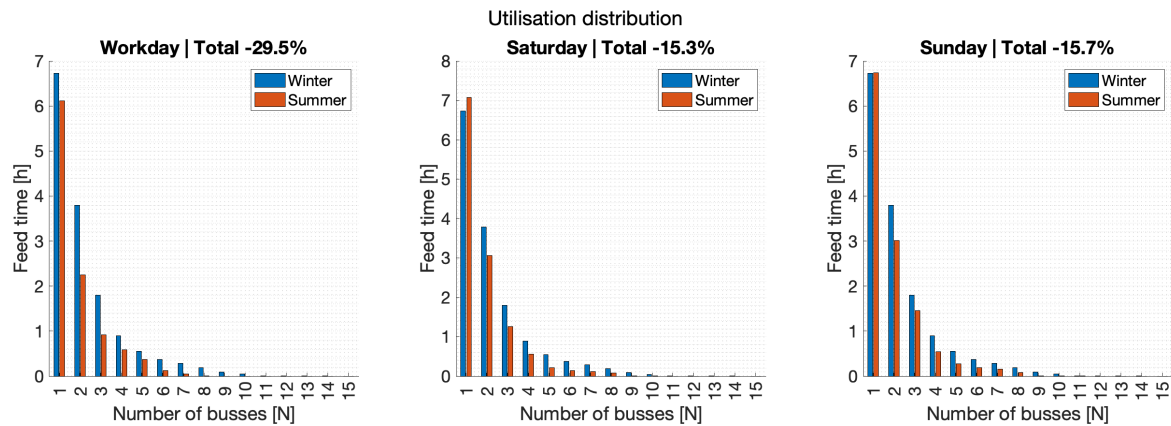


Figure 5.2: Distribution of number of busses fed by the same substation during full-grid operation

Table 5.1 shows an analysis of the bus time distribution for the different schedules between winter and summer. From this table we can see that in winter nearly half of the time other busses are available to share energy with. In summer this percentage of time with more than one bus fed by the same substation is decreased significant (For the regular schedule by nearly 29%). Due to this decrease in potential sharing possibilities may have an impact on the usage of the braking resistor. When no other busses are available to share energy with, the left-over regenerative braking energy will be burned in the braking resistor.

Table 5.1: Time analysis for number of busses  $N$  fed by substation

|                   | Workday   |           | Saturday  |           | Sun-/Holiday |           |
|-------------------|-----------|-----------|-----------|-----------|--------------|-----------|
|                   | Winter    | Summer    | Winter    | Summer    | Winter       | Summer    |
| $t(N = 1)$        | 6.7h 31%  | 6.1h 36%  | 6.7h 31%  | 7.0h 35%  | 6.7h 34%     | 6.7h 54%  |
| $t(N > 1)$        | 14.7h 69% | 10.4h 64% | 14.8h 69% | 12.5h 65% | 14.7h 69%    | 12.5h 66% |
| $\Delta t(N > 1)$ | -5%       |           | -4%       |           | -3%          |           |

## 5.2. Substation power

The substation power demand profile can be used to analyse the impact of the implementation of storage systems on the total power demand and energy consumption per substation. Figure 5.3 shows an example of a substation power profile as generated by the simulations. The data is from substation 12, which is responsible for feeding sections 23 and 24. In the zoomed in plot, the dotted line shows the actual power delivered by the substation, whereas the solid lines show the section power demand. As can be seen in the figure, when the power demand from one section becomes negative (when a bus is braking in this section and no other bus in this section is able to consume this energy), the energy is forwarded to any other section fed by the substation. When this occurs, the total amount of power delivered by the substation decreases. From now on, the ability for sections to share power through the substation with each other via the same bus-bar will be referred as the section-substation relationship.

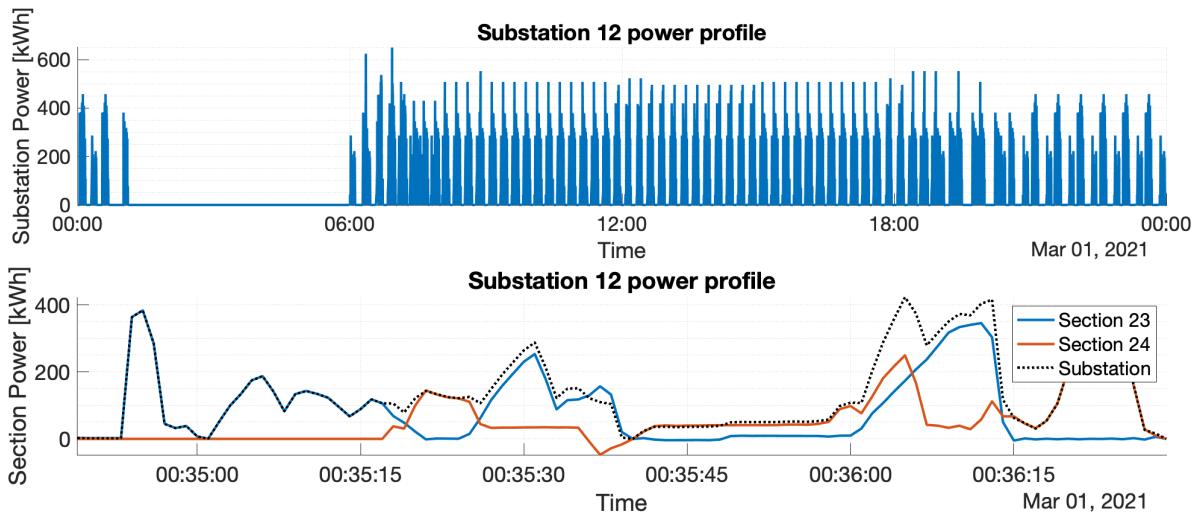


Figure 5.3: Example substation power profile

### 5.3. Substation energy

From the substation power profiles, using equation 5.2, one can determine the energy delivered by the substation to the grid. Figure 5.4 shows the distribution of energy consumption between different substations for a day in summer and winter. As expected, the amount of energy consumed in winter is higher than the energy consumption in summer, probably due to the impact of the HVAC consumption. The actual reason for this reduction will be discussed later on.

$$E_{ss} = \int_{t=0}^{t=t_{max}} P_{ss}(t) dt \tag{5.2}$$

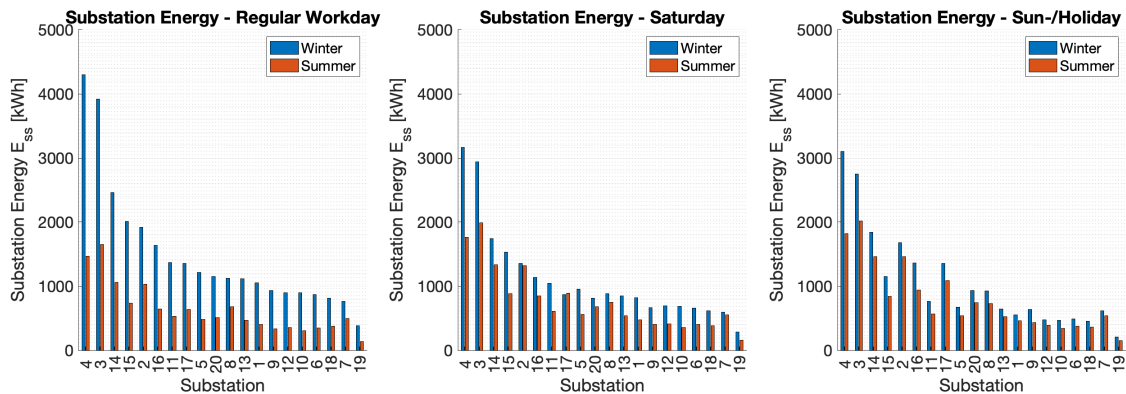


Figure 5.4: Substation energy for all scenarios

#### 5.3.1. Substation energy validation

Using the simulated substation power profiles, and the different available scenarios and their occurrences, the total simulated substation location energy can be determined.

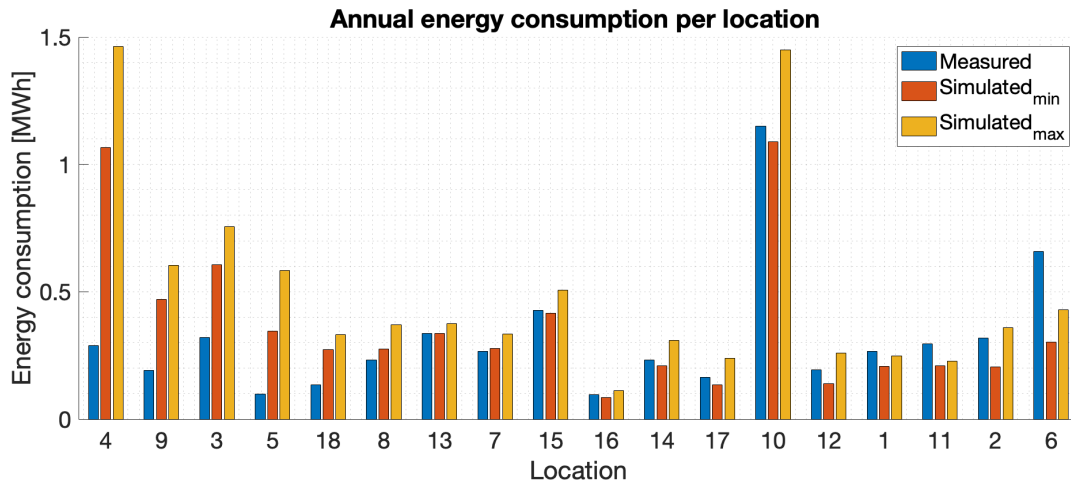


Figure 5.5: Simulated vs. measured substation location energy consumption based on measurement data and simulation outcomes

Figure 5.5 shows the annual measured substation location energy consumption and the simulated consumption for both the min and max profiles. For most substation locations, the difference between the measured values and the simulated values is relative small, but for some substation locations the difference is high. Some clarifications for this phenomena are:

- **Varying power profiles:** The calculation of the annual substation location energy consumption is based upon one measurement per schedule type, modified only once for the summer scenario, generating a total of six power profiles. This sample size may be too small to be extrapolated to determine the annual energy consumption.
- **HVAC Profiles:** In the simulation, the HVAC profile is heavily simplified. In reality, the HVAC consumption is very dependent on (probabilistic) weather conditions, and may therefore also introduce errors while extrapolating to annual consumption.
- **Bilateral connections** are not considered in the simulations. With the implementation of bilateral connections, energy is able to flow from one substation location to sections connected to other substation locations, thereby changing the energy distribution between different substation locations. The simulation results for substation location 6 are lower than the measured values. From the data it is known that implementing bilateral connections increases the total energy for this substation location by 40%, so the higher measured value does originate from the implementation of bilateral connections. Since the consumption for this location is increased, a decrease is expected in connected sections.
- **Negative bus power profiles** are assumed to be energy that is generated while braking, available for natural sharing or burned in the braking resistor, while in reality this negative value is the amount of energy that is injected to the grid to be used by other busses (purely natural sharing). This explains the big difference in energy consumption for substation location 4, which is feeding high traffic sections. In this substation location, more energy is shared naturally, thereby decreasing the actual energy consumption.

## 5.4. Available regenerative energy

The negative values from the bus power profiles can be considered as available regenerative power, which will be either injected into the grid, or burned in the burning resistor on the bus. The total amount of available regenerative energy can be determined using equation 5.3. Table 5.3 shows the amount, relative difference to total substation energy and seasonal change in the amount of available regenerative braking energy.

$$E_{av} = \int_{t=0}^{t=t_{max}} P(P < 0, t) dt \quad (5.3)$$

Table 5.2: Available regenerative energy in the Arnhem grid

|                 | Workday |    |        |     | Saturday |    |        |     | Sun-/Holiday |    |        |     |
|-----------------|---------|----|--------|-----|----------|----|--------|-----|--------------|----|--------|-----|
|                 | Winter  |    | Summer |     | Winter   |    | Summer |     | Winter       |    | Summer |     |
| $E_{av}$ [kWh]  | 1710    | 6% | 1932   | 15% | 1416     | 6% | 2337   | 15% | 1395         | 7% | 2326   | 15% |
| $\Delta E_{av}$ | +9%     |    |        |     | +9%      |    |        |     | +8%          |    |        |     |

## 5.5. Braking resistor energy

The braking resistor burns any excess power in a section when no other consumers are available in the section or connected sections through the section-substation relationship. The amount of power burned in the braking resistor  $P_{br}$  is calculated during the simulation and stored per bus in a vector over time. Figure 5.6 shows an example of braking resistor power profile.

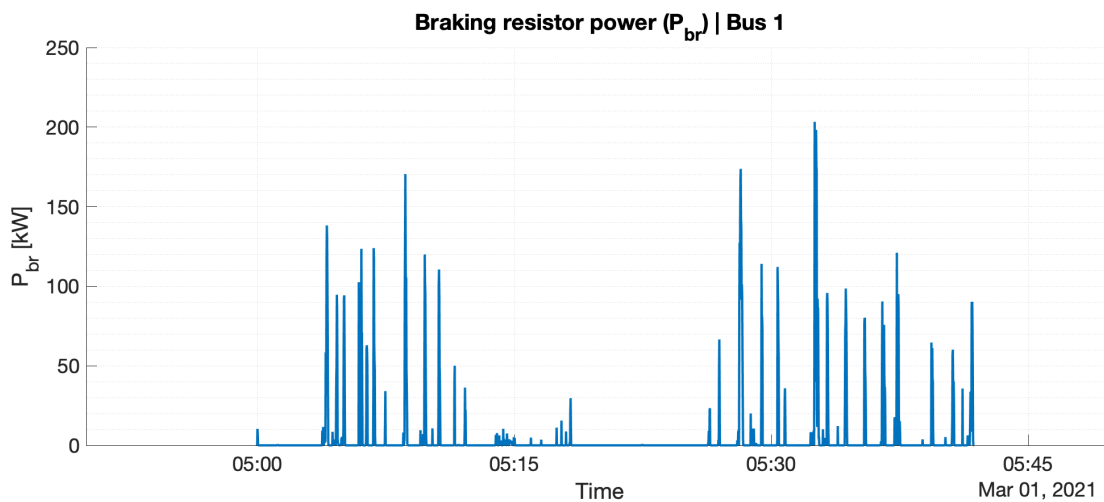


Figure 5.6: Braking resistor power profile, outcome of pre-simulation power distribution (PSPD) calculation for a bus on line 6 departing at 05:00

Using the braking resistor power profiles and equation 5.4, one is able to determine the total amount of energy burned in the braking resistor per bus. Since for every time instance, the actual location of the bus (and thus from which substation it is fed) is available, the distribution of the total amount of braking energy burned in each substation can be determined. Figure 5.7 shows the distribution of braking energy between different substations for winter and summer operation. Table 5.3 shows the difference in braking resistor energies for all different scenarios. In summer, the relative energy burned in the braking resistor is increased by 8-9%.

$$E_{br} = \int_{t=0}^{t=t_{max}} P_{br}(t) dt \quad (5.4)$$

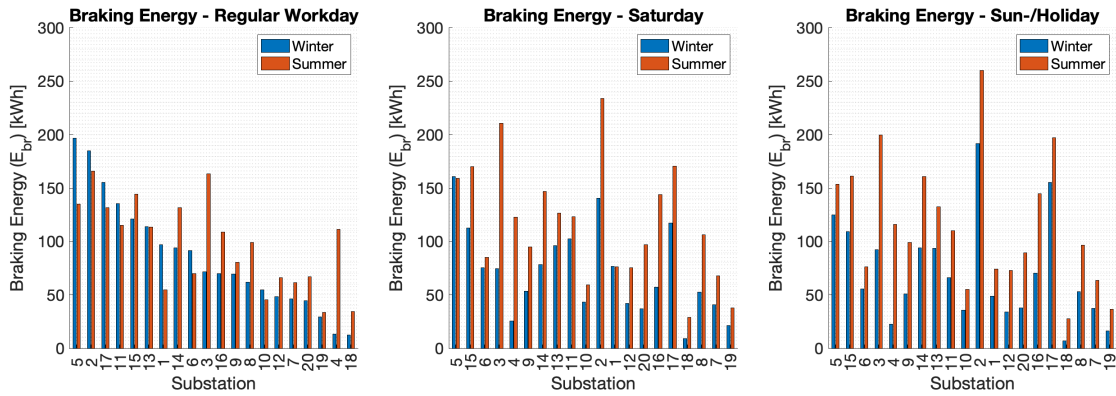


Figure 5.7: Braking energy per substation

|                 | Workday |        | Saturday |        | Sun-/Holiday |        |      |     |      |    |      |     |
|-----------------|---------|--------|----------|--------|--------------|--------|------|-----|------|----|------|-----|
|                 | Winter  | Summer | Winter   | Summer | Winter       | Summer |      |     |      |    |      |     |
| $E_{br}$ [kWh]  | 1710    | 6%     | 1932     | 15%    | 1416         | 6%     | 2337 | 15% | 1395 | 7% | 2326 | 15% |
| $\Delta E_{br}$ | +9%     |        | +9%      |        | +8%          |        |      |     |      |    |      |     |

Table 5.3: Increase in braking resistor power over different scenarios, absolute and relative to the total energy consumption

## 5.6. Energy distribution

In order to get more insights in the different energy flows in the trolley-gird, a deeper analysis can be performed on the available profiles. The energy flows in the grid can be visualised by figure 5.8. In this figure, the energy flows for two different scopes are defined. The first scope is on a grid level, the second one on a bus level. The reason why this distinction is necessary is due to the energy loop within the grid scope. The coming sections will give more insight in the scopes and their energy profiles.

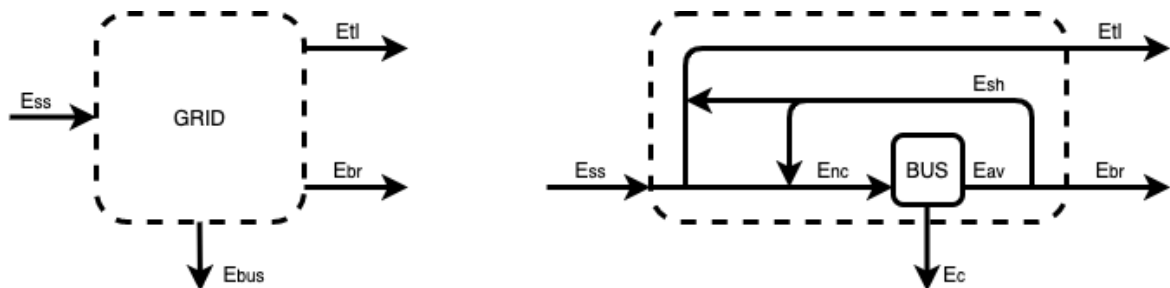


Figure 5.8: Energy distribution of trolley-grid.

### 5.6.1. Grid level

On a grid level, the energy flow model has an input for the total amount of energy delivered by the substations ( $E_{ss}$ ), and two outputs for the total amount of energy burned in the braking resistor ( $E_{br}$ ) and the energy lost as transmission losses in the overhead lines. ( $E_{tl}$ ) Table 5.4 shows the outcomes of the baseline simulations for all possible scenarios. From this data we can observe that;

- The total amount of energy burned in the braking resistor is increased by 9 % in the summer.
- The total energy consumption is decreased in the summer.
- Transmission losses are not depending on change in either power profile or schedule.

|                 | <b>Workday</b> |     |        |     | <b>Saturday</b> |     |        |     | <b>Sun-/Holiday</b> |     |        |     |
|-----------------|----------------|-----|--------|-----|-----------------|-----|--------|-----|---------------------|-----|--------|-----|
|                 | Winter         |     | Summer |     | Winter          |     | Summer |     | Winter              |     | Summer |     |
| $E_{bus}$       | 27560          | 91% | 10338  | 82% | 20227           | 91% | 12544  | 82% | 19091               | 90% | 12993  | 82% |
| $E_{br}$        | 1711           | 6%  | 1932   | 15% | 1417            | 6%  | 2337   | 15% | 1396                | 7%  | 2327   | 15% |
| $E_{tl}$        | 920            | 3%  | 391    | 3%  | 667             | 3%  | 442    | 3%  | 610                 | 3%  | 469    | 3%  |
| $E_{ss}$        | 30191          |     | 12662  |     | 22311           |     | 15323  |     | 21097               |     | 15788  |     |
| $\Delta E_{ss}$ |                |     | -58%   |     |                 |     | -31%   |     |                     |     | -25%   |     |

Table 5.4: Increase in braking resistor power over different scenarios, absolute and relative to the total energy consumption

In order to get more insight in the distribution of excess energy, the grid can be analysed at a bus level, thereby incorporating the effect of natural sharing and the energy loops created by this phenomena.

### 5.6.2. Bus level

On a bus level, the energy flow model has two inputs, one being the energy fed directly from the substation, and one being the energy fed from other busses. The sum of these two inputs is the total energy needed by the bus ( $E_{nc}$ ), calculated by integrating over all positive values of the bus power demand profiles. This energy demand can be calculated before the simulations when integrating over the positive values of the bus power demand profiles. Equation 5.5 can be used to determine this energy. The outputs of the model consist out of the energy shared to other busses ( $E_{sh}$ ), the energy burned in the braking resistor ( $E_{br}$ ), and the energy consumed by the bus itself ( $E_c$ ). The energy consumed by the bus itself consists out of multiple parts of which the most important are the traction energy and the energy needed for the HVAC. The available regenerative energy  $E_{av}$  can be calculated using equation 5.3. Table 5.5 shows the outcomes of the baseline simulations for all possible scenarios.

$$E_{av} = \int_{t=0}^{t=t_{max}} P(P < 0, t) dt \quad (5.5)$$

Table 5.5: Excess energy destination analysis

|                 | <b>Workday</b> |     |        |     | <b>Saturday</b> |     |        |     | <b>Sun-/Holiday</b> |     |        |     |
|-----------------|----------------|-----|--------|-----|-----------------|-----|--------|-----|---------------------|-----|--------|-----|
|                 | Winter         |     | Summer |     | Winter          |     | Summer |     | Winter              |     | Summer |     |
| $E_{sh}$        | 1635           | 49% | 833    | 30% | 1025            | 42% | 1018   | 30% | 873                 | 38% | 1138   | 33% |
| $E_{br}$        | 1711           | 51% | 1932   | 70% | 1417            | 58% | 2337   | 70% | 1396                | 62% | 2327   | 67% |
| $E_{av}$        | 3346           |     | 2765   |     | 2442            |     | 3355   |     | 2268                |     | 3464   |     |
| $\Delta E_{av}$ |                |     | -17%   |     |                 |     | 37%    |     |                     |     | 53%    |     |

Figure 5.9 shows the results of table 5.5 separated by season. A trend line is added to see the impact of changing schedule in a season on the share of excess energy. Where the braking resistor energy share increases for a less-dense schedule in winter, it decreases in summer. This is an important observation since it shows that the combination of scheduling and power profile determines the excess energy share distribution, and thus that these factors are not independent.

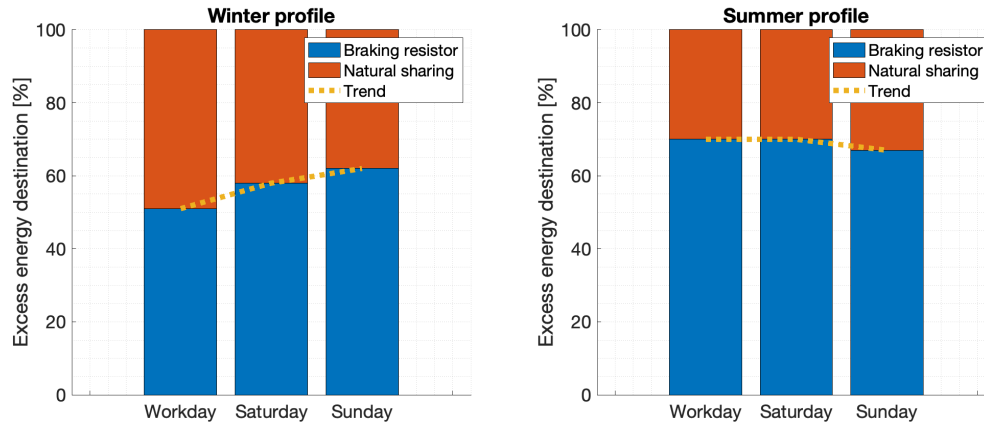


Figure 5.9: Excess energy share in different scenarios

## 5.7. Transmission losses

As described in section 4.6, the transmission losses are an output of the implemented grid model. Since the transmission losses are calculated at every time sample, an accurate analysis of these losses can be made. Figure 5.10 shows the transmission losses for every substation, using a regular week scenario. These relative losses have been calculated using equation 5.1. In this equation,  $E_{loss}$  is the calculated amount of transmission losses in the grid.  $E_{in}$  is the amount of energy supplied by the substation.

$$E_{loss} = \frac{E_{loss}[\text{kWh}]}{E_{in}[\text{kWh}]} \cdot 100 [\%] \quad (5.6)$$

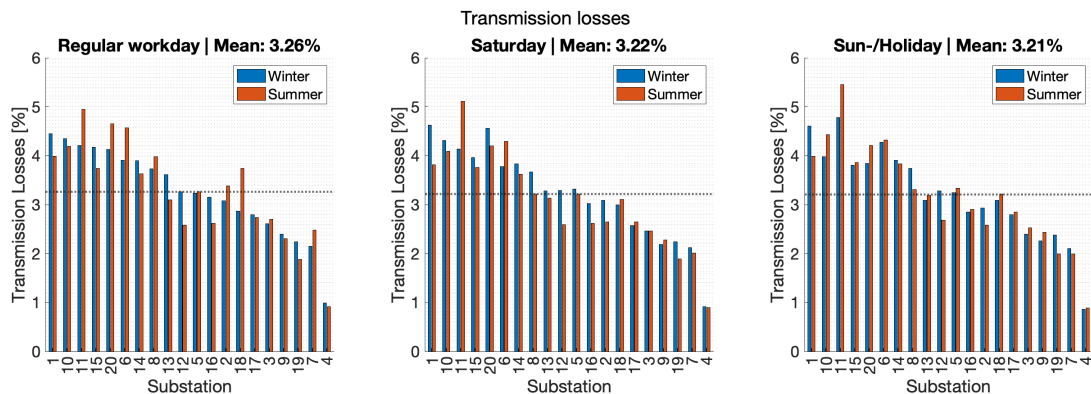


Figure 5.10: Transmission losses for all substations

In previous research on the topic of transmission losses in the Arnhem grid, a constant value for the transmission losses of 16.7% is assumed [38]. The results of this analysis show that the actual transmission losses are lower. Figure 5.10 shows the relative transmission losses per substation, and the average relative transmission losses. The average of the simulated transmission losses is 3.17 %.

From figure 5.10 and the results on transmission losses in table 5.4 one can conclude that the transmission losses are independent from the seasonal changes and the changes in timetable. The absolute values however do change, but are small compared to the losses in the braking resistor.

## 5.8. Peak substation power

The bus power profiles show clearly power peaks when a bus is accelerating. The feeding substation should be sized large enough to deliver these accelerating power peaks. Since a substation can be

feeding multiple sections, on which at some time multiple busses can be connected, big substation power peaks can occur in the case that two busses are accelerating at the same time. Every section has a maximum current, and using the simulation results, an analysis can be performed on how often these maximum currents are exceeded. Figure 5.11 shows an example of the section current of a day. This figure shows that the maximum current limit is not exceeded often. Also, a lot of headroom remains unused most of the time. This headroom could be used to extend the grid functionalities by for example placing EV chargers on the grid. When this type of constant power loads are added to the grid, the substation power profile will increase and thereby potentially cause more overloading situations.

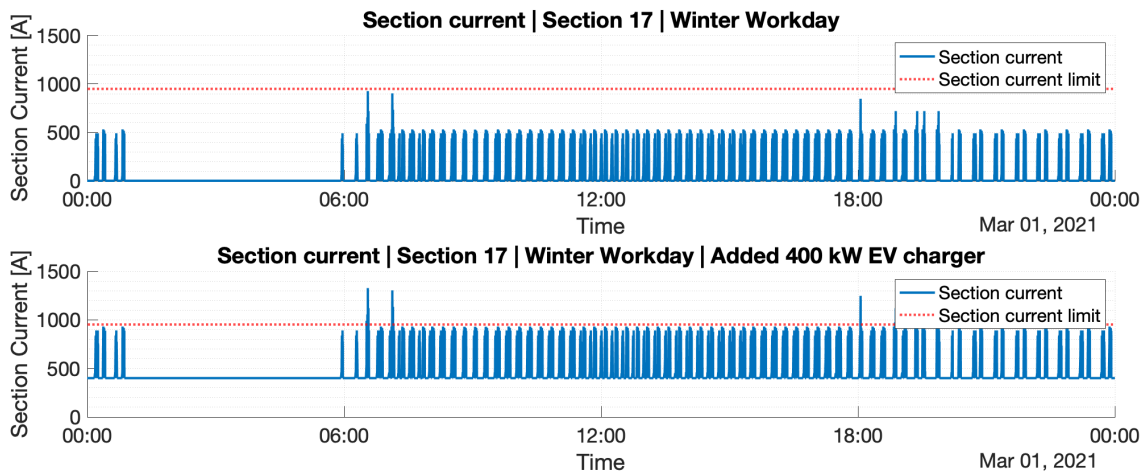


Figure 5.11: Daily substation current profile

## 5.9. Conclusions

This chapter shows results of the baseline simulations of the Arnhem grid. Some main conclusions are found on the normal operation of the Arnhem grid. First, the combination of scheduling and seasonal power profile changes determines the share in excess energy. These factors are not independent. Second, simulations show that the transmission losses are nearly constant while using different schedules and (seasonal changing) power profiles. Lastly, extending the grid with for example EV chargers is limited by some (rare) peaks in substation current demand. The next chapter will use these results in order to research if placing stationary storage can improve the grid efficiency or enable implementation of EV chargers.



# 6

## Simulation results & Discussion

*While chapter 5 shows the simulation results of the Arnhem grid without storage (current case), this section will implement storage in order to maximize recuperation of braking energy, reduce transmission losses and increase substation headroom for the implementation of auxiliary constant power loads in the trolley-grid. The performance of the charge schemes as presented in chapter 4 can be analyzed when implemented in the simulated Arnhem grid. This chapter will give insights on the impact of the location of the storage, the charge scheme parameters and also gives a recommendation on sizing for various applications.*

### 6.1. Stationary storage for reduction of transmission losses

In this section, the results of the simulations focused on the reduction of transmission losses will be presented. First, an analysis will be performed on the reduction of transmission losses using an isolated section, thereby leaving out the possibility for a section to share energy to other sections through the substation. A location analysis will be performed on this isolated scenario for both of the available charge schemes. Next, the section-substation relationship will be implemented to give a more realistic representation of the Arnhem grid. The results can be used to give a recommendation on the best location and charge scheme to be used in order to reduce the transmission losses.

#### 6.1.1. Simulation setup

The total amount of transmission losses is a direct output of the simulation framework, thereby simplifying the performance index of a implemented ESS. For these simulations only the location of the storage is changed. Both charge schemes will be considered using the following ESS assumptions:

- For CS2,  $P_{th}$  is set to 60 kW, thereby filtering out any HVAC demand and only support the grid when traction power is requested.
- The ESS is sized at 1 kWh, as proposed in section 4.7.3. The implemented charge schemes and their parameters will only store energy for a short time. For CS1, energy is fed back to the grid as soon as there is a power demand. Since  $P_{th}$  for CS2 is set relatively low, also in this charge scheme, no accumulation of energy is expected.

#### 6.1.2. Isolated section results

Section 24 will be used as an example section for the simulation of the reduction of transmission losses. Figure 6.1 shows the section 24 on the map and a simplified geological representation of this section. For this specific section, the feed-in point from the substation is near the end of the section, indicated by FED in the figure. The location of the storage is changed with steps of 100 meters. The total length of section 24 is 1390 m, resulting in 13 simulations over this section.

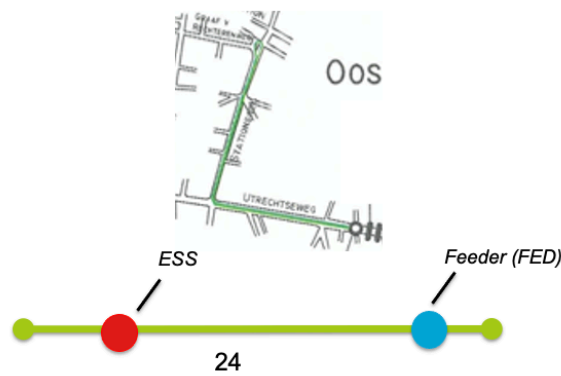


Figure 6.1: Map and simplified representation of the isolated model of section 24

Figure 6.2 shows the absolute reduction in transmission losses with different location of the stationary ESS. The positive values in the reduction indicate the positions for which the storage is capable of reducing the total transmission losses when compared to the situation with no storage. As can be seen in the plot, not all locations have a positive effect in the reduction of the transmission losses. When storage is placed near the feed-in point, the transmission losses are always increased compared to the baseline. When storage is placed at the beginning of the section (far away from the feed-in point) only CS2 is able to reduce the transmission losses. The plots show a optimal position. Looking at the absolute values, the total reduction, even at the optimal location is small ( $\sim 800$  Wh/day).

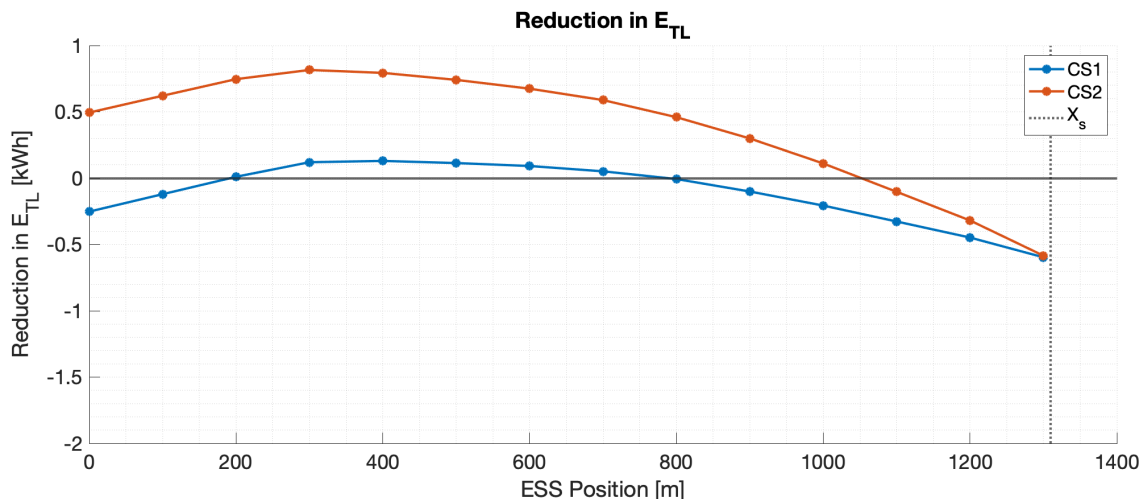


Figure 6.2: Reduction in transmission losses for section 24 in isolated state

In order to reduce the number of simulations for the full Arnhem grid, three locations will be considered in the full-grid simulations:

- **EOL** (End of line), the end of the section with the biggest distance from the feed-in point. For section 24 this is the ESS located at  $x = 0m$ .
- **FED** (Feed-in point), the location where the section is connected to the grid, for section 24 this is 1300 meters.
- **EOL/2** halfway down the line, for section 24 this is 650 meters.

Table 6.1.a gives an overview of the absolute reduction in transmission losses using these three locations. As can be seen in this table, CS2 has the maximum reduction of the absolute values of the transmission losses at EOL/2, which is in line with figure 6.2. In the table, the charge scheme

with maximum reduction for that location is marked green. Table 6.1.b shows the relative impact on the transmission losses and table 6.1.c shows the maximum change in reduction between different locations. The maximum change in transmission losses for all locations is around 2%.

Table 6.1: Change in transmission losses for section 24 (Connected), a) absolute, b) relative to baseline, c) impact of location

| $\Delta E$ [kWh] | Section 24 (isolated) |       |
|------------------|-----------------------|-------|
| E base [kWh]     | 22,45                 |       |
| x                | CS1                   | CS2   |
| EOL              | -0,25                 | 0,50  |
| EOL/2            | 0,07                  | 0,63  |
| FED              | -0,61                 | -0,61 |

a)

| $\Delta E$ [%] | Section 24 (isolated) |        |
|----------------|-----------------------|--------|
| x              | CS1                   | CS2    |
| EOL            | -1,11%                | 2,23%  |
| EOL/2          | 0,31%                 | 2,81%  |
| FED            | -2,72%                | -2,72% |

b)

| $\Delta E$ [kWh]   | Section 24 (isolated) |       |
|--------------------|-----------------------|-------|
| x                  | CS1                   | CS2   |
| Max $\Delta$ [kWh] | 0,07                  | 0,63  |
| Max $\Delta$ [%]   | 0,31%                 | 2,81% |

c)

### 6.1.3. Connected section results

As described in section 3.1.3, some sections are connected to each other by the section-substation relationship, enabling them to share regenerative braking power to other sections. In the example in section 6.1.2, section 24 is isolated from the other sections connected to the substation. In reality, section 24 is connected to section 23 via the bus-bar in substation 1. Figure 6.3 shows the section 24 on the map and a simplified geological representation of this section including the relation with section 23.

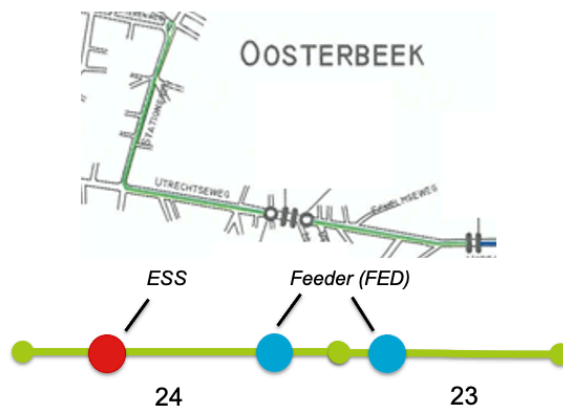


Figure 6.3: Map and simplified representation of the connected model of section 24

The same simulation as in section 6.1.2 can now be performed with the section-substation relationship implemented. Figure 6.4 shows the absolute reduction in transmission losses for this scenario. One can see from this plot that neither CS1 nor CS2 is able to reduce the transmission losses.

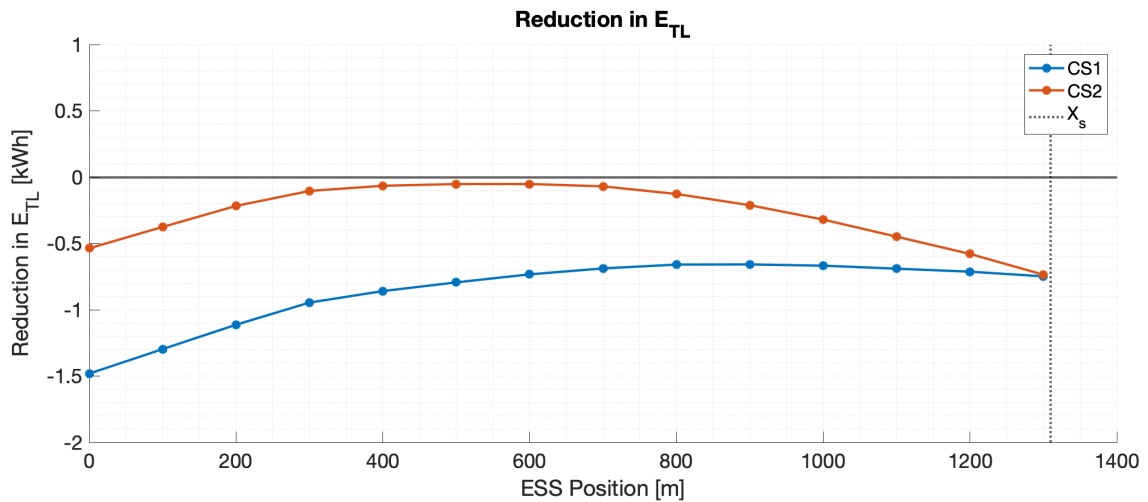


Figure 6.4: Reduction in transmission losses for section 24 in connected state

Table 6.2 shows an overview of the comparison between section 24 when it is isolated, and when connected to section 23. From this table one can conclude that only in the isolated situation, reduction of transmission losses by implementing stationary storage is possible in this section. Some clarifications for this result can be:

- The charge scheme does not consider the location of bus, but determines its set-point only on the substation power profiles. This may cause a scenario where energy is fed from the storage, while the distance from the feed-in point to the bus is smaller. In this situation, the transmission losses are increased.
- Connecting section 24 and 23 increases the natural sharing over regenerative braking energy between busses. This impacts the amount of transmission losses, even in the baseline simulation. With more natural sharing, less energy will be stored and discharged from the storage, resulting in less utilization of the storage when it might be beneficial for the reduction in transmission losses.

Table 6.2: Section 24 results for both connected and isolated operation

| $\Delta E$ [kWh] | Section 24 (isolated) |       | Section 24 |       |
|------------------|-----------------------|-------|------------|-------|
| E base [kWh]     | 22,45                 |       | 22,88      |       |
| x                | CS1                   | CS2   | CS1        | CS2   |
| EOL              | -0,25                 | 0,50  | -1,48      | -0,54 |
| EOL/2            | 0,07                  | 0,63  | -0,70      | -0,05 |
| FED              | -0,61                 | -0,61 | -0,75      | -0,75 |

| $\Delta E$ [%] | Section 24 (isolated) |        | Section 24 |        |
|----------------|-----------------------|--------|------------|--------|
| x              | CS1                   | CS2    | CS1        | CS2    |
| EOL            | -1,11%                | 2,23%  | -6,47%     | -2,36% |
| EOL/2          | 0,31%                 | 2,81%  | -3,06%     | -0,22% |
| FED            | -2,72%                | -2,72% | -3,28%     | -3,28% |

| $\Delta E$         | Section 24 (isolated) |       | Section 24 |        |
|--------------------|-----------------------|-------|------------|--------|
| x                  | CS1                   | CS2   | CS1        | CS2    |
| Max $\Delta$ [kWh] | 0,07                  | 0,63  | (0,70)     | (0,05) |
| Max $\Delta$ [%]   | 0,31%                 | 2,81% | -3,06%     | -0,22% |

### 6.1.4. Full grid results

The simulations on the reduction of transmission losses have been performed for the whole Arnhem grid. In these simulations, only the three positions as described in section 6.1.2 are be considered. Table 6.3.a shows the results of the full grid simulations. From this table one can see that in most of the sections in the Arnhem grid, reduction of transmission losses is not possible. In the cases where reduction is possible, the storage is placed either at the end of the section, of halfway the section. The reduction of transmission losses occurs when the distance of the storage to the bus is smaller than the distance from the feed-in point to the bus. When storage is placed at the feed-in point, no reduction is expected. table 6.3.a confirms this.

Table 6.3: Full grid simulations on reduction of transmission losses. a) Positive effect is green. b) row based colouring on optimal location per charge scheme (green is best, red is worst, orange is in between)

| a)                          |            |        |        | b)         |       |        |                             |
|-----------------------------|------------|--------|--------|------------|-------|--------|-----------------------------|
| $\Delta E$ [kWh]<br>Section | CS1<br>FED | EOL/2  | EOL    | CS2<br>FED | EOL/2 | EOL    | $\Delta E$ [kWh]<br>Section |
| 2                           | -2,60      | -1,56  | -3,66  | -2,60      | 1,25  | 1,43   | 2                           |
| 3                           | -2,52      | -2,98  | -4,58  | -2,52      | -1,88 | -2,91  | 3                           |
| 5                           | -0,29      | -0,28  | -0,62  | -0,29      | -0,22 | -0,46  | 5                           |
| 6                           | -0,17      | -0,14  | -0,27  | -0,17      | -0,09 | -0,16  | 6                           |
| 8                           | -0,18      | -0,15  | -0,19  | -0,18      | -0,15 | -0,17  | 8                           |
| 9                           | -3,88      | -2,65  | -6,62  | -3,88      | -2,08 | -4,39  | 9                           |
| 12                          | -3,54      | -2,14  | -4,81  | -3,54      | -1,72 | -3,38  | 12                          |
| 13                          | -2,41      | -0,62  | -2,59  | -2,41      | -0,61 | -1,88  | 13                          |
| 14                          | -3,46      | -10,10 | -19,34 | -3,46      | -5,97 | -11,95 | 14                          |
| 15                          | -8,47      | -3,36  | -10,27 | -8,47      | -2,77 | -6,57  | 15                          |
| 16                          | -5,27      | -3,15  | -7,65  | -5,27      | -1,65 | -3,93  | 16                          |
| 17                          | -4,83      | -5,17  | -10,82 | -4,83      | -1,40 | -4,33  | 17                          |
| 18                          | -4,40      | -4,57  | -11,21 | -4,40      | -1,05 | -4,04  | 18                          |
| 19                          | -0,61      | -0,81  | -2,35  | -0,61      | 0,32  | -0,64  | 19                          |
| 20                          | -0,64      | -0,12  | -0,91  | -0,64      | 0,47  | 0,16   | 20                          |
| 21                          | -0,45      | -1,23  | -2,29  | -0,45      | -0,96 | -1,83  | 21                          |
| 22                          | -1,18      | 0,32   | -0,56  | -1,18      | 1,30  | 1,15   | 22                          |
| 23                          | -1,08      | -1,04  | -1,48  | -1,08      | -0,86 | -1,11  | 23                          |
| 24                          | -1,08      | -0,79  | -1,76  | -1,08      | 0,06  | -0,49  | 24                          |
| 25                          | -0,77      | -0,21  | -1,55  | -0,77      | 0,89  | 0,51   | 25                          |
| 26                          | -2,26      | -1,95  | -4,33  | -2,26      | -1,01 | -2,46  | 26                          |
| 27                          | -1,94      | -3,65  | -6,56  | -1,94      | -2,39 | -4,30  | 27                          |
| 28                          | -3,61      | -3,93  | -6,88  | -3,61      | -2,67 | -4,55  | 28                          |
| 29                          | -3,42      | -1,99  | -4,46  | -3,42      | 0,74  | 0,30   | 29                          |
| 30                          | -3,27      | -4,20  | -7,15  | -3,27      | -1,83 | -2,94  | 30                          |
| 31                          | -3,66      | -2,17  | -5,41  | -3,66      | 0,33  | -1,05  | 31                          |
| 32                          | -1,93      | 0,02   | -0,85  | -1,93      | 2,60  | 3,70   | 32                          |
| 33                          | -2,52      | -3,14  | -5,87  | -2,52      | -1,25 | -2,32  | 33                          |
| 34                          | -2,50      | -6,59  | -14,65 | -2,50      | -3,71 | -9,89  | 34                          |
| 35                          | -3,68      | -7,92  | -12,59 | -3,68      | -6,24 | -9,48  | 35                          |
| 36                          | -2,83      | -2,95  | -5,88  | -2,83      | -1,91 | -3,57  | 36                          |
| 39                          | -3,74      | -2,60  | -3,88  | -3,74      | 0,85  | 1,19   | 39                          |
| 40                          | -3,37      | -5,19  | -9,36  | -3,37      | -3,33 | -6,13  | 40                          |
| 41                          | -2,34      | -3,87  | -7,46  | -2,34      | -2,27 | -4,39  | 41                          |
| 42                          | -1,18      | -0,75  | -2,10  | -1,18      | 0,69  | 0,43   | 42                          |
| 43                          | -1,26      | -1,50  | -2,64  | -1,26      | -1,06 | -1,75  | 43                          |
| 44                          | -0,20      | 0,02   | 0,02   | -0,20      | 0,32  | 0,52   | 44                          |
| 45                          | -0,22      | -0,37  | -0,58  | -0,22      | -0,31 | -0,50  | 45                          |
| 46                          | -0,52      | -1,06  | -1,67  | -0,52      | -0,95 | -1,47  | 46                          |
| 47                          | -0,54      | 0,12   | -0,33  | -0,54      | 0,85  | 0,92   | 47                          |
| 48                          | -0,73      | -0,69  | -2,07  | -0,73      | 0,09  | -0,94  | 48                          |
| 49                          | -0,75      | -1,20  | -2,24  | -0,75      | -0,75 | -1,48  | 49                          |

Also, in table 6.3.b the optimal location is indicated in green. This data can be used in further research, to indicate at which position the location has the best (or least negative) effect on the transmission losses when CS1 or CS2 are used in other applications (e.g. recuperation of regenerative braking energy). For both CS1 and CS2, one can see that the middle of the section has the best (or least negative) effect on the transmission losses.

### 6.1.5. CS2 for reduction of transmission losses and implementation of bus location

From the results in the previous sections, one can find that using stationary storage for the reduction of transmission losses is not always possible, and if reduction occurs, the absolute value of reduction is small compared to the baseline transmission losses. However CS2 performs better in the reduction of transmission losses than CS1. A clarification for this result can be that, since CS2 only supports the grid above a set threshold, supporting the grid on high power demands from a location closer to the bus is helping the reduction in transmission losses. Further research can be performed on the tuning of the parameters for CS2 to find higher reduction in the losses.

The small reduction in transmission losses can also be a result of the relative short sections in specifi-

cally the Arnhem grid. In the scenario where sections would be longer (e.g. other cities), transmission losses might play a bigger role in the total loss distribution in the grid, and therefore, implementing an ESS in this scenario might be more beneficial.

Since the bus location is an important parameter in the reduction of transmission losses, further research on location-dependent charge schemes might be performed.

## 6.2. Stationary storage storage for recuperation of braking energy

In this section, the results of the simulations focused on recuperation of regenerative braking energy are presented. First, the simulation setup is discussed including the seasonal variations that will be considered. The results will be presented for both charge schemes, and a comparison is made between them. Location and charge scheme parameters will remain fixed in these simulations, after which a recommendation will be made on the implementation of stationary storage in the Arnhem grid.

### 6.2.1. Simulation setup

The efficiency of the implementation of stationary storage for the recuperation of regenerative braking energy can be measured based on the reduction in total energy fed from the substation. When braking energy is stored and discharged after storing, the total amount of energy fed from the substation is expected to decrease. Both charge schemes will be considered using the following ESS assumptions:

- For CS2,  $P_{th}$  is set to 60 kW, thereby filtering out any HVAC demand and only support the grid when traction power is requested.
- The ESS is sized at 1 kWh, as proposed in section 4.7.3. The implemented charge schemes and their parameters will only store energy for a short time. For CS1, energy is fed back to the grid as soon as there is a request. Since  $P_{th}$  for CS2 is set relatively low, also in this charge scheme, no accumulation of energy is expected.
- Change in location on the section of the stationary storage is expected to only affect the transmission losses, therefore in these simulations the location on the section will be fixed. From table 6.3.b one can observe that for most sections, placing the storage halfway down the section has the best (or least negative) impact on the reduction of transmission losses. In the simulations focusing on the recuperation of regenerative braking the stationary storage will therefore be placed halfway down the section.

The seasonal changes in the power profiles of the busses, and the different schedules will have an impact on the amount of braking energy available for regenerative braking. First, since the number of busses is decreased in the summer, natural energy sharing is expected to decrease. This phenomena is in line with the results in section 5.6.2. Second, the share of braking energy will increase in summertime due to the fact that available regenerative braking power is first fed to the bus HVAC, of which the demand is smaller in summer. Therefore the energy available for storage will increase. In these simulations, the seasonal changes can be observed by looking at the difference in efficiency for the different scenarios.

### 6.2.2. Operation of stationary storage used for recuperation of braking energy.

The operation of the stationary storage can be analyzed looking at the simulated power profiles of the storage and the storage SOC. The actual reduction in substation energy can be observed by integrating the substation power profiles. Figure 6.5 shows an overview of the operation of the storage implemented in the simulated Arnhem grid. From this figure we can observe the following phenomena:

- Negative substation power indicates an excess of power in the grid. This energy will be burned in the braking resistors on the busses. From the power plot, one can see that, if stationary storage is implemented, no negative substation power is present. This indicates that (nearly) all braking resistor energy is stored.

- Mainly in summertime, reduction of peaks can be observed, indicating that the total substation energy is decreased. The decrease of these peaks is especially visible since in this specific simulation, CS2 is implemented, which can be tuned for peak reduction using the power threshold.
- The ESS positive (charge) power profiles are in line with the available braking power based on the negative values of the substation plot in the baseline simulation.
- The negative (discharge) power profiles are constant when discharging, which is in line with the fixed support power in CS2.
- SOC limits are not reached, indicating that the sizing is sufficient for the application.

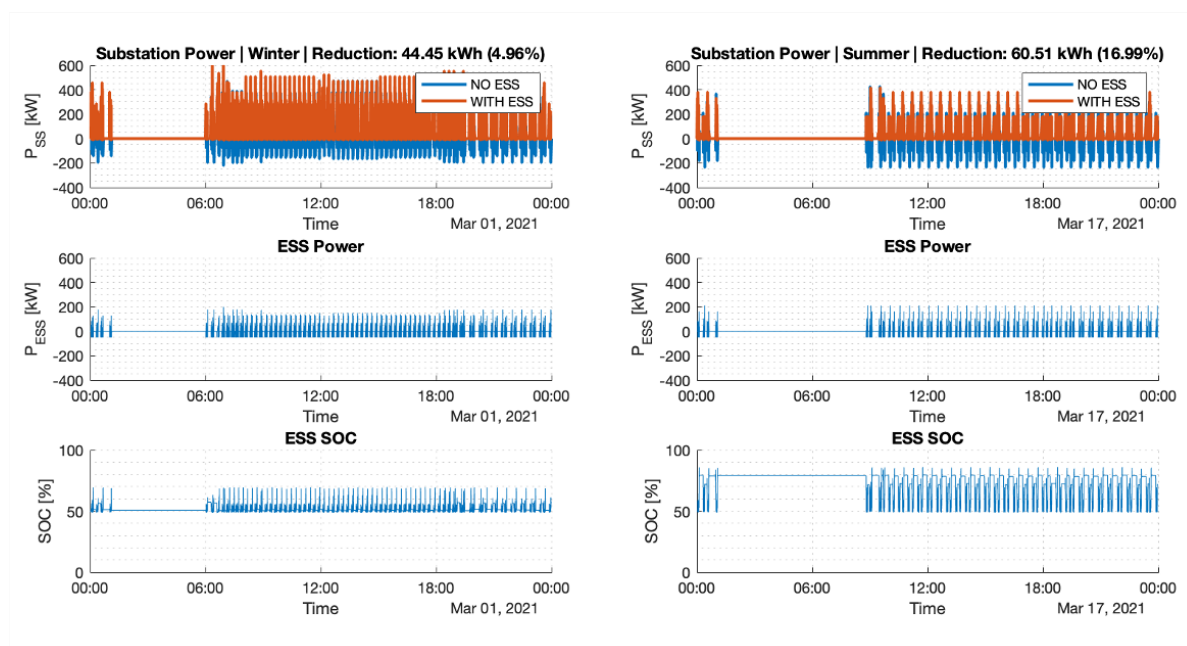


Figure 6.5: ESS Simulation results; CS2, 1-day full grid simulation, regular workday, max profiles

### 6.2.3. Full grid simulation

After confirming correct operation of the storage for the recuperation of braking energy, the simulation is performed for the full Arnhem grid. Table 6.4 shows the results for the reduction in total substation energy for all sections. The table shows reduction in total energy consumption for every scenario, and their seasonal weighted average. This weighted average is based on the occurrence of the timetables as described in section 3.5.1.

Table 6.4: Relative reduction in substation energy [%] for CS1 and CS2 implemented stationary storage. a) CS1 b) CS2 (Efficiency colouring from green to red, green is best, red is worse)

| ΔE CS1 | Winter  |          |        |         |          |        | Summer  |          |        |         |          |        | Average (weighted) [%] |
|--------|---------|----------|--------|---------|----------|--------|---------|----------|--------|---------|----------|--------|------------------------|
|        | S1      |          | S2     |         | S3       |        | S4      |          | S5     |         | S6       |        |                        |
|        | Regular | Saturday | Sunday |                        |
| 5      | 0,28    | 0,73     | 0,66   | 6,79    | 6,24     | 5,72   | 6,78    | 6,26     | 5,74   | 1,69    |          |        |                        |
| 6      | 0,28    | 0,73     | 0,66   | 6,82    | 6,26     | 5,75   | 6,80    | 6,29     | 5,78   | 1,70    |          |        |                        |
| 8      | 0,28    | 0,73     | 0,67   | 6,83    | 6,28     | 5,76   | 6,78    | 6,27     | 5,76   | 1,70    |          |        |                        |
| 9      | 1,64    | 2,28     | 3,01   | 8,79    | 9,45     | 8,81   | 8,74    | 9,10     | 8,71   | 3,39    |          |        |                        |
| 12     | 1,65    | 2,28     | 3,03   | 8,84    | 9,48     | 8,87   | 8,79    | 9,13     | 8,75   | 3,40    |          |        |                        |
| 36     | 1,64    | 2,27     | 3,00   | 8,76    | 9,38     | 8,77   | 8,74    | 9,09     | 8,70   | 3,39    |          |        |                        |
| 26     | 3,43    | 4,03     | 4,59   | 11,12   | 9,85     | 9,83   | 11,15   | 9,86     | 9,88   | 5,24    |          |        |                        |
| 27     | 3,39    | 3,99     | 4,55   | 11,07   | 9,75     | 9,76   | 11,15   | 9,81     | 9,81   | 5,22    |          |        |                        |
| 41     | 3,39    | 4,00     | 4,57   | 11,06   | 9,82     | 9,81   | 11,18   | 9,94     | 9,94   | 5,24    |          |        |                        |
| 33     | 5,42    | 6,63     | 8,51   | 17,57   | 17,26    | 17,24  | 17,26   | 17,40    | 17,36  | 8,52    |          |        |                        |
| 34     | 5,36    | 6,52     | 8,37   | 17,32   | 17,02    | 17,04  | 17,31   | 17,40    | 17,45  | 8,53    |          |        |                        |
| 14     | 8,49    | 9,19     | 10,05  | 14,17   | 15,58    | 15,59  | 13,72   | 14,85    | 14,80  | 9,92    |          |        |                        |
| 15     | 8,66    | 9,31     | 10,25  | 14,42   | 15,85    | 15,90  | 13,65   | 14,82    | 14,79  | 9,88    |          |        |                        |
| 16     | 8,68    | 9,28     | 10,27  | 14,40   | 15,87    | 15,92  | 13,71   | 14,90    | 14,86  | 9,94    |          |        |                        |
| 42     | 3,87    | 4,55     | 4,64   | 15,30   | 15,22    | 13,81  | 15,39   | 15,30    | 14,00  | 6,47    |          |        |                        |
| 43     | 3,85    | 4,51     | 4,61   | 15,19   | 15,23    | 13,81  | 15,19   | 15,14    | 13,88  | 6,37    |          |        |                        |
| 30     | 8,87    | 8,80     | 7,77   | 19,22   | 18,15    | 17,47  | 18,93   | 17,70    | 17,29  | 10,88   |          |        |                        |
| 31     | 8,96    | 8,91     | 7,81   | 19,34   | 18,16    | 17,43  | 19,10   | 17,85    | 17,32  | 10,99   |          |        |                        |
| 39     | 10,33   | 12,20    | 10,33  | 18,68   | 17,33    | 16,37  | 18,11   | 16,75    | 16,51  | 12,20   |          |        |                        |
| 40     | 10,29   | 12,09    | 10,29  | 18,42   | 17,12    | 16,27  | 17,74   | 16,44    | 16,30  | 12,00   |          |        |                        |
| 17     | 14,50   | 15,14    | 16,71  | 25,12   | 25,48    | 25,57  | 22,60   | 22,23    | 22,17  | 16,80   |          |        |                        |
| 18     | 14,57   | 15,21    | 16,83  | 25,05   | 25,42    | 25,50  | 22,78   | 22,38    | 22,35  | 16,88   |          |        |                        |
| 35     | 14,38   | 15,03    | 16,62  | 24,87   | 25,24    | 25,32  | 22,28   | 21,91    | 21,86  | 16,50   |          |        |                        |
| 48     | 3,49    | 4,09     | 3,64   | 11,78   | 12,83    | 10,77  | 11,96   | 13,03    | 10,93  | 5,39    |          |        |                        |
| 49     | 3,51    | 4,06     | 3,64   | 11,72   | 12,80    | 10,83  | 11,92   | 13,04    | 11,05  | 5,37    |          |        |                        |
| 13     | 4,96    | 5,34     | 5,14   | 12,66   | 12,73    | 11,86  | 10,66   | 11,76    | 11,09  | 6,25    |          |        |                        |
| 19     | 4,95    | 5,32     | 5,09   | 12,83   | 12,84    | 11,91  | 10,97   | 12,05    | 11,34  | 6,37    |          |        |                        |
| 28     | 9,15    | 10,24    | 13,04  | 21,72   | 21,19    | 22,84  | 20,45   | 19,36    | 21,60  | 12,24   |          |        |                        |
| 29     | 9,28    | 10,26    | 12,99  | 21,58   | 21,02    | 22,67  | 20,71   | 19,60    | 21,94  | 12,47   |          |        |                        |
| 2      | 8,29    | 8,42     | 7,97   | 12,38   | 14,61    | 14,67  | 12,68   | 15,00    | 14,97  | 9,48    |          |        |                        |
| 3      | 8,22    | 8,36     | 7,92   | 12,18   | 14,38    | 14,47  | 12,24   | 14,53    | 14,56  | 9,21    |          |        |                        |
| 25     | 6,75    | 7,28     | 7,21   | 21,81   | 21,01    | 20,80  | 22,17   | 21,37    | 21,13  | 10,12   |          |        |                        |
| 23     | 4,87    | 5,44     | 6,45   | 16,64   | 16,57    | 16,66  | 16,71   | 16,65    | 16,68  | 7,61    |          |        |                        |
| 24     | 4,87    | 5,43     | 6,37   | 16,69   | 16,61    | 16,69  | 16,99   | 16,91    | 16,94  | 7,72    |          |        |                        |
| 22     | 5,59    | 5,76     | 6,98   | 13,54   | 15,25    | 14,78  | 13,91   | 15,60    | 15,12  | 7,68    |          |        |                        |
| 32     | 9,55    | 10,36    | 10,35  | 18,31   | 19,21    | 18,43  | 18,89   | 19,76    | 19,05  | 11,97   |          |        |                        |
| 44     | 1,37    | 1,37     | 1,42   | 8,13    | 6,79     | 6,77   | 8,25    | 6,92     | 6,90   | 2,77    |          |        |                        |
| 45     | 1,34    | 1,34     | 1,40   | 8,20    | 6,83     | 6,82   | 8,15    | 6,89     | 6,87   | 2,73    |          |        |                        |
| 20     | 5,45    | 6,17     | 5,42   | 11,20   | 11,09    | 10,67  | 11,17   | 11,21    | 10,77  | 6,78    |          |        |                        |
| 21     | 5,38    | 6,11     | 5,35   | 11,10   | 11,01    | 10,57  | 11,01   | 11,08    | 10,65  | 6,67    |          |        |                        |
| 46     | 6,82    | 6,72     | 6,80   | 21,89   | 21,56    | 21,85  | 22,10   | 21,79    | 22,04  | 9,98    |          |        |                        |
| 47     | 6,98    | 6,87     | 6,97   | 22,13   | 21,80    | 22,11  | 22,18   | 21,86    | 22,12  | 10,25   |          |        |                        |

From table 6.4 the following phenomena can be observed:

- In general, as expected, the efficiency of the stationary storage is higher in the summer. This is caused due to the increase in excess energy in the sections.
- Sections that are connected to the same substation are performing nearly the same. This is expected due to the fact that energy (and thus also excess regenerative braking energy) can be shared between these sections. A storage implemented in efficiency lies in the change in transmission losses, which, compared to the total energy are small.

A deeper analysis on the efficiency of the storage is performed by looking at known parameters of the connected sections. Figure 6.6 shows two scatter plots of known section data versus ESS efficiency. The first plot shows a negative exponential trend on the efficiency in relation with the section utilisation. The second plots shows a linear trend between the amount of braking resistor energy and the storage efficiency. When the energy consumption of the braking resistor would be measured in every section a recommendation can be made on high efficiency sections.

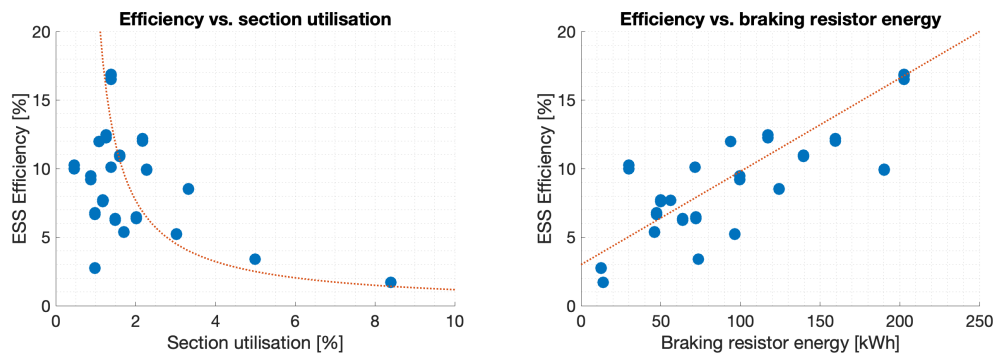


Figure 6.6: Analysis on ESS efficiency in different sections based on known section parameters.

In order to get insights in the differences between the performance of CS1 and CS2, table 6.5 shows the difference between the reduction in total substation energy for every section. This table also shows the weighted amount of braking energy available in the section. From this data one can observe that the differences between CS1 and CS2 are small. This is mainly because the parameters for CS2 have been set to a relative small threshold value, and therefore the peak reducing abilities of this charge scheme are not utilized optimal. In most scenarios CS1 performs better. It can be observed that for sections with high braking energy, CS1 always performs better.

Table 6.5: Comparing difference in substation energy reduction between implementation of CS1 and CS2, row coloured on efficiency, green is better

| AE CS1/2 | Winter  |          |        | Summer  |          |        | E_br<br>(measured+weighed)<br>(kWh) |
|----------|---------|----------|--------|---------|----------|--------|-------------------------------------|
|          | S1      | S2       | S3     | S4      | S5       | S6     |                                     |
|          | Regular | Saturday | Sunday | Regular | Saturday | Sunday |                                     |
| 5        | 0,00    | 0,00     | 0,00   | 0,01    | -0,02    | -0,02  | 36,68                               |
| 6        | 0,00    | 0,00     | -0,01  | 0,02    | -0,03    | -0,03  | 36,68                               |
| 8        | 0,00    | 0,00     | 0,00   | 0,05    | 0,01     | 0,00   | 36,68                               |
| 9        | -0,02   | -0,01    | -0,02  | 0,05    | 0,35     | 0,10   | 95,4                                |
| 12       | -0,01   | -0,01    | -0,01  | 0,05    | 0,35     | 0,12   | 95,4                                |
| 36       | -0,02   | -0,03    | -0,03  | 0,02    | 0,29     | 0,07   | 95,4                                |
| 26       | -0,04   | -0,05    | -0,05  | -0,03   | -0,01    | -0,05  | 100,78                              |
| 27       | -0,05   | -0,06    | -0,07  | -0,08   | -0,06    | -0,05  | 100,78                              |
| 41       | -0,07   | -0,06    | -0,07  | -0,12   | -0,12    | -0,13  | 100,78                              |
| 33       | -0,09   | -0,08    | -0,10  | 0,31    | -0,14    | -0,12  | 124,19                              |
| 34       | -0,14   | -0,20    | -0,27  | 0,01    | -0,38    | -0,41  | 124,19                              |
| 14       | 0,02    | 0,07     | -0,04  | 0,45    | 0,73     | 0,79   | 180,04                              |
| 15       | 0,21    | 0,29     | 0,16   | 0,77    | 1,03     | 1,11   | 180,04                              |
| 16       | 0,17    | 0,20     | 0,10   | 0,69    | 0,97     | 1,06   | 180,04                              |
| 42       | -0,08   | -0,06    | -0,08  | -0,09   | -0,08    | -0,19  | 78,07                               |
| 43       | -0,02   | -0,04    | -0,02  | 0,00    | 0,09     | -0,07  | 78,07                               |
| 30       | -0,17   | -0,16    | -0,14  | 0,29    | 0,45     | 0,18   | 118,17                              |
| 31       | -0,18   | -0,16    | -0,18  | 0,24    | 0,31     | 0,11   | 118,17                              |
| 39       | -0,09   | -0,08    | -0,09  | 0,57    | 0,58     | -0,14  | 148,02                              |
| 40       | 0,01    | 0,07     | 0,01   | 0,68    | 0,68     | -0,03  | 148,02                              |
| 17       | -0,30   | -0,26    | -0,24  | 2,52    | 3,25     | 3,40   | 171,23                              |
| 18       | -0,28   | -0,25    | -0,22  | 2,27    | 3,04     | 3,15   | 171,23                              |
| 35       | -0,13   | -0,06    | -0,04  | 2,59    | 3,33     | 3,46   | 171,23                              |
| 48       | -0,07   | -0,09    | -0,05  | -0,18   | -0,20    | -0,16  | 48,47                               |
| 49       | -0,04   | -0,05    | -0,05  | -0,20   | -0,24    | -0,22  | 48,47                               |
| 13       | 0,00    | 0,00     | 0,00   | 2,00    | 0,97     | 0,77   | 67,42                               |
| 19       | -0,09   | -0,10    | -0,12  | 1,86    | 0,79     | 0,57   | 67,42                               |
| 28       | -0,11   | -0,06    | -0,04  | 1,27    | 1,83     | 1,24   | 109,79                              |
| 29       | -0,24   | -0,17    | -0,25  | 0,87    | 1,42     | 0,73   | 109,79                              |
| 2        | -0,26   | -0,24    | -0,25  | -0,30   | -0,39    | -0,30  | 80,19                               |
| 3        | -0,10   | -0,10    | -0,10  | -0,06   | -0,15    | -0,09  | 80,19                               |
| 25       | -0,12   | -0,11    | -0,09  | -0,36   | -0,36    | -0,33  | 68,04                               |
| 23       | -0,01   | 0,00     | 0,01   | -0,07   | -0,08    | -0,02  | 49,72                               |
| 24       | -0,09   | -0,09    | -0,11  | -0,30   | -0,30    | -0,25  | 49,72                               |
| 22       | -0,11   | -0,13    | -0,20  | -0,37   | -0,35    | -0,34  | 49,32                               |
| 32       | -0,29   | -0,31    | -0,37  | -0,58   | -0,55    | -0,62  | 80,71                               |
| 44       | -0,03   | -0,04    | -0,03  | -0,12   | -0,13    | -0,13  | 15,5                                |
| 45       | -0,01   | -0,01    | -0,01  | -0,05   | -0,06    | -0,05  | 15,5                                |
| 20       | -0,08   | -0,10    | -0,08  | 0,03    | -0,12    | -0,10  | 47,69                               |
| 21       | -0,04   | -0,04    | -0,06  | 0,09    | -0,07    | -0,08  | 47,69                               |
| 46       | -0,02   | -0,03    | -0,04  | -0,21   | -0,23    | -0,19  | 27,56                               |
| 47       | -0,19   | -0,20    | -0,20  | -0,05   | -0,06    | -0,01  | 27,56                               |

### 6.3. Stationary storage for increased substation capacity

In section 6.2 the main goal is to maximize the recuperation of braking energy by storing the energy in the ESS and reuse it when needed. In order for this principle to work, the ESS should be sized sufficient and the SOC has to remain below the maximum SOC in order to store energy at all times. It is shown that for the recuperation of braking energy, CS1 performs better than CS2. The aggressive method of charge and discharge of the ESS seems to be the best method looking at maximizing the recuperation of braking energy. Whereas CS1 is better in recuperation of braking energy, it does not have any parameters to tune the charge scheme for other services. CS2 does have these parameters, and thus can be tuned for different applications than maximizing recuperation alone.

From the analysis in chapter 5, it is found that the substations are not overloaded regularly, but a lot of capacity of the substation is used only for some (not often occurring) peaks in the power demand. These peaks make the implementation of constant power loads (for example EV chargers) to the trolley-grid impossible. Figure 6.7 shows the substation power over a day with and without the implementation of a tuned charge scheme, assuming an empty ESS at the start of the day. For this specific substation, the maximum power is 800 kW. The headroom that is available for the implementation of constant power loads is indicated by the purple box. For this specific scenario, roughly 120 kW is available for these loads, but this limitation only originates from the power demand peak in the morning.

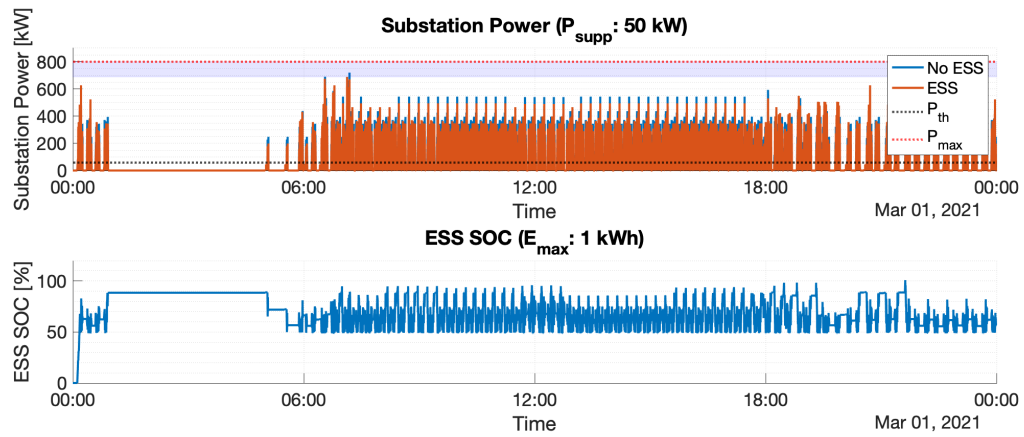


Figure 6.7: Substation headroom without tuned threshold

In CS2, two parameters are available for tuning.  $P_{th}$  determines the threshold of total power demand from which the storage is going to inject a set power ( $P_{set}$ ) into the grid. These parameters give the possibility to tune the charge scheme in order to only support on large power peaks, thereby possibly increasing the substation headroom. Figure 6.8 shows the results of a simulation where the charge schema is specifically tuned to focus on the high power demand peaks. Again, the headroom for constant power loads is indicated by the purple box. In this scenario, one can see that the headroom is extended significant, now opening the opportunity to implement constant power loads to the grid.

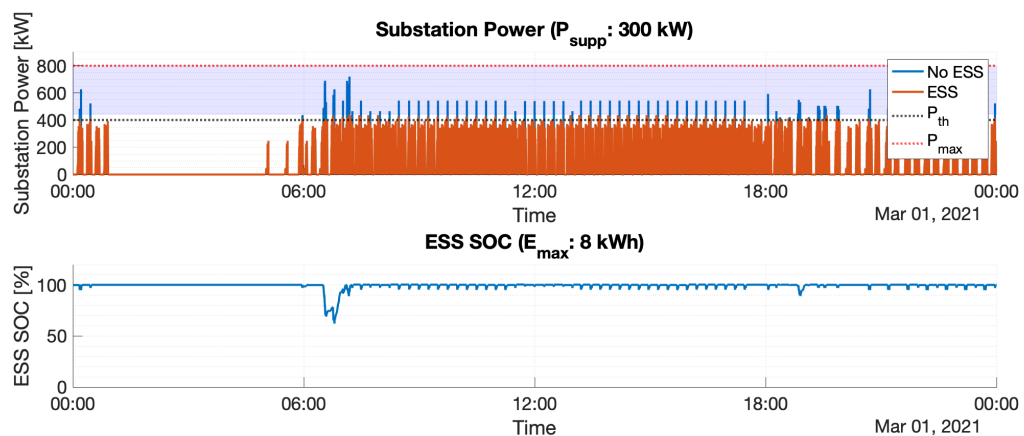


Figure 6.8: Substation headroom with tuned threshold

## 6.4. Recommendation on sizing

In order to size the storage properly, one can use the results from the extremes of all scenario simulations with (assumed) infinite SOC. Since the complete behaviour of the storage can be simulated, the maximal deviation of the storage SOC in both positive and negative directions can be used as a base for the optimal size. Keeping in mind the limitations of the storage medium (20% - 80% SOC), one can use equation 6.1 to determine the optimal size.

Figure 6.9 shows the ESS operation and SOC when no sizing is performed (and thus infinite storage  $C_{\infty}$  is assumed). This SOC profile can be used in combination with equation 6.1 to determine the optimal size of the storage. In this equation, the utilized part of the storage, indicated by the maximum SOC deviation gives the factor of  $C_{\infty}$  to size the storage. In order to compensate for the SOC limits this size is resized with a factor of 1.4 (hereby increasing the size by 40%, 2 times 20% for each limit).

$$C_{opt} = 1.2C_{\infty} \cdot \frac{50 - \max(\Delta SOC)}{100} \text{ [kWh]} \quad (6.1)$$

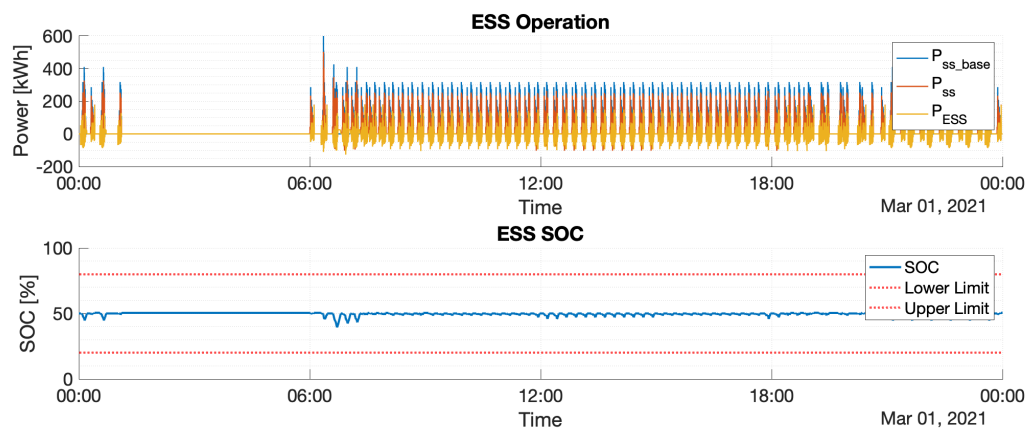


Figure 6.9: ESS Operation with over-sized storage

Figure 6.10 shows the results after sizing the storage using equation 6.1. In this plot one can see that the sizing is sufficient to not violate any SOC limitations.

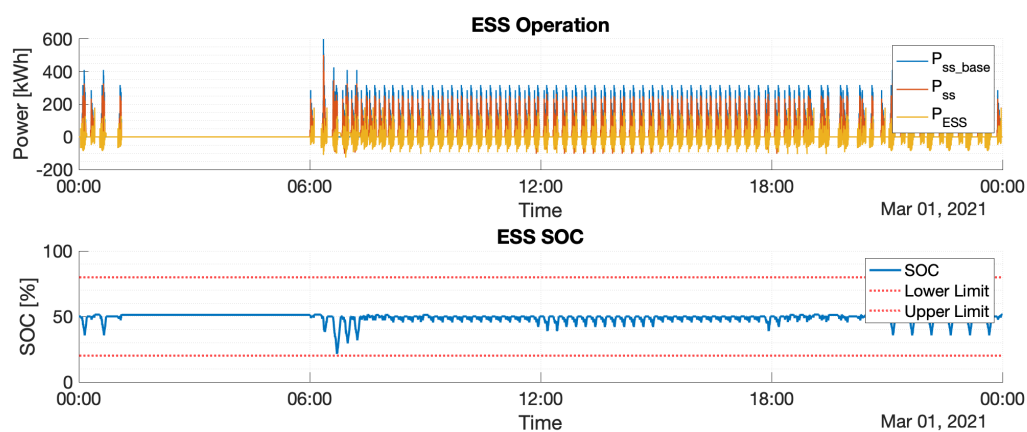


Figure 6.10: ESS Operation with properly sized storage

## 6.5. Conclusions

This chapter discussed the results of the implementation of stationary storage for different use-cases. From the results, one can conclude that;

- Using stationary ESS only for reduction of transmission losses with CS1 or CS2 is not beneficial due to the small impact on the total energy consumption when compared to the situation without storage implemented.
- When stationary ESS is implemented, the best (or least negative) impact on the reduction of the transmission losses is when it is positioned halfway down the line.
- The section substation relationship has a negative effect on the reduction of transmission losses using stationary ESS since the proposed charge schemes are not a function of the bus location.
- Placing stationary ESS for the increase of recuperation of braking energy is beneficial. Up to 17% of reduction in substation energy can be achieved in some sections with high braking resistor utilisation. The reduction of total substation energy is related to the amount of excess energy in the section (or connected sections).
- Implemented storage with parameters for CS2 set to maximum recuperation of braking energy gives worse results than with CS1. However CS2 has multiple parameters, so it can be tuned for other services as well.

- CS2 allows tuning for specific applications apart from maximum recuperation. Tuning this charge scheme allows an increase of substation power headroom for the application of constant power loads on the trolley-grid like EV chargers or the implementation of in-motion charging busses
- A method has been presented to determine proper sizing from the simulation results, not violating any of the SOC limitations of the storage medium.

The next chapter will combine the baseline results from chapter 5 and the results from chapter 6 in order to answer the research questions and give specific recommendations for the Arnhem grid.

# 7

## Conclusions

*This chapter describes main conclusions regarding the simulation results. Recommendations for further work are given and the research questions are answered.*

The implementation of stationary storage and some of the design parameters of these systems are simulated using the Arnhem grid as a case study. First, the available data-set of the Arnhem grid was explored in chapter 3, an analysis has been performed on the grid without the implementation of storage in order to get insights in the operation in chapter 5. Next, stationary storage systems were implemented in the simulation framework and the results were presented in chapter 6. The main objectives discussed are;

- Reduction of the braking power lost in the on-board braking resistor
- Reduction of transmission losses in the catenary wires
- Increase of substation headroom for the implementation of constant power loads on the trolley-grid such as EV chargers or the implementation of in-motion charging busses

Furthermore, a recommendation can be made on sizing and location of storage from the results of the simulation.

### 7.1. Grid analysis

From the baseline simulation of the Arnhem grid, the following conclusions can be found. First, the combination of scheduling and seasonal power profile changes determines the share in excess energy. These factors are found to be not independent. Second, simulation shows that the transmission losses are nearly constant while using different schedules and (seasonal changing) power profiles. Lastly, extending the grid with for example EV chargers is limited by some (rare) peaks in substation current demand.

From this data **RQ1** can be answered:

***RQ1:*** *What is the magnitude of transmission losses and braking resistor energy distribution in the Arnhem grid?*

It is found that in the Arnhem grid, the transmission losses are at the same level throughout the year for both seasonal changing power profiles and scheduling. On average, the transmission losses are 3%, thereby not having a significant impact on the total energy consumption. The braking resistor energy distribution is determined by the combination of scheduling and seasonal changes. These factors are found to be not independent.

Since the results on transmission losses are dependent on the section lengths, this conclusion is only valid for the investigated Arnhem grid. Grid setups with longer sections will be subject to a larger amount of transmission losses.

## 7.2. Reduction of transmission losses

Using stationary ESS only for reduction of transmission losses with the proposed charge schemes is not beneficial due to the small impact on the total energy consumption. In most cases, when stationary storage is implemented, the best (or least negative) impact on the reduction of the transmission losses is when it is positioned halfway down the line. The section substation relationship has a negative effect on the reduction of transmission losses using stationary ESS since the proposed charge schemes do not consider the actual bus location.

From this data **RQ2** can be answered:

**RQ2:** *What is the location, size and charge schema of stationary storage to allow the minimal transmission losses?*

It is found that in the Arnhem grid, using stationary storage only for the reduction of transmission losses with the proposed charge schemes is not beneficial. Only in some cases reduction is possible, but in most cases placing storage for this purpose only increases the transmission losses. However, this study shows that, in most cases, when the storage is placed halfway down the line, the decrease (or least increase) of transmission losses is minimal. A method for sizing of the storage is presented based on the maximum available braking energy. It is important to mention that the proposed charge schemes do not consider the bus location, making them less beneficial for the reduction of transmission losses. Research can be performed on schemes that do include the bus positions.

## 7.3. Maximal recuperation of braking energy

Placing stationary storage systems for the increase of recuperation of braking energy is beneficial. Up to 17% of reduction in substation energy can be achieved in some sections. The reduction of total substation energy is related to the amount of excess energy in the section (or connected sections). Two charge schemes are proposed in this work. The first charge scheme (CS1) charges any time there is excess energy in the grid, and discharges as soon as there is a power demand on the connected section. The second charge scheme (CS2) charges any time there is excess energy in the grid, but only discharges if the section demand is above a set threshold. Implemented storage with parameters for CS2 set to maximum recuperation of braking energy gives worse results than with CS1. However, since CS2 has more parameters, it can be tuned for other services as well.

From this data **RQ3** can be answered:

**RQ3:** *What is the location, size and charge schema of stationary storage to allow the maximum recuperation of regenerative braking energy?*

It is found that, for the Arnhem grid, the maximum recuperation of braking energy can be achieved using an aggressive charge scheme that charges **only** when any excess energy is available, and discharges when there is an energy demand. Up to 17% of reduction in substation energy can be achieved in some sections with high braking resistor utilisation. A method for sizing of the storage is presented which is a function of the maximum available braking energy.

## 7.4. Increase of grid power capacity

The presented tuneable charge scheme, CS2, allows tuning for specific applications apart from maximum recuperation. Tuning this charge scheme allows increase of substation power headroom for the application of constant power loads on the trolley-grid such as EV chargers or the implementation of in-motion charging busses.

# Bibliography

- [1] *Translink Library*, 2020 (accessed June 11, 2020). URL <https://www.translink.nl/library>.
- [2] Parthena Apostolidou and N.P. Papanikolaou. Energy saving estimation of athens trolleybuses considering regenerative braking and improved control scheme. *Resources*, 7, 07 2018. doi: 10.3390/resources7030043.
- [3] Ricardo Barrero, Joeri Van Mierlo, and Xavier Tackoen. Energy savings in public transport. *IEEE vehicular technology magazine*, 3(3):26–36, 2008.
- [4] Mikołaj Bartłomiejczyk. Smart grid technologies in electric power supply systems of public transport. *Transport*, 180:1144–1154, 2017.
- [5] Mikołaj Bartłomiejczyk, Roman Hrbáč, Vítězslav Stýskala, and Marcin Połom. Trolleybus with traction batteries for autonomous running. 2013.
- [6] M. Bartłomiejczyk. Practical application of in motion charging: Trolleybuses service on bus lines. In *2017 18th International Scientific Conference on Electric Power Engineering (EPE)*, pages 1–6, 2017.
- [7] Mikołaj Bartłomiejczyk. Super capacitor energy bank medcom ucer-01 in gdynia trolleybus system. pages 2124–2128, 10 2016. doi: 10.1109/IECON.2016.7793086.
- [8] Mikołaj Bartłomiejczyk and Slobodan Mircevski. Reducing of energy consumption in public transport — results of experimental exploitation of super capacitor energy bank in gdynia trolleybus system. 09 2014. doi: 10.1109/EPEPEMC.2014.6980616.
- [9] Mikołaj Bartłomiejczyk and Marcin Połom. Spatial aspects of tram and trolleybus supply system. pages 211–215, 09 2015.
- [10] Dirk Baumeister, M Salih, M Wazifehdust, P Steinbusch, M Zdrallek, S Mour, L Lenuweit, P Deskovic, and H Ben Zid. Modelling and simulation of a public transport system with battery-trolleybuses for an efficient e-mobility integration. In *1st E-Mobility Power System Integration Symposium*, 2017.
- [11] J Belt, V Utgikar, and I Bloom. Calendar and phev cycle life aging of high-energy, lithium-ion cells containing blended spinel and layered-oxide cathodes. *Journal of Power Sources*, 196(23): 10213–10221, 2011.
- [12] Ira Bloom, BW Cole, JJ Sohn, Scott A Jones, Edward G Polzin, Vincent S Battaglia, Gary L Henriksen, Chester Motloch, Richardson Richardson, T Unkelhaeuser, et al. An accelerated calendar and cycle life study of li-ion cells. *Journal of power sources*, 101(2):238–247, 2001.
- [13] Breng. Dienstregeling 2019, arnhem stad. 2019.
- [14] Ricardo de Castro, Claudio Pinto, Rui Esteves Araújo, Pedro Melo, and Diamantino Freitas. Optimal sizing and energy management of hybrid storage systems. In *2012 IEEE Vehicle Power and Propulsion Conference*, pages 321–326. IEEE, 2012.
- [15] Eugenio Faggioli, Piergeorgio Rena, Veronique Danel, X Andrieu, Ronald Mallant, and Hans Kahlen. Supercapacitors for the energy management of electric vehicles. *Journal of Power Sources*, 84(2):261–269, 1999.
- [16] Pablo García, Juan P Torreglosa, Luis M Fernández, and Francisco Jurado. Control strategies for high-power electric vehicles powered by hydrogen fuel cell, battery and supercapacitor. *Expert Systems with Applications*, 40(12):4791–4804, 2013.

- [17] Nima Ghaviha, Javier Campillo, Markus Bohlin, and Erik Dahlquist. Review of application of energy storage devices in railway transportation. *Energy Procedia*, 105:4561–4568, 2017.
- [18] Catalin Goia, Luiza Popa, Claudia Popescu, and Mihai Octavian Popescu. Supercapacitors used as an energy source to drive the short urban electric vehicles. In *2011 7TH INTERNATIONAL SYMPOSIUM ON ADVANCED TOPICS IN ELECTRICAL ENGINEERING (ATEE)*, pages 1–6. IEEE, 2011.
- [19] Štefan Hamacek, Mikołaj Bartłomiejczyk, Roman Hrbáč, Stanislav Mišák, and Vítězslav Stýskala. Energy recovery effectiveness in trolleybus transport. *Electric Power Systems Research*, 112: 1–11, 2014.
- [20] Štefan Hamacek, Mikołaj Bartłomiejczyk, Roman Hrbáč, Stanislav Mišák, and Vítězslav Stýskala. Energy recovery effectiveness in trolleybus transport. *Electric Power Systems Research*, 112: 1–11, 2014.
- [21] A Hammar, Pascal Venet, Richard Lallemand, Gerard Coquery, and Gerard Rojat. Study of accelerated aging of supercapacitors for transport applications. *IEEE transactions on industrial electronics*, 57(12):3972–3979, 2010.
- [22] Xuebing Han, Minggao Ouyang, Languang Lu, and Jianqiu Li. A comparative study of commercial lithium ion battery cycle life in electric vehicle: Capacity loss estimation. *Journal of Power Sources*, 268:658–669, 2014.
- [23] Victor Isaac Herrera, Aitor Milo, Haizea Gaztañaga, Javier Ramos, and Haritza Camblong. Adaptive and non-adaptive strategies for optimal energy management and sizing of a dual storage system in a hybrid electric bus. *IEEE Transactions on Intelligent Transportation Systems*, 20(9): 3435–3447, 2018.
- [24] D. Iannuzzi, P. Pighetti, and P. Tricoli. A study on stationary supercapacitor sets for voltage droops compensation of streetcar feeder lines. In *Electrical Systems for Aircraft, Railway and Ship Propulsion*, pages 1–8, 2010.
- [25] Diego Iannuzzi, Flavio Ciccarelli, and Davide Lauria. Stationary ultracapacitors storage device for improving energy saving and voltage profile of light transportation networks. *Transportation Research Part C: Emerging Technologies*, 21(1):321–337, 2012.
- [26] Diego Iannuzzi, Davide Lauria, and Pietro Tricoli. Optimal design of stationary supercapacitors storage devices for light electrical transportation systems. *Optimization and Engineering*, 13(4): 689–704, 2012.
- [27] Walter Lhomme, Philippe Delarue, Philippe Barrade, Alain Bouscayrol, and Alfred Rufer. Design and control of a supercapacitor storage system for traction applications. In *Fourtieth IAS Annual Meeting. Conference Record of the 2005 Industry Applications Conference, 2005.*, volume 3, pages 2013–2020. IEEE, 2005.
- [28] M. Połom M. Bartłomiejczyk. Nowoczesna koncepcja rozwoju transportu trolejbusowego : projekt slide-In, autobusy (modern concept of development of trolleybus transport: Slide-In project,). 2015.
- [29] Fabian Meishner and Dirk Uwe Sauer. Wayside energy recovery systems in dc urban railway grids. *eTransportation*, 1:100001, 2019. ISSN 2590-1168. doi: <https://doi.org/10.1016/j.etrans.2019.04.001>. URL <http://www.sciencedirect.com/science/article/pii/S2590116819300013>.
- [30] Joachim J Mwambeleko, Thanatchai Kulworawanichpong, and Kenedy A Greyson. Tram and trolleybus net traction energy consumption comparison. In *2015 18th International Conference on Electrical Machines and Systems (ICEMS)*, pages 2164–2169. IEEE, 2015.
- [31] Gholam-Abbas Nazri and Gianfranco Pistoia. *Lithium batteries: science and technology*. Springer Science & Business Media, 2008.

- [32] Noshin Omar, Mohamed Abdel Monem, Yousef Firouz, Justin Salminen, Jelle Smekens, Omar Hegazy, Hamid Gaulous, Grietus Mulder, Peter Van den Bossche, Thierry Coosemans, et al. Lithium iron phosphate based battery—assessment of the aging parameters and development of cycle life model. *Applied Energy*, 113:1575–1585, 2014.
- [33] D. Haskins D. K. G. Mackinger M. Pandion A. Randacher D. Steiner P. G. Andersson, D. W. Backhaus and Y. Tremblay. *How to build and operate an efficient trolleybus system*. 2015.
- [34] T. Ratniyomchai, S. Hillmansen, and P. Tricoli. Optimal capacity and positioning of stationary supercapacitors for light rail vehicle systems. In *2014 International Symposium on Power Electronics, Electrical Drives, Automation and Motion*, pages 807–812, 2014.
- [35] Alexandre Ravey, Nicolas Watrin, Benjamin Blunier, David Bouquain, and Abdellatif Miraoui. Energy-source-sizing methodology for hybrid fuel cell vehicles based on statistical description of driving cycles. *IEEE Transactions on Vehicular Technology*, 60(9):4164–4174, 2011.
- [36] Alexandre Ravey, Robin Roche, Benjamin Blunier, and Abdellatif Miraoui. Combined optimal sizing and energy management of hybrid electric vehicles. In *2012 IEEE Transportation Electrification Conference and Expo (ITEC)*, pages 1–6. IEEE, 2012.
- [37] Rehda Sadoun, Nassim Rizoug, P Bartholomeüs, B Barbedette, and Philippe Le Moigne. Influence of the drive cycles on the sizing of hybrid storage system battery-supercapacitor supplying an electric vehicle. In *IECON 2011-37th Annual Conference of the IEEE Industrial Electronics Society*, pages 4106–4112. IEEE, 2011.
- [38] Bram Scheurwater. The potential of renewable energy sources for powering of trolleybus grids: An arnhem case-study. 11 2020.
- [39] Junyi Shen, Serkan Dusmez, and Alireza Khaligh. Optimization of sizing and battery cycle life in battery/ultracapacitor hybrid energy storage systems for electric vehicle applications. *IEEE Transactions on industrial informatics*, 10(4):2112–2121, 2014.
- [40] K. Shiokawa and R. Takagi. Numerical optimisation of the charge/discharge characteristics of way-side energy storage systems by the embedded simulation technique using the railway power network simulator rtss. pages 583–592, 09 2012. ISBN 9781845646165. doi: 10.2495/CR120491.
- [41] G. Stana and V. Brazis. Modeling of two-trolleybus motion with braking energy exchange and transmission resistance. In *2018 25th International Workshop on Electric Drives: Optimization in Control of Electric Drives (IWED)*, pages 1–6, 2018.
- [42] Ehsan Tara, Soheil Shahidinejad, Shaahin Filizadeh, and Eric Bibeau. Battery storage sizing in a retrofitted plug-in hybrid electric vehicle. *IEEE Transactions on Vehicular Technology*, 59(6): 2786–2794, 2010.
- [43] Phatiphat Thounthong, Stephane Rael, and Bernard Davat. Energy management of fuel cell/battery/supercapacitor hybrid power source for vehicle applications. *Journal of Power Sources*, 193(1):376–385, 2009.
- [44] Abhishek Singh Tomar, Bram Veenhuizen, Lejo Buning, and Ben Pyman. Estimation of the size of the battery for hybrid electric trolley busses using backward quasi-static modelling. In *Multidisciplinary Digital Publishing Institute Proceedings*, volume 2, page 1499, 2018.
- [45] S. Vazquez, S. M. Lukic, E. Galvan, L. G. Franquelo, and J. M. Carrasco. Energy storage systems for transport and grid applications. *IEEE Transactions on Industrial Electronics*, 57(12):3881–3895, 2010.
- [46] Wikipedia-bijdragers. Arnhemse trolleybus — wikipedia, de vrije encyclopedie, 2021. URL [https://nl.wikipedia.org/w/index.php?title=Arnhemse\\_trolleybus&oldid=58862403](https://nl.wikipedia.org/w/index.php?title=Arnhemse_trolleybus&oldid=58862403). [Online; accessed 4-mei-2021].
- [47] Jia Ying Yong, Vigna K Ramachandaramurthy, Kang Miao Tan, and Nadarajah Mithulanathan. A review on the state-of-the-art technologies of electric vehicle, its impacts and prospects. *Renewable and Sustainable Energy Reviews*, 49:365–385, 2015.